People's Democratic Republic of Algeria
ministry of higher education and scientific research

National Polytechnic School

Process Control Laboratory

King Abdullah University of Science and Technology

Control Engineering Department

Final Project Thesis

Thesis submitted for the degree of state engineer

Observer Design for Time Scale Systems

Chaouach Lotfi Mustapha

defended publicly 02/07/2020

Jury members :

President	D.BOUDANA	Doctor	NPS- Algiers
Supervisors	M. TADJINE	Professor	NPS- Algiers
	T.M. LALEG/B.Ben Nasser	Professor/Doctor	KAUST-KSA
Examiner	M.CHAKIR	MCA	NPS- Algiers

ENP 2020

People's Democratic Republic of Algeria
ministry of higher education and scientific research

National Polytechnic School

Process Control Laboratory

King Abdullah University of Science and Technology

Control Engineering Department

Final Project Thesis

Thesis submitted for the degree of state engineer

Observer Design for Time Scale Systems

Chaouach Lotfi Mustapha

defended publicly 02/07/2020

Jury members :

President	D.BOUDANA	Doctor	NPS- Algiers
Supervisors	M. TADJINE	Professor	NPS- Algiers
	T.M.LALEG/B.Ben Nasser	Professor/Doctor	KAUST- KSA
Examiner	M.CHAKIR	MCA	NPS- Algiers

ENP 2020

ملخص

في هذه الأطروحة ، تم النظر الى مشكل القياس و التقدير في أنظمة المقياسات الزمنية المتعددة. سنجرب القيام بتطوير طريقة جديدة لهذا الصنف من الأنظمة, سنبدأ أولا بتقديم بعض طرق كالمان الغير خطية التي التكيفية التي تقوم بقياس الأنظمة الزمنية المتعددة. من مقياس كالمان قمنا بانشاء نسخة معممة من مقياس كالمان الموسع عل الأنظمة الزمنية المتعذدة. سنقوم أيضا بعرض نسخة موسعة من المقياس الغير خطي التكيفي لتشخيص الأخطاء في الأنظمة الزمنية. الحيابات و المبرهنات تعتمد على الأدوات المعرفة في نضرية الأنظمة الزمنية.
فعالية تقنيات القياس و التقدير المدروسة موضحة عبر عدة محاكاة رقمية كما نقدم أيضا دراسة مقارنة بين نسخة مقياس كالمان في الوقت المتقطع و نسخة مقياس كالمان المتوسع لأنظمة الزمن المتعددة في حالة تتبع جسم متحرك.

كلمات دالة :, مقياس غير تنظرية المقياس الزمني ، أنظمة المقياسات الزمنية المتعددة ، تقدير الحالة ، تشخيص الأخطاء.الدالة المعدلة.

Résumé

Dans ce projet de fin d'études, le problème d'estimation des signaux d'état et du diagnostic des systèmes à échelles de temps est abordé. Nous essayons de développer de nouveaux observateurs et estimateurs pour cette catégorie de systèmes en commençant dans un premier temps par introduire certains observateurs adaptatifs non linéaires pour le diagnostic des défauts et le filtre de Kalman pour les systèmes à échelles de temps.
Nous établirons à partir du filtre de Kalman à échelles de temps une généralisation de la version discrète du filtre de Kalman étendu au cas des échelles de temps puis nous proposerons une extension des observateurs adaptatifs pour le diagnostic de défauts aux échelles de temps.
L'ensemble des calculs et des démonstrations se base principalement sur les notions et outils introduits dans théorie de l'analyse et du calcul dans les échelles de temps.
L'efficacité des observateurs étudiés ou développés sera illustrée au travers de résultats découlant de simulations numériques. Nous ferons notamment une étude comparative entre les versions discrètes et échelles de temps du filtre de Kalman étendu dans un scénario de poursuite de cible.

Mots clés: time scale theory, time scale systems, estimation d'état, diagnostic de défauts.

Abstract

In this thesis, the problem of state signals estimation and diagnosis on time scale systems is addressed. We will try to develop new observers for this category of systems, starting first by introducing certain adaptive nonlinear observers for fault diagnosis and the time scale Kalman filter.
We establish from the time scale Kalman filter a generalization of the discrete version of the extended Kalman filter to the time scale case, we will also propose an extension of the adaptive nonlinear state observers for fault diagnosis on time scales.
The calculations and demonstrations are mainly based on the tools and notions introduced in the theory of time scale analysis.
The effectiveness of the observers studied or developed will be illustrated through the numerical simulations results. We also make a comparative study between the discrete and time scale versions of the extended Kalman filters in a target tracking scenario.

Key words: time scale theory, time scale systems, state estimation,fault diagnosis.

Acknowledgment

I would like to express my deep gratitude to my advisors **Pr.Mohamed Tadjine** and **Pr.Meriem-Taous Laleg Kirati** for their help, patience and guidance through this thesis. Without their persistent support this dissertation would not have been possible.
I want to thank **Pr.Mohamed Tadjine** for sharing an invaluable knowledge and for instilling in me a genuine passion for engineering and science.
I want to thank **Pr.Meriem-Taous Laleg Kirati** for being an amazing person and supervisor and sharing with me her great knowledge.
I want to thank **Dr.Bacem Ben Nasser** who always steered me in the right direction and never hesitated to help me whenever I needed it.
I would also like to express my gratitude to all teachers that enhanced my knowledge and fueled my passion for science and engineering.

I would like to thank my friends with whom I have spent these last five years at the National Polytechnic School learning, exchanging, laughing and evolving.
I wish to thank my whole family members, especially my mother and father and my siblings for their unconditional and endless support and love.
At last, I would like to address distinguished thanks to the **most singular person** in the creation and with whom I have been able to establish an equally singular and powerful bond.

Dedicated to my mother and father, siblings, aunts and uncles, my grand father and grand mother, my friends and family and all those whom I care about...

Contents

List of figures

List of tables

List of Symbols

General Introduction **12**

1 Time Scale Calculus **14**
1.1 Introduction 15
1.2 Background on time scale calculus 15
1.2.1 Basic definitions 15
1.2.2 Differentiation 16
1.2.3 Integration 18
1.2.4 Exponential functions on time scales 21
1.2.5 Lyapunov and Riccati Equations 24
1.3 Controllability and Observability 25
1.3.1 Controllability 26
1.3.2 Observability 27
1.4 Stability and stabilisability of time scale linear systems 27
1.5 Conclusion 30

2 State of the art on Fault Estimation and Diagnosis **31**
2.1 Introduction 32
2.2 Basics of fault diagnosis in dynamic systems 32
2.2.1 Terminology 32
2.2.2 Faults types 32
2.2.3 Faults modeling 33
2.3 Fault estimation using adaptive observers 36
2.3.1 Generalities around the adaptive observers 36
2.3.2 Non linear lipschitzian systems observation 36
2.3.3 The considered class of nonlinear systems 38
2.3.4 Adaptive state observer design 39

2.3.5 Simulation example . . . 44
2.4 Conclusion . . . 50

3 Time Scale Observer Design **51**
3.1 Introduction . . . 52
3.2 Kalman filter on time scales . . . 52
3.2.1 Time scale Kalman filter equations . . . 52
3.2.2 Fault estimation feature . . . 54
3.3 Extended Kalman filter for time scale systems . . . 56
3.3.1 Time scale extended Kalman filter equations . . . 56
3.3.2 Error stochastic stability . . . 57
3.4 Observer based control on time scales . . . 65
3.5 LQG/LTR case . . . 66
3.6 Simulation examples . . . 67
3.6.1 Kalman filter . . . 67
3.6.2 Extended Kalman filter . . . 74
3.6.3 Observer based control . . . 76
3.6.4 LQG/LTR . . . 81
3.7 Adaptive non linear fault estimation observers . . . 85
3.7.1 Fast fault estimation observer . . . 86
3.7.2 Proportional integral observer . . . 88
3.7.3 PI H_∞ observer . . . 90
3.7.4 Simulation . . . 92
3.8 Conclusion . . . 98

4 Application to the Radar Target Tracking **99**
4.1 Introduction . . . 100
4.2 Generalities around the target tracking . . . 100
4.2.1 Model of target trajectories . . . 100
4.2.2 Measurement equation . . . 103
4.2.3 Radar tracking using EKF . . . 103
4.3 Simulation . . . 104
4.4 Conclusion . . . 112

General Conclusion **113**

Bibliography **115**

List of Tables

1.1 Classification of points on $\mathbb{T}$ 16
1.2 Examples of time scale sets 16
1.3 Classical examples 21

3.1 Time scales considered for simulation 67

List of Figures

1.1 Hilger Complex Plane [27] 22
1.2 Example of Hilger complex planes with given graininess 22

2.1 Time evolution of faults: (a)abrupt fault (b)gradual fault (c)intermittend fault 33
2.2 Flexible link arm [20] 35
2.3 Conventional adaptive observer state estimation 45
2.4 Conventional adaptive observer fault estimation 46
2.5 Fast fault estimation observer state estimation 47
2.6 Fast fault estimation observer fault estimation 48
2.7 PI H_∞ observer state estimation 49
2.8 PI H_∞ observer fault estimation 50

3.1 Time scale Kalman filter simulation for $\mathbb{T} = 2\mathbb{Z}$. 68
3.2 Time scale Kalman filter simulation for $\mathbb{T} = \mathbb{H}_n$. 68
3.3 Time scale Kalman filter simulation for $\mathbb{T} = \mathbb{P}_{12}$. 69
3.4 Time scale Kalman filter simulation for $\mathbb{T} = 2\mathbb{Z}$ for $t \leq 8$ and $\mathbb{T} = \mathbb{H}_n$ for $t > 8$. 70
3.5 Time scale Kalman filter simulation for $\mathbb{T} = \mathbb{N}^{\frac{1}{2}}$. 70
3.6 Time scale Kalman filter with fault estimation feature for $\mathbb{T} = 2\mathbb{Z}$. 71
3.7 Time scale Kalman filter with fault estimation feature for $\mathbb{T} = \mathbb{H}_n$. 72
3.8 Time scale Kalman filter with fault estimation feature for $\mathbb{T} = \mathbb{N}^{\frac{1}{2}}$. 72
3.9 Time scale Kalman filter with fault estimation feature for $\mathbb{T} = 2\mathbb{Z}\ \mathbb{H}_n\ \mathbb{N}^{\frac{1}{2}}$. . 73
3.10 Time scale extended Kalman filter motor shaft angle estimation and its estimation error. 74
3.11 Time scale extended Kalman filter motor shaft angular velocity estimation and its estimation error 75
3.12 Time scale extended Kalman filter rod angle estimation and its estimation error. 75
3.13 Time scale extended Kalman filter Rod angular velocity estimation and its estimation error. 76
3.14 Inverted Pendulum. 77
3.15 Practically generated time scale set. 78

3.16 Observer based control simulation in noisy scenario 79
3.17 Observer based control simulation in non noisy scenario 80
3.18 LTR controller case1 simulation 82
3.19 LTR controller case2 simulation 83
3.20 LQG case controller simulation 83
3.21 LTR controller case1 estimation error 84
3.22 LTR controller case2 estimation error 84
3.23 Time scale fast fault estimation observer state estimation. 92
3.24 Time scale fast fault estimation observer state estimation error 93
3.25 Time scale fast fault estimation observer fault estimation. 93
3.26 Time scale fast fault estimation observer fault estimation error. 94
3.27 Time scale PI H_∞ observer state estimation. 95
3.28 Time scale PI H_∞ observer state estimation error 96
3.29 Time scale PI H_∞ observer fault estimation. 96
3.30 Time scale PI H_∞ observer fault estimation error. 97

4.1 Kalman filter algorithm scheme. [28] 104
4.2 Linear trajectory and measurements generation. 106
4.3 Target tracking using discrete EKF. 106
4.4 Discrete extended Kalman filter targes position estimation error. 107
4.5 Target tracking using time scale extended Kalman filter. 107
4.6 Time scale extended Kalman filter target position estimation error. 108
4.7 Maneuvering target trajectory. 109
4.8 Maneuvering target tracking using discrete extended Kalman filter. 110
4.9 Maneuvering target tracking using time scale extended Kalman filter. . . . 110
4.10 Maneuvering target position estimation error. 111

List of Symbols

$\mathbb{R}$	set of real numbers.
$\mathbb{Q}$	set of rational numbers.
$\mathbb{Z}$	set of integers.
$\mathbb{C}$	set of complex numbers.
$\mathbb{T}$	time scale set.
σ	forward jump operator.
ρ	backward jump operator.
$\emptyset$	empty set.
μ	graininess function.
C_{rd}	set of rd-continuous functions.
I	identity matrix.
$\mathcal{R}$	set of all regressive and rd-continuous functions.
$\mathbb{C}_\mu$	set of Hilger complex numbers.
ξ_μ	cylinder transformation.
$W_C[t_0, t_f]$	controllability Gramian.
$\Gamma_C[A, B]$	controllability matrix.
$W_O[t_0, t_f]$	observability Gramian.
$\Gamma_O[A, C]$	observability matrix.
$\varsigma(A)$	the spectrum of the matrix A.
$\|x\|$	the Euclidean norm of the vector x.
$\|M\|$	the induced matrix norm of the matrix M.

General Introduction

Introduction

State estimation is a control engineering area of major importance due to the role that it plays in studying the problem of system inner signals reconstruction from limited measurements. This control engineering strategy has become essential in any control application that deals with engineered processes control and monitoring or system calibration.
System states estimation is performed using states observers . These tools provide an estimate of the internal state of a given real system by observing its indirect effects using system's inputs and outputs. Since the previous century, observers theory has been widely developed for continuous and discrete time linear and non linear systems.
Discrete and continuous states observers have already demonstrated high effectiveness and suitability for application in different engineering domains such as aerospace, telecommunication ...etc thanks to the simplicity of their implementation and their efficiency [8].
Actually, systems may also be described and characterized by continuous and discrete dynamics at the same time. This is especially profound in many technological systems, in which logic decision making and embedded control actions are combined with continuous physical processes [17].
To capture the evolution of these systems, specially dedicated mathematical models are needed. In 1988 Stefan Hilger, under the direction of Bern Aulbach, introduced the theory of time scales in order to unify discrete and continuous analysis [14]. As a result, we can generalize a process to account for both cases, or any combination of the two under some topological conditions.
It's important to notice that many other time scales than just the set of real numbers or integers can be handled by this process and this leads to more general results.
This theory represents a major asset to give an appropriate description to systems with

hybrid or time non uniform dynamics which are also known as *time scale systems.*

Motivation

Despite the growing interests in this new theory and the different studies already done in the literature, time scale theory is recent and no well developed for control and estimation applications.
The motivation behind this thesis relies on the development of time scale observers from the extension of already established discrete and continuous observers for estimation and diagnosis. Indeed, to achieve the main goal of this thesis we take continuous and discrete observers and generalize their dynamical properties to the arbitrary time scale case.
The observers considered are the extended Kalman filter (EKF) and different adaptive state observers for fault diagnosis on Lipschitzian nonlinear systems.

Thesis outline

The thesis is organised as follows:

- In chapter 1, we introduce the basics of time scale calculus and the main tools or equations that will be used to establish our proofs in the third chapter. We also introduce in this chapter the notions that characterize the dynamical properties of time scale systems.

- Chapter 2 deals with fault estimation and diagnosis, we introduce here the basics of fault diagnosis in dynamical systems and we present fault estimation using adaptive observers

- Chapter 3 gathers all our contributions to the topic, we introduce the time scale Kalman filter presented in [6]. We develop then different time scale observers and bring a theoretical and numerical analysis of these observers performances through the study of the observer based control case on time scales. These observers are assessed through different numerical simulations.

- In chapter 4, we unfold a radar target tracking scenario using the classical EKF and the new time scale EKF.

A general conclusion and a bibliographic appendix complete this document.

CHAPTER 1

Time Scale Calculus

1.1 Introduction

Time Scale calculus is a contemporary theory that was introduced by the German mathematician Stefan Hilger in his PhD thesis in 1988 in order to accomplish a unification of both theories of differential and difference equations[14]. Thus this theory unifies the classical integral and differential calculus with the calculus of finite differences.
Time scale theory offers a new formalism to study hybrid systems that are characterized by discrete continuous dynamics, it has a tremendous potential for applications to any field that requires a simultaneous description and modelling of discrete and continuous data[5].

1.2 Background on time scale calculus

In this section, we will state the basic definition of the main concepts and notions connected to time scales and the tools that will be used in chapters to come.

1.2.1 Basic definitions

Definition 1.2.1. *[5] A time scale is an arbitrary non empty closed subset of the real numbers* $\mathbb{R}$.

Thus $\mathbb{R}$, $\mathbb{Z}$, $\mathbb{N}$, $\mathbb{N}_0$
as are $[0,1]\cup[2,3]$, $[0,1]\cup\mathbb{N}$.
While $\mathbb{Q}$, $\mathbb{R}\backslash\mathbb{Q}$, $\mathbb{C}$, $(0,1)$ are not time scales.
We assume that a time scale $\mathbb{T}$ has the topology that it inherits from the real numbers set[5].
Any time scale that is a combination of any of the above sets is called a hybrid time scale[5].

Definition 1.2.2. *[5] Let* $\mathbb{T}$ *be a time scale. For* $t\in\mathbb{T}$ *we define the forward jump operator* $\sigma:\mathbb{T}\to\mathbb{T}$ *by*

$$\sigma(t)=\inf\{s\in\mathbb{T}:s>t\},$$

While the backward jump operator $\rho:\mathbb{T}\to\mathbb{T}$ *is defined by*

$$\rho(t)=\sup\{s\in\mathbb{T}:s<t\}.$$

We admit that inf($\emptyset$) =sup($\mathbb{T}$) (i.e., $\sigma(t)=t$ if $\mathbb{T}$ has a maximum t) and sup($\emptyset$) =inf($\mathbb{T}$) (i.e., $\rho(t)=t$ if $\mathbb{T}$ has a minimum t).
If $\sigma(t)>t$, we say that t is *right-scattered*, while if $\rho(t)<t$ we say that t is *left-scattered*.
We say that a point is *isolated* if it is right-scattered and left-scattered at the same time.
Also, if $t<$sup($\mathbb{T}$) and $\sigma(t)=t$, then t is called right-dense, and if $t>$inf($\mathbb{T}$) and $\rho(t)=t$, then t is called *left-dense.* Points that are right-dense and left-dense at the same time are called dense.

t right-scattered	$\sigma(t) > t$
t right-dense	$\sigma(t) = t$
t left-scattered	$\rho(t) < t$
t left-dense	$\rho(t) = t$

Table 1.1: Classification of points on $\mathbb{T}$

Definition 1.2.3. *[5] The graininess function is defined by*

$$\mu(t) = \sigma(t) - t \tag{1.1}$$

The set $\mathbb{T}^\kappa$ is derived from the time scale $\mathbb{T}$ as follows[5]:
If $\mathbb{T}$ has a left-scattered maximum m, then $\mathbb{T}^\kappa = \mathbb{T} - \{m\}$.Otherwise, $\mathbb{T}^\kappa = \mathbb{T}$.
To sum up.

$$\mathbb{T}^\kappa = \begin{cases} \mathbb{T}\backslash(\rho(\sup\mathbb{T}), \sup\mathbb{T}] & \text{if } \sup\mathbb{T} < \infty \\ \mathbb{T} & \text{if } \sup\mathbb{T} = \infty \end{cases} \tag{1.2}$$

Finally, if $f : \mathbb{T} \to \mathbb{R}$ is a function, then we define the function $f^\sigma : \mathbb{T} \to \mathbb{R}$ by

$$f^\sigma(t) = f(\sigma(t)) \quad \text{fort} \in \mathbb{T}.$$

$\mathbb{T}$	$\mu(t)$	$\sigma(t)$	$\rho(t)$
$\mathbb{R}$	0	t	t
$\mathbb{Z}$	1	$t+1$	$t-1$
$h\mathbb{Z}$	h	$t+h$	$t-h$
$q^{\mathbb{N}}$	$(q-1)t$	qt	$\frac{t}{q}$
$\mathbb{N}_0^2$	$2\sqrt{t}+1$	$(\sqrt{t}+1)^2$	$(\sqrt{t}-1)^2$

Table 1.2: Examples of time scale sets

1.2.2 Differentiation

We consider a function $f : \mathbb{T} \to \mathbb{R}$ and define the so-called *delta* or Hilger *derivative* of f at a point $t \in \mathbb{T}^\kappa$.

Definition 1.2.4. *[5] Assume $f : \mathbb{T} \to \mathbb{R}$ is a function and let $t \in \mathbb{T}^\kappa$. Then we define $f^\Delta(t)$ to be the number (provided it exists) with the property that given any $\epsilon > 0$, there is a neighborhood U of t (i.e.,$U = (t-\delta, t+\delta) \cap \mathbb{T}$ for some $\delta > 0$) such that*

$$|[f(\sigma(t)) - f(s)] - f^\Delta(t)[\sigma(t) - s]| \leq \epsilon|\sigma(t) - s| \quad \textit{for all } s \in U.$$

We call $f^\Delta(t)$ the delta (or Hilger) derivative of f at t.

We say that f is delta (or Hilger) differentiable (or simply: differentiable) on $\mathbb{T}^\kappa$ provided f^Δ exists for all $t \in \mathbb{T}^\kappa$. Then, we call the function $f^\Delta : \mathbb{T}^\kappa \to \mathbb{R}$ the (delta) derivative of f on $\mathbb{T}^\kappa$.
We state now an important theorem that gives some easy and useful relationships concerning the delta derivative.

Theorem 1.2.1. *[5] Assume $f : \mathbb{T} \to \mathbb{R}$ is a function and let $t \in \mathbb{T}^\kappa$. Then we have the following:*

i) If f is differentiable at t, then f is continuous at t.

ii) If f is continuous at t and t is right-scattered, then f is differentiable at t with:

$$f^\Delta(t) = \frac{f(\sigma(t)) - f(t)}{\mu(t)}.$$

iii) If t is right-dense, then f is differentiable at t if the limit

$$\lim_{s\to t} \frac{f(t) - f(s)}{t - s}.$$

exists as a finite number. In this case

$$f^\Delta(t) = \lim_{s\to t} \frac{f(t) - f(s)}{t - s}.$$

iv) If f is differentiable at t, then

$$f(\sigma(t)) = f(t) + \mu(t) f^\Delta(t).$$

Notice that the last property in theorem1.2.1 is our main equation to run the different simulations.
We can give the following examples:

a. When $\mathbb{T} = \mathbb{R}$, then (if the limits exists)

$$f^\Delta(t) = \lim_{s\to t} \frac{f(t) - f(s)}{t - s} = f'(t).$$

b. When $\mathbb{T} = \mathbb{Z}$, then

$$f^\Delta(t) = f(t + 1) - f(t) = \Delta f(t).$$

c. When $\mathbb{T} = q^{\mathbb{Z}}$ for $q > 1$, then

$$f^{\Delta}(t) = \frac{f(qt) - f(t)}{(q-1)t}.$$

It's important to be able to find derivatives of sums, products, and quotients of differentiable functions. We state here an important theorem that gives us the main formulas that allow us to make these calculations

Theorem 1.2.2. *[5] Assume $f, g : \mathbb{T} \to \mathbb{R}$ are differentiable at $t \in \mathbb{T}^{\kappa}$. Then:*

i) The sum $f + g : \mathbb{T} \to \mathbb{R}$ is differentiable at t with:

$$(f+g)^{\Delta}(t) = f^{\Delta}(t) + g^{\Delta}(t).$$

ii) For any constant α, $\alpha f : \mathbb{T} \to \mathbb{R}$ is differentiable at t with

$$(\alpha f)^{\Delta}(t) = \alpha f^{\Delta}(t).$$

iii) The product $fg : \mathbb{T} \to \mathbb{R}$ is differentiable at t with

$$(fg)^{\Delta}(t) = f^{\Delta}(t)g(t) + f(\sigma(t))g^{\Delta}(t) = f(t)g^{\Delta}(t) + f^{\Delta}(t)g(\sigma(t)).$$

iv) If $f(t)f(\sigma(t)) \neq 0$,then $\frac{1}{f}$ is differentiable at t with

$$\left(\frac{1}{f}\right)^{\Delta}(t) = -\frac{f^{\Delta}(t)}{f(t)f(\sigma(t))}.$$

v) If $g(t)g(\sigma(t)) \neq 0$, then $\frac{f}{g}$ is differentiable at t and

$$\left(\frac{f}{g}\right)^{\Delta} = \frac{f^{\Delta}(t)g(t) - f(t)g\Delta(t)}{g(t)g(\sigma(t))}.$$

1.2.3 Integration

In order to describe the classes of functions that are "integrable", we introduce the following two concepts.

Definition 1.2.5. *[5] A function $f : \mathbb{T} \to \mathbb{R}$ is called regulated provided its right sided limits exist (finite) at all right-dense points in $\mathbb{T}$ and its left sided limits exist (finite) at all left-dense points of $\mathbb{T}$.*

Definition 1.2.6. *[5] A function $f : \mathbb{T} \to \mathbb{R}$ is called rd-continuous provided it is continuous at right-dense points in $\mathbb{T}$ and its left sided limits exist(finite) at left-dense points in $\mathbb{T}$.*

Remark. *The set of rd-continuous functions $f : \mathbb{T} \to \mathbb{R}$ is denoted by:*

$$C_{rd} = C_{rd}(\mathbb{T}) = C_{rd}(\mathbb{T}, \mathbb{R}).$$

The set of functions $f : \mathbb{T} \to \mathbb{R}$ that are differentiable and whose derivative is rd-continuous is denoted by[5]:

$$C^1_{rd} = C^1_{rd}(\mathbb{T}) = C^1_{rd}(\mathbb{T}, \mathbb{R}).$$

Some results concerning rd-continuous and regulated functions are contained in the following theorem.

Theorem 1.2.3. *[5] Assume $f : \mathbb{T} \to \mathbb{R}$.*

- *i) If f is continuous, then f is rd-continuous.*
- *ii) If f is rd-continuous, then f is regulated.*
- *iii) The jump operator σ is rd-continuous.*
- *iv) If f is regulated or rd-continuous, then so is f^σ.*
- *v) Assume f is continuous. If $g : \mathbb{T} \to \mathbb{R}$ is regulated or rd-continuous, then $f \circ g$ has that property too.*

Definition 1.2.7. *[5] A continuous function $f : \mathbb{T} \to \mathbb{R}$ is called pre-differentiable with (region of differentiation) D, provided $D \subset \mathbb{T}^\kappa$, $\mathbb{T}^\kappa \backslash D$ is countable and contains no right-scattered elements of $\mathbb{T}$, and f is differentiable at each $t \in D$.*

Let's introduce now the main existence theorem for pre-antiderivatives.

Theorem 1.2.4. *[5] Let f be a regulated function. Then there exists a function F which is pre-differentiable with region of differentiation D such that*

$$F^\Delta(t) = f(t) \qquad \textit{holds for all}\, t \in D.$$

Definition 1.2.8. *[5] Assume $f : \mathbb{T} \to \mathbb{R}$ is a regulated function. Any function F as in theorem1.2.4 is called a pre-antiderivative of f. We define the indefinite integral of a regulated function f by*

$$\int f(t)\Delta t = F(t) + C.$$

Where C is an arbitrary constant and F is a pre-antiderivative of f. The Cauchy integral is defined by

$$\int_r^s f(t)\Delta t = F(s) - F(r) \quad \text{for all } r, s \in \mathbb{T}.$$

A function $F : \mathbb{T} \to \mathbb{R}$ is called an antiderivative of $f : \mathbb{T} \to \mathbb{R}$ provided

$$F^{\Delta}(t) = f(t) \quad \text{holds for all } t \in \mathbb{T}^{\kappa} \ .$$

Theorem 1.2.5. *[5] Every rd-continuous function has an antiderivative. In particular if $t_0 \in \mathbb{T}$, then F is defined by*

$$F(t) = \int_{t_0}^t f(\tau)\Delta\tau \quad \text{for } t \in \mathbb{T}.$$

is an antiderivative of f.

Theorem 1.2.6. *[5] if $f \in C_{rd}$ and $t \in \mathbb{T}^{\kappa}$, then*

$$\int_t^{\sigma(t)} f(\tau)\Delta\tau = \mu(t)f(t).$$

Theorem 1.2.7. *[5] If $a, b, c \in \mathbb{T}$, $\alpha \in \mathbb{R}$, and $f, g \in C_{rd}$, then:*

i) $\displaystyle\int_a^b [f(t) + g(t)]\,\Delta t = \int_a^b f(t)\Delta t + \int_a^b g(t)\Delta t;$

ii) $\displaystyle\int_a^b \alpha f(t)\Delta t = \alpha \int_a^b f(t)\Delta t;$

iii) $\displaystyle\int_a^b f(t)\Delta t = -\int_b^a f(t)\Delta t;$

iv) $\displaystyle\int_a^b f(t)\Delta t = \int_a^c f(t)\Delta t + \int_c^b f(t)\Delta t;$

v) $\displaystyle\int_a^a f(t)\Delta t = 0;$

vi) if $f(t) \geq 0$ for all $a \leq t < b$, then $\displaystyle\int_a^b f(t)\Delta t \geq 0.$

Time Scale $\mathbb{T}$	$\mathbb{R}$	$\mathbb{Z}$
$\rho(t)$	t	$t-1$
$\sigma(t)$	t	$t+1$
$\mu(t)$	0	1
$f^{\Delta}(t)$	$f'(t)$	$\Delta f(t)$
$\int_a^b f(t)\Delta t$	$\int_a^b f(t)dt$	$\sum_{t=a}^{b-1} f(t)$ (if $a<b$)
Rd-continuous f	continuous f	any f

Table 1.3: Classical examples

1.2.4 Exponential functions on time scales

In this subsection, we introduce the generalized exponential functions on time scales.

Definition 1.2.9. *[5] A function $p : \mathbb{T} \to \mathbb{R}$ is called regressive if*

$$1 + \mu(t)p(t) \neq 0 \quad \textit{for all}\, t \in \mathbb{T}.$$

Definition 1.2.10. *[5] An $m \times n$ matrix-valued function A is rd-continuous if each of its entries are rd-continuous.*
Furthermore, if $m = n$, A is said to be regressive (denoted by $A \in \mathcal{R}$) if

$$I + \mu(t)A(t) \quad \textit{is invertible for all}\, t \in \mathbb{T}^k.$$

Remark. *The set of all regressive and rd-continuous functions is given by*

$$\mathcal{R} = \mathcal{R}(\mathbb{T}) = \mathcal{R}(\mathbb{T}, \mathbb{R}).$$

In the matrix case we write:

$$\mathcal{R}(\mathbb{T}, \mathbb{R}^{m\times n}).$$

In Laplace transforms of continuous time signals, we have the s plane. In the z-transform of discrete time signals, there is the unit circle. In time scales, both are special cases of the Hilger circle which contains the Hilger complex numbers defined as follows:

Definition 1.2.11. *[5]For $\mu > 0$, we define the Hilger complex numbers by*

$$\mathbb{C}_\mu = z \in \mathbb{C} : z \neq -\frac{1}{\mu}.$$

When $\mu = 0$, let $\mathbb{C}_0 = \mathbb{C}$.

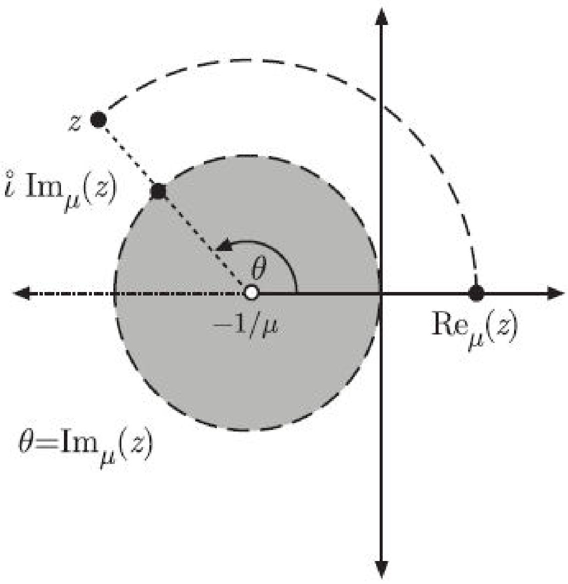

Figure 1.1: Hilger Complex Plane [27]

Remark. *When $\mu \neq 0$ the Hilger real part of μ is*

$$\mathrm{Re}_\mu(z) = \frac{|\mu z + 1| - 1}{\mu}.$$

and the Hilger imaginary part is

$$\mathrm{Im}_\mu(z) = \frac{\mathrm{Arg}(\mu z + 1)}{\mu}.$$

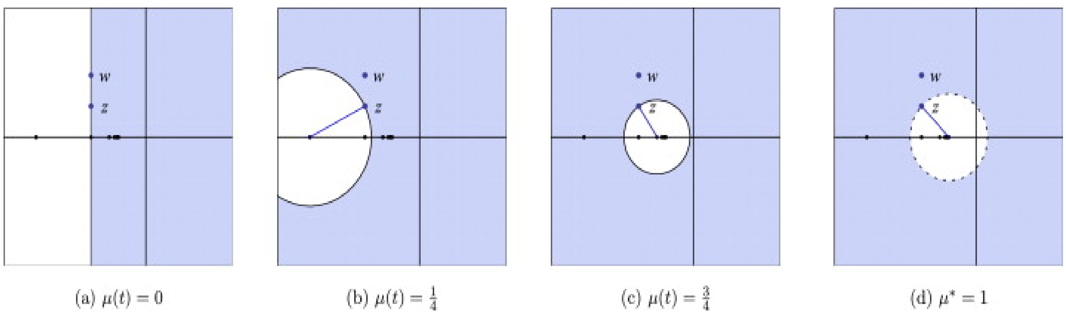

Figure 1.2: Example of Hilger complex planes with given graininess

To express the exponential function we need to define first the cylinder transformation whose range is the set Z_μ defined as follows.

Definition 1.2.12. *[5]For $\mu > 0$, we define the strip*

$$\mathbb{Z}_\mu = \left\{ z \in \mathbb{C} : -\frac{\pi}{\mu} < Im(z) \leq \frac{\pi}{\mu} \right\}.$$

When $\mu = 0$, let $\mathbb{Z}_0 = \mathbb{C}$.

Definition 1.2.13. *[5] For $\mu > 0$, we define the cylinder transformation $\xi_\mu : \mathbb{C}_\mu \to \mathbb{Z}_\mu$ by*

$$\xi_\mu = \frac{1}{\mu} Log(\mu z + 1), \tag{1.3}$$

where Log represents the principal logarithm function. For $\mu = 0$, we define $\xi_0(z) = z$ for all $z \in \mathbb{C}$.
i.e., $\xi_\mu(z) = \begin{cases} \frac{Log(1+\mu z)}{\mu} & if \quad \mu \neq 0 \\ z & if \quad \mu = 0 \end{cases}$

Theorem 1.2.8. *[5]Suppose that A is regressive and rd-continuous. Then the initial value problem*

$$X^\Delta(t) = A(t)X(t) \quad , X(t_0) = I$$

has a unique $n \times n$ matrix-valued solution X.

Definition 1.2.14. *[5] The solution X from theorem1.2.8 is called the matrix exponential function on $\mathbb{T}$ and is denoted by $e_A(., t_0)$. Where $e_A(t, s) = exp\left\{ \int_s^t \xi_{\mu(\tau)}(A(\tau))\Delta\tau \right\}$*

Theorem 1.2.9. *[5] Let A be regressive and rd-continuous.Then for $r, s, t \in \mathbb{T}$,*

i) $e_A(t, s)e_A(s, r) = e_A(t, r)$,

ii) $e_A(t, t) = e_0(t, s) = I$,

iii) $e_A(\sigma(t), s) = (I + \mu(t)A(t))e_A(t, s)$,

iv) $e_A(t, \sigma(s)) = e_A(t, s)(I + \mu(s)A)^{-1}$,

v) $e_A^{-1}(t, s) = e_A(s, t)$,

vi) $(e_A(., s))^\Delta = Ae_A(., s)$,

vii) $(e_A(t, .))^\Delta = -e_A^\sigma(t, .)A = e_A(t, .)(I + \mu(s)A)^{-1}A$.

As examples, let's assume that A is a $n \times n$ matrix. We have:

a. If $\mathbb{T} = \mathbb{Z}$, then

$$e_A(t, t_0) = \begin{cases} \prod_{\tau=t_0}^{t-1}[I + A(\tau)] & \text{if } A(t) \neq \text{-}I. \\ (I + A)^{t-t_0} & \text{if } I + A \text{ is a constant and invertible.} \end{cases}$$

b. If $\mathbb{T} = \mathbb{R}$, then

$$e_A(t,t_0) = \begin{cases} exp\left\{\int_{t_0}^{t} A(\tau)d\tau\right\} & \text{if } A \text{ is continuous and } A(s)A(t) = A(t)A(s) \text{ for all } s,t \in \mathbb{T}. \\ e^{A(t-t_0)} & \text{if } A(t) \text{ is constant.} \end{cases}$$

c. If $\mathbb{T} = h\mathbb{Z}$, then

$$e_A(t,t_0) = \begin{cases} \prod_{\tau=t_0}^{\frac{t}{h-1}} [I + hA(h\tau)] & \text{if } A(t) \text{ is regressive.} \\ \left(I + hA\right)^{\frac{t-t_0}{h}} & \text{if } I + hA \text{ is a constant and invertible .} \end{cases}$$

d. If $\mathbb{T} = q^{\mathbb{N}_0}$ for $q > 1$, then

$$e_A(t,1) = \prod_{\tau \in \mathbb{T}\cap(0,t)} [I + (q-1)\tau A(\tau)].$$

Theorem 1.2.10. *[5] Let $A \in \mathcal{R}$ be an $n \times n$ matrix-valued function on $\mathbb{T}$ and suppose that $f : \mathbb{T} \to \mathbb{R}^n$ is rd-continuous. Let $t_0 \in \mathbb{T}$ and $x_0 \in \mathbb{R}^n$. Then the solution of the initial value problem*

$$x^{\Delta}(t) = A(t)x(t) + f(t), \qquad x(t_0) = x_0.$$

is given by

$$x(t) = e_A(t,t_0)x_0 + \int_{t_0}^{t} e_A(t,\sigma(\tau))f(\tau)\Delta\tau.$$

Theorem 1.2.11. *[5] Let $t_0 \in \mathbb{T}, x, f \in C_{rd}$ and $A \in R^+$.Then*

$$x^{\Delta}(t) \leq A(t)x(t) + f(t), \quad \text{for all } t \in \mathbb{T}^{\kappa}.$$

implies

$$x(t) \leq x(t_0)e_A(t,t_0) + \int_{t_0}^{t} e_A(t,\sigma(\tau))f(\tau)\Delta\tau, \quad \text{for all } t \in \mathbb{T}_{t_0}^{\kappa}$$

1.2.5 Lyapunov and Riccati Equations

In the next chapters, we will use the notion of Lyapunov and Riccati equations on time scales to obtain or demonstrate some results.

Definition 1.2.15. *[29]A square matrix-valued function A is said to be symmetric if it is equal to its transpose,i.e. $A = A^T$.*

Definition 1.2.16. *[29] A symmetric matrix-valued function A is said to be positive definite (denoted $A > 0$) if $x^T Ax > 0$ for any nonzero vector x. A symmetric matrix-valued function A is said to be positive semi-definite (denoted $A \geq 0$) if ($x^T Ax \geq 0$) for any nonzero vector x.*

Definition 1.2.17. *[29] Let $P \in C^1_{rd}(\mathbb{T}, \mathbb{R}^{n\times n})$ be symmetric, A generalized Lyapunov function is given by*

$$x^T(t)P(t)x(t).$$

We will use the Lyapunov functions to demonstrate the error and stochastic error stability of some observers in the third chapter.

Definition 1.2.18. *[29] Let X be positive definite and let A,B,C be constant matrices. Then a Riccati equation of the first form is given by*

$$\begin{aligned} X^{\Delta}(t) = C + AX(t) + (I+\mu(t)A)X(t)A^T - (I+\mu(t)A) \\ X(t)B^T(C+\mu(t)BX(t)B^T)^{-1}BX(t)(I+\mu(t)A^T). \end{aligned} \tag{1.4}$$

And a Riccati equation of the second form is given by

$$\begin{aligned} -X^{\Delta}(t) = C + AX^{\sigma}(t) + (I+\mu(t)A)X^{\sigma}(t)A^T - (I+\mu(t)A) \\ X^{\sigma}(t)B^T(C+\mu(t)BX^{\sigma}(t)B^T)^{-1}BX^{\sigma}(t)(I+\mu(t)A^T). \end{aligned} \tag{1.5}$$

We will use these two equations in the third chapter.
The equation 1.4(1) will be used to describe the evolution of the error covariance of the Kalman Filter and predict its value.
The equation 1.5(2) will be used to compute the value parameter of the optimal state feedback in the third chapter.

1.3 Controllability and Observability

These two concepts have been introduced by R.E.Kalman in the early 1960s. Both allow a control system classification without necessarily finding their solution in closed form.
Because of this usefulness, It's important to lay down the foundations of linear control on time scales and introduce those two notions for these systems.
In this section we will consider the time scale invariant linear system

$$\begin{aligned} x^{\Delta}(t) = Ax(t) + Bu(t) \\ y(t) = Cx(t) \end{aligned} \tag{1.6}$$

where $t \in \mathbb{T}$, $x \in \mathbb{R}^n$ is the state, $u \in \mathbb{R}^m$ is the input , $y \in \mathbb{R}^p$ is the output and $A \in \mathbb{R}^{n\times n}$, $B \in \mathbb{R}^{n\times m}$, $C \in \mathbb{R}^{p\times n}$.
Here u is assumed to be rd-continuous. A is assumed to be regressive and C is assumed to be of rank n.

Remark. *Although system 1.6 seems to be a very natural extension from the continuous and discrete cases, to examine the rank condition for controllability in the classical sense, one must assume that the graininess function is differentiable, an assumption that is not satisfied in general for time scales (see Example 1.56 in [5]). To step this issue the linear system 1.6 has been altered in [29]. But for the work done in this thesis, we will focus only on system 1.6. Nevertheless, I strongly encourage to read the third chapter in [29].*

1.3.1 Controllability

Let's consider the state equation

$$x^{\Delta}(t) = Ax(t) + Bu(t) \tag{1.7}$$

When we refer to a linear system being "controllable", we mean there exist inputs such that the state vector "can be driven" to the origin for any given initial condition. If all of the states of the linear system are controllable, then we have the following definition for complete controllability.

Definition 1.3.1. *[29] The state equation 1.7 is said to be completely controllable on* $[t_0, t_f]$ *if for all* $x_0 \in \mathbb{R}^n$*, there exists* u *such that the solution* x *of 1.7 with* $x(t_0) = x_0$ *satisfies* $x(t_f) = 0$.

The generalized controllability criterion is

Theorem 1.3.1. *[29] The state equation 1.7 is completely controllable if and only if the controllability Gramian* $W_C\left[t_0, t_f\right]$ *is invertible where*

$$W_C\left[t_0, t_f\right] = \int_{t_0}^{t_f} e_A(t_0, \sigma(\tau)) BB^T e_A^T(t_0, \sigma(\tau)) \Delta\tau.$$

Let's look now at the generalized Kalman rank condition for controllability of linear systems on time scales.

Theorem 1.3.2. *[16] The state equation 1.7 is completely controllable if and only if the* $n \times (nm)$ *controllability matrix* $\Gamma_C\left[A, B\right]$ *has full rank* n*, where*

$$\Gamma_C\left[A, B\right] = \left[B \ AB \ A^2B \ \ldots \ A^{n-1}B\right]$$

.

1.3.2 Observability

We refer to a linear system being "observable" if given the output y and input u, we can find our initial condition x_0. If this is true regardless of the initial time and initial state, we have the following definition for complete observability.[29]

Definition 1.3.2. *[29] The linear system 1.6 is said to be completely observable on* $[t_0, t_f]$ *where, if for any* $x(t_0)$ *and a known* u, $x(t_0)$ *can be uniquely determined by* $y(t)$.
On the other hand, the linear system 1.6 is said to be unobservable if given $x(t_0) = x_0$ *and the input* $u(t) = 0$, *there exists a finite time* t_f *such that* $y(t) = 0$ *for all* $t \in [t_0, t_f)$.

Theorem 1.3.3. *[29] The linear system 1.6 is completely observable if and only if the observability Gramian* $W_O[t_0, t_f]$ *is invertible, where*

$$W_O[t_0, t_f] = \int_{t_0}^{t_f} e_A^T(\tau, t_0) C^T C e_A(\tau, t_0) \Delta\tau.$$

The generalized Kalman rank condition for observability of linear systems on time scales is as follows.

Theorem 1.3.4. *[29] The linear system 1.6 is completely observable if and only if the* $(np) \times n$ *observability matrix* $\Gamma_O[A, C]$ *has full rank* n, *where*

$$\Gamma_O[A, C] = \begin{bmatrix} C \\ CA \\ . \\ . \\ CA^{n-1} \end{bmatrix}$$

1.4 Stability and stabilisability of time scale linear systems

In this section we introduce the uniform exponential stability of linear systems on time scales and give the characterisation of stabilisability of linear systems.
These two concepts will be needed to explain some simulation results.
In this section, we consider the time invariant linear system on the time scale $\mathbb{T}$

$$x^{\Delta}(t) = Ax(t), \tag{1.8}$$

where $x(t) \in \mathbb{R}^n$, $A \in \mathbb{R}^{n \times n}$ and $t \in \mathbb{T}$.

Remark. *In general, the exponential stability of a linear system on time scale cannot be characterised by the spectrum of its matrix.*
Fortunately, this can be done for uniform exponential stability. For this reason, when we talk about stability in the next sections we will mean the uniform exponential stability.
Moreover, The spectrum decides of about the classical exponential stability of system 1.8 only if the matrix A is diagonalisable.[2]
In this particular case, all what will be developed for uniform exponential stability can be stated for classical exponential stability. This will be useful to explain some filters behaviors.

Let's start with the basic definitions

Definition 1.4.1. *[2] Let's consider the non linear system*

$$x^{\Delta}(t) = f(x(t)), \qquad x(t_0) = x_0, \tag{1.9}$$

where $x(t) \in \mathbb{R}^n$, $x_0 \in \mathbb{R}^n$, $t, t_0 \in \mathbb{T}$ and f is of class $\mathcal{C}^1$. We assume that the state $x = 0$ is the unique equilibrium of 1.9. The unique forward trajectory determined by x_0 and t_0 evaluated at the time $t \geq t_0$ is denoted by $p(t, x_0, t_0)$.
The equilibrium of 1.9 is uniformly exponentially stable if there exist constants $\alpha < 0$, $M \geq 1$ and $\delta > 0$ such that for every $t_0 \in \mathbb{T}$

$$\|x_0\| < \delta \implies \|p(t, x_0, t_0)\| \leq M \|x_0\| e^{\alpha(t-t_0)}, \qquad \forall t \geq t_0$$

A system with the above property is called uniformly exponentially stable

Remark. *If μ is unbounded, then for any f the system 1.9 is not uniformly exponentially stable.*

Definition 1.4.2. *[2]Let's consider now the nonlinear control system on the time scale $\mathbb{T}$*

$$x^{\Delta}(t) = g(x(t), u(t)), x(t_0) = x_0, \tag{1.10}$$

where $x(t) \in \mathbb{R}^n$, $u(t) \in \mathbb{R}^m$, $x_0 \in \mathbb{R}^n$, $t, t_0 \in \mathbb{T}$ and $t \geq t_0$. We assume that $g : \mathbb{R}^n \times \mathbb{R}^m \to \mathbb{R}^n$ is a function of class $\mathcal{C}^1$ with respect to the variables x and u. We also assume that the state $x = 0$ is an equilibrium of 1.10 for $u = 0$.(i.e.$g(0, 0) = 0$.)
A mapping $k : \mathbb{R}^n \to \mathbb{R}^m$ of class $\mathcal{C}^1$ such that $k(0) = 0$ will be called feedback. Applying the feedback k to system 1.10 we get the closed-loop system

$$x^{\Delta}(t) = f(x(t)), \qquad x(t_0) = x_0, \tag{1.11}$$

where $f(x) = g(x, k(x))$.
The feedback k stabilises system1.10 uniformly exponentially if $x = 0$ is a uniform exponentially stable equilibrium point of the closed loop system 1.11 [2].
System 1.10 will be called uniformly exponentially stabilisable if there exists a feedback stabilising the system 1.10 uniformly exponentially.

System 1.10 will be called linearly uniformly exponentially stabilisable if there exists a linear feedback $u = Kx$, $K \in \mathbb{R}^{m\times n}$, stabilising the system 1.10 uniformly exponentially.
For linear systems we will consider only linear feedbacks.

Let's announce an important proposition.

Proposition 1.4.1. *[2] The following conditions are equivalent:*

(i) System 1.8 is uniformly exponentially stable.

(ii) There exist constants $\alpha < 0$ and $M \geq 1$ such that for all $t_0 \in \mathbb{T}$

$$\|e_A(t, t_0)\| \leq Me^{\alpha(t-t_0)} \qquad \forall t \in \mathbb{T} \text{ and } t \geq t_0.$$

We announce the following theorem.

Theorem 1.4.1. *[10] The following conditions are equivalent:*

(i) There exists uniform exponentially stable linear system 1.8 on time scale $\mathbb{T}$.

(ii) There exists $\overline{\mu} > 0$ such that $\mu(t) \leq \overline{\mu}$ for all $t \in \mathbb{T}$.

This theorem expresses the boundedness of the graininess on a time scale as a necessary condition to the stability of any system that evolves in it.

Theorem 1.4.2. *[2] Let $\mu(t) \leq \overline{\mu}$ for all $t \in \mathbb{T}$. Assume that the eigenvalues of A are distinct, real and each $\lambda \in \varsigma(A)$ satisfies $\lambda \in (-\frac{1}{\overline{\mu}}, 0)$. Then the system 1.8 is uniform exponential stable.*

Not only the fact that this theorem shows that uniform exponential stability can be characterized by the eigenvalues of the matrix A, but it also gives a location in the Hilger complex plane for the placement of poles when we stabilise a system with a state feedback. Let us consider the linear control system defined on the time scale $\mathbb{T}$.

$$x^{\Delta}(t) = Ax(t) + Bu(t), \tag{1.12}$$

where $x(t) \in \mathbb{R}^n$, $u(t) \in \mathbb{R}^m$, $A \in \mathbb{R}^{n\times n}$, $B \in \mathbb{R}^{n\times m}$. u is also assumed to be rd-continuous and A regressive.
under theses conditions the following theorem has been stated in [3]

Theorem 1.4.3. *[3] Assume that $\mu(t)$ is bounded. If system 1.12 is controllable, then it is stabilizable.*

Remark. *The theorem above is of utmost importance, because we will work with bounded graininess time scales.*

1.5 Conclusion

This first chapter is dedicated to introduce essential notions and theorems to deal with any problem related to time scale systems.
First we recalled theoretical basics and notions that constitute calculus in time scale theory, these notions allow us to define what is a time scale system and describe its behavior through delta derivative equations.
After that we gave an overview of tools that allow the analysis of time scale systems dynamical properties. We have seen that controlability and observability for time scale linear systems are the same as continuous linear systems. We have also seen that graininess operator is a key parameter to analyse time scale systems stability.
This graininess important role in systems stability constrains us to assume that graininess values are always known in next chapters.

CHAPTER 2

State of the art on Fault Estimation and Diagnosis

2.1 Introduction

In this chapter, we focus on the state of the art on fault estimation and diagnosis. We talk in general about diagnosis and details around the diagnosis and introduce important results about adaptive observers for fault diagnosis for Lipschitzian non linear systems. These observers have a major interest because of their ability to adapt the state observation to faults that could strike system components by locating and estimating those faults.

2.2 Basics of fault diagnosis in dynamic systems

2.2.1 Terminology

In this part, we recall the definition of some terms as they are stated in [15].

- **Fault:** an unauthorized deviation of at least one characteristic property or a system parameter from its nominal value.

- **Fault detection:** Determination if a fault is present in the system as well as the instant of its occurrence.

- **Fault location:** determination of the type, location and time of a fault appearance; it follows the fault detection.

- **Fault identification:** determination of the severity level of the fault as well as its temporal behavior; it follows the fault location.

- **Fault diagnosis:** Determination of the type, size, location and time of the appearance of a fault; it follows fault detection and includes isolation and identification.

2.2.2 Faults types

Faults may happen for different reasons such as components aging, friction...etc. According to the organ where they appear, the faults are classified into three principal categories [20]: sensor faults, actuator faults and components faults.

- **Actuator faults:** these are slippages between signals supplied by the control unit and those applied to the system.

- **Sensor faults:** they characterize abnormal deviations between real signals and measured values supplied by sensors. Their effects are harmful on looped systems.

- **Component fault:** they characterize anomalies in the system itself. This type of fault causes a change in the system dynamic.

The faults can also be differentiated following their time behavior.
A fault which appears abruptly is qualified as an *abrupt fault*. On the other hand, when a fault has a slow evolution it is qualified as a *gradual fault*.
A non persistent abrupt fault that disappears and reappears randomly is known as an *intermittent fault*.

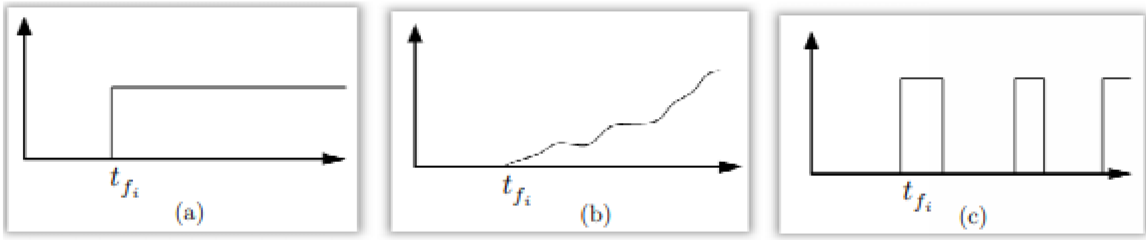

Figure 2.1: Time evolution of faults: (a)abrupt fault (b)gradual fault (c)intermittend fault

2.2.3 Faults modeling

Model-based diagnosis techniques are usually designed around a dynamic model that describes the behavior of the system in normal situations. [20]
The appearance of a fault leads to an abnormal change in the behavior of the system. Faults are then detected if the measured variables deviate from those calculated from the model.
Unfortunately, disturbances, measurement noise and non-modeled dynamics also generate inconsistencies between the behavior of the system and the mathematical model that is describing it.
The diagnosis of a fault is therefore possible only if we know the symptoms associated with this one, i.e. if we know the impact of this fault on the behavior of the process and are able to discern it from that generated by model imperfections and other faults. It is therefore necessary to establish a list of all the faults to be diagnosed as well as the model describing the dynamic behavior of the process generated by these faults and which takes account of the imperfections of the model. [20]

we consider the non-linear systems which can be described by the following differential equation system:

$$\begin{cases} \dot{x}(t) = Ax(t) + Bu(t) + \Phi(x(t)) + D\delta(t) \\ y(t) = Cx(t) + \omega(t) \end{cases} \tag{2.1}$$

Where $x(t) \in \mathbb{R}^n$, $u(t) \in \mathbb{R}^m$, $y(t) \in \mathbb{R}^p$ represent the state vector, the control signal and the measured outputs respectively . $\Phi(x(t)) : \mathbb{R}^n \to \mathbb{R}^n$ is a function that represents the model nonlinearities.
The vector $\delta(t) \in \mathbb{R}^l$ which is distributed via the known D matrix represents the effect of the external disturbances and model uncertainties. $\omega(t) \in \mathbb{R}^p$ is the measurement noise.
Just like disturbances, faults are represented by some unknown additive signals as follows:

$$\begin{cases} \dot{x}(t) = Ax(t) + B(u(t) + f_a(t)) + \Phi(x(t)) + E_c f_c(t) + D\delta(t) \\ y(t) = Cx(t) + E_s f_s(t) + \omega(t) \end{cases} \tag{2.2}$$

Where the vectors $f_a(t) \in \mathbb{R}^m$, $f_c(t) \in \mathbb{R}^{q_c}$ and $f_s(t) \in \mathbb{R}^{q_s}$ represent actuator faults, component faults and sensor faults respectively. The matrices B, E_c and E_s locate the incidence of these faults.
The system described by the equations 2.2 can be represented as follows [20]:

$$\begin{cases} \dot{x}(t) = Ax(t) + Bu(t) + \Phi(x(t)) + E(t)f(t) + W_1 d(t) \\ y(t) = Cx(t) + Ff(t) + W_2 d(t) \end{cases} \tag{2.3}$$

Where $f = \begin{bmatrix} f_a^T & f_c^T & f_s^T \end{bmatrix}^T$, $E = \begin{bmatrix} B & E_c & 0_{n\times q_s} \end{bmatrix}$, $F = \begin{bmatrix} 0_{p\times m} & 0_{p\times q_c} & E_s \end{bmatrix}$, $d = \begin{bmatrix} \delta^T & \omega^T \end{bmatrix}^T$, $W_1 = \begin{bmatrix} D & 0_{n\times m} \end{bmatrix}$ and $W_2 = \begin{bmatrix} 0_{p\times l} & I_p \end{bmatrix}$.
The effect of a fault f_i can be distinguished from disturbances effect if $E_i \notin span(W_1)$. As well as, the effect of a fault f_i is distinguishable from the other faults if E is a full rank matrix. [20]
It's also worth noting that the measurement noise can hide the sensor calibration faults and slow the detection of gradual faults.

Remark. f_i $(i = 1...(m + q_c + q_s))$ *refers to the components of the vector* f.

Remark. E_i $(i = 1...(m + q_c + q_s))$ *refers to the column vector of* E *that corresponds to* f_i.

Remark. *It's important to notice that modeling with additive faults can lead to a number of faults higher than the real one. [20]*

We consider the model of a flexible link arm given by the following equations [23]:

$$\begin{cases} \dot{\theta}_m(t) = \omega_m(t) \\ \dot{\omega}_m(t) = \frac{k}{J_m}(\theta_l(t) - \theta_m(t)) - \frac{b}{J_m}\omega_m(t) + \frac{k_\tau}{J_m}u(t) \\ \dot{\theta}_l(t) = \omega_l(t) \\ \dot{\omega}_l(t) = -\frac{k}{J_l}(\theta_l(t) - \theta_m(t)) - \frac{mgh}{J_t}\sin(\theta_l(t)) \end{cases} \tag{2.4}$$

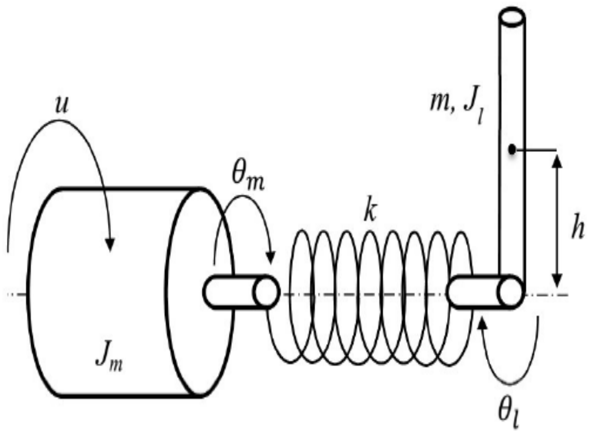

Figure 2.2: Flexible link arm [20]

Where θ_m and θ_l are the angular positions of the motor shaft and the rod respectively, ω_m and ω_l are their respective angular velocities. u represents the control torque applied by the motor, J_m the rotor inertia momentum, J_l the rod inertia momentum, k the bond elasticity constant, m the rod mass, g the gravity constant, h the distance between the rotation axis of the rod and its center of gravity, b the viscous friction coefficient and k_τ is some positive constant.We suppose that θ_m and ω_m are measured.
If we define the state of the system $x = \begin{bmatrix} x_1 & x_2 & x_3 & x_4 \end{bmatrix}^T = \begin{bmatrix} \theta_m & \omega_m & \theta_l & \omega_l \end{bmatrix}^T$, the system 2.4 can be written in the form (2.1) such that

$$A = \begin{bmatrix} 0 & 1 & 0 & 0 \\ -\frac{k}{J_m} & -\frac{b}{J_m} & \frac{k}{J_m} & 0 \\ 0 & 0 & 0 & 1 \\ \frac{k}{J_t} & 0 & -\frac{k}{J_t} & 0 \end{bmatrix},\ B = \begin{bmatrix} 0 \\ \frac{k_\tau}{J_m} \\ 0 \\ 0 \end{bmatrix},\ C = \begin{bmatrix} 1 & 0 & 0 & 0 \\ 0 & 1 & 0 & 0 \end{bmatrix},\ \Phi(x) = \begin{bmatrix} 0 \\ 0 \\ 0 \\ \frac{-mgh}{J_t} sin(x_3) \end{bmatrix}.$$

Many faults can occur in this system. In this example, we will only deal with components faults.
The deformation of the flexible connection and another mechanical fault which manifests itself by an abnormal increase in viscous friction in the bond. It is clear that the impact of these two faults on the model results in abnormal variations of the parameters k and b. Thus, the model of the system with the parametric variations due to these faults can be written

$$\begin{cases} \dot{x} = (A + \Delta A)x + Bu + \Phi(x) \\ y = Cx \end{cases} \tag{2.5}$$

where

$$\Delta A = \begin{bmatrix} 0 & 0 & 0 & 0 \\ -\frac{\Delta k}{J_m} & -\frac{\Delta b}{J_m} & \frac{\Delta k}{J_m} & 0 \\ 0 & 0 & 0 & 0 \\ \frac{\Delta k}{J_t} & 0 & -\frac{\Delta k}{J_t} & 0 \end{bmatrix}$$

Δk, Δb represent respectively the abnormal variations of k and b.
If we put $Ef = \Delta Ax$, the system 2.5 becomes:

$$\begin{cases} \dot{x} = Ax + Bu + \Phi(x) + Ef \\ y = Cx \end{cases} \tag{2.6}$$

where

$$f = \begin{bmatrix} f_1 \\ f_2 \end{bmatrix} = \begin{bmatrix} \Delta k(x_3 - x_1) \\ \Delta b x_2 \end{bmatrix}, E = \begin{bmatrix} 0 & \frac{1}{J_m} & 0 & -\frac{1}{J_t} \\ 0 & -\frac{1}{J_m} & 0 & 0 \end{bmatrix}^T$$

2.3 Fault estimation using adaptive observers

2.3.1 Generalities around the adaptive observers

An adaptive observer is an observer that aims to estimate, in addition to the state, the unknown process parameters. [20]
The estimation of the unknown parameters is guaranteed only if the persistent excitation condition is satisfied. [20]
Their major limitation is that they require the system to satisfy some structure specifying the unknown parameters location relative to the outputs.[20]

Let's define now what is the persistent excitation.

Definition 2.3.1. *[4] A signal $\Psi(\tau) : \mathbb{R} \rightarrow \mathbb{R}^{\rho \times \mu}$ satisfies the persistent excitation property if there exist some positive real constants T, k_1 and k_2 so that $\forall t \geq 0$*

$$I_\rho k_1 \geq \int_t^{t+T} \Psi(\tau)\Psi(\tau)^T d\tau \geq I_\rho k_2 \tag{2.7}$$

2.3.2 Non linear lipschitzian systems observation

Nonlinear systems observers synthesis problem consists mainly in looking for a correction term that is able to dominate the nonlinear part in the dynamic of the observation error. The difficulty of this problem is largely linked to the analytical properties of these nonlinearities . The class of nonlinear systems that has attracted the most attention is that of the so-called Lipschitzian systems which are described by the following equation system

$$\begin{cases} \dot{x} = Ax + Bu + \Phi(x,u,t) \\ y = Cx \end{cases} \tag{2.8}$$

The nonlinear term $\Phi(x,u)$ satisfies locally the following Lipschitz continuity condition

$$\|\Phi(x,u,t) - \Phi(\hat{x},u,t)\| \leq l_\Phi \|x - \hat{x}\| \tag{2.9}$$

$\forall x, \hat{x} \in \mathbb{D}^n \subset \mathbb{R}^n$, and $u \in \mathbb{R}^m$, where the constant $l_\Phi \in \mathbb{R}^+$, called the Lipschitz constant, is independent of x and u values. If 2.9 is satisfied $\forall x, \hat{x} \in \mathbb{R}^n$, the function $\Phi(x,u,t)$ is globally lipschitzian.

Remark. *system 2.8 can describe globally or locally the behavior of many real systems. [20]*

Remark. *Any non linear system in the general form $\dot{x} = \mathcal{G}(x,u,t)$ which has the origin as an equilibrium point can be written as 2.8 if $\mathcal{G}(x,u,t)$ is continuously differentiable with respect to x. [20]*

Conventional state observers for system 2.8 have generally the following structure [20] :

$$\dot{\hat{x}} = A\hat{x} + Bu + \Phi(\hat{x},u,t) + L(y - C\hat{x}) \tag{2.10}$$

The estimation error dynamic $\tilde{x} = x - \hat{x}$ is given by

$$\dot{\tilde{x}} = (A - LC)\tilde{x} + \tilde{\Phi} \tag{2.11}$$

where $\tilde{\Phi} = \Phi(x,u,t) - \Phi(\hat{x},u,t)$.
Subsequently, we need to determinate a gain L that allows the linear term in2.11 to dominate the non linear term $\tilde{\Phi}$ to guarantee the convergence of $\tilde{x}$ to the origin.
Obviously, the eigenvalues placement in the the left half plane isn't sufficient to guarantee the stability of 2.11, especially when the Lipschitz constant value reaches high values[20].
A sufficient and necessary condition for the stability of 2.8 is provided by the following theorem

Theorem 2.3.1. *[20] We consider the error system 2.11 with (C, A) as an observable pair and Φ satisfies 2.9. The error $\tilde{x}$ is asymptotically stable if the gain L can be chosen so that $(A - LC)$ is stable and*

$$\min_{\omega \geq 0}(\sigma_{\min}(A - LC - j\omega I_n)) > l_\Phi \tag{2.12}$$

2.3.3 The considered class of nonlinear systems

In the context of faults estimation and reconstruction using observers, the systems considered are usually linear or non-linear in the following form [24]

$$\begin{cases} \dot{x} = Ax + \Phi(x,u) + Ef \\ y = Cx \end{cases} \tag{2.13}$$

where $x \in \mathbb{R}^n$ is the state vector, $u \in \mathbb{R}^m$ the input vector, $y \in \mathbb{R}^p$ the output vector and $f \in \mathbb{R}^q$ an unknown vector that models the faults effect on the system.
$\Phi(x,u) : \mathbb{R}^n \times \mathbb{R}^m \rightarrow \mathbb{R}^n$ is a known non-linear function and $A \in \mathbb{R}^{n\times n}$, $B \in \mathbb{R}^{n\times m}$, $E \in \mathbb{R}^{n\times q}$ and $C \in \mathbb{R}^{n\times p}$ are constant matrices with $\text{rank}(C) = p$ and $\text{rank}(E) = q$.
We suppose that the pair (C, A) is observable or at least detectable and the non-linear function $\Phi(x,u)$ doesn't alter the system observability (detectability).

Hypothesis 2.1. *The input u and the faults vector f are bounded. Moreover, u ensures the x state boundness even in faulty mode.*

Hypothesis 2.2. *The function $\Phi(x,u)$ is lipschitzian with respect to x uniformly in u. i.e., there exists a known real constant $l_\Phi > 0$ so that*

$$\|\Phi(x,u) - \Phi(\hat{x},u)\| \leq l_\Phi \|x - \hat{x}\| \ (2.14)$$

Hypothesis 2.3. *The matrices E and C satisfy the following condition*

$$\text{rank}(CE) = \text{rank}(E) \tag{2.15}$$

Hypothesis 2.4. *the following equality*

$$rank(\begin{bmatrix} sI_n - A & -E \\ C & 0_{p\times q} \end{bmatrix}) = n + \text{rank}(E) \tag{2.16}$$

is satisfied $\forall s \in \mathbb{C}$ *such as* $\text{Re}(s) \geq 0$.

The hypothesis 2.3 is known as *the observer matching condition* [13]. This condition signifies that $\text{rank}(E) \leq \text{rank}(C)$ $(q \leq p)$ and that the faults appear only in the dynamics of q outputs. [21]
The hypothesis 2.4 is known as the *minimal phase condition* [24]. It indicates that all the invariant zeros of (A, E, C) have a negative real part. (for more details check [20])
It also ensures for the system 2.13, the detectability of x and f.

2.3.4 Adaptive state observer design

In this part, we recall some adaptive state observers and their error stability condition.

Conventional adaptive state observer

The adaptive state observer that corresponds to the system 2.13 is given by the equations [20]

$$\begin{cases} \dot{\hat{x}} = A\hat{x} + \Phi(\hat{x}, u) + E\hat{f} + L(y - C\hat{x}) \\ \dot{\hat{f}} = \Gamma F(y - C\hat{x}) \end{cases} \tag{2.17}$$

where $\hat{x}$ and $\hat{f}$ are the estimates of x and f respectively, $L \in \mathbb{R}^{n\times p}$ the observer gain, $F \in \mathbb{R}^{q\times p}$ a matrix to determinate and $\Gamma \in \mathbb{R}^{q\times q}$ a symmetric and positive definite matrix. From 2.13 and 2.17, the estimation error dynamics $\tilde{x} = x - \hat{x}$ and $\tilde{f} = f - \hat{f}$ are given by the following equations

$$\begin{cases} \dot{\tilde{x}} = (A - LC)\tilde{x} + \tilde{\Phi} + E\tilde{f} \\ \dot{\tilde{f}} = \dot{f} - \Gamma FC\tilde{x} \end{cases} \tag{2.18}$$

where $\tilde{\Phi} = \Phi(x, u) - \Phi(\hat{x}, u)$. The theorem below provides a sufficient condition for the asymptotic stability of the system 2.18. (for the demonstration or more details see demonstration of **theorem 2.1** in [29])

Theorem 2.3.2. *[20] If we consider the system 2.13 under the hypothesis 2.2-2.4 and the observer 2.17. If there are some real and positive constant ϵ and two matrices $P \in \mathbb{R}^{n\times n}$ symmetric and positive definite and $F \in \mathbb{R}^{q\times p}$ such that*

$$(A - LC)^T P + P(A - LC) + \epsilon^{-1}PP + \epsilon\Phi^2 I_n < 0 \tag{2.19}$$

$$E^T P = FC \tag{2.20}$$

then if $\dot{f} = 0$, the estimations errors $\tilde{x}$ and $\tilde{f}$ which dynamics are given by 2.18 are asymptotically stable.

the observer synthesis problem consists in determining the matrices L and F such that the inequality 2.19 is satisfied under the equality constraint 2.20.
In [20] a systematic method is proposed which consists in transforming 2.19 and 2.20 into a convex optimization problem formulated in terms of affine or linear matrix inequalities (LMI).
The LMI problem is in this case:
minimise η such that

$$\begin{bmatrix} \eta I_n & (E^T P - FC)^T \\ * & \eta I_q \end{bmatrix} \tag{2.21}$$

and

$$\begin{bmatrix} A^T P + PA - C^T M^T - MC + \epsilon l_\Phi^2 I_n & P \\ * & -\epsilon I_n \end{bmatrix} < 0 \tag{2.22}$$

with $L = P^{-1}M$.

Extension to sensor faults case

If we take into account only the case of sensor faults, the system 2.13 can be written into the form

$$\begin{cases} \dot{x} = Ax + \Phi(x, u) \\ y = Cx + E_s f_s \end{cases} \tag{2.23}$$

where the vector $f_s \in \mathbb{R}^s$ models the effect of sensor faults and $E_s \in \mathbb{R}^{p \times q_s}$ is its distribution matrix which is supposed to be a full rank matrix.
in [20] the problem of reconstruction of sensor faults is transformed into a problem of reconstruction of actuators faults. The following system is considered

$$\begin{cases} \dot{x}_s = -A_s x_s + A_s y \\ y_s = x_s \end{cases} \tag{2.24}$$

where $y_s \in \mathbb{R}^p$ and the matrix $A_s \in \mathbb{R}^{p \times p}$ is Hurwitz. The association of both systems 2.23 and 2.24 in a single system gives us

$$\begin{cases} \dot{\overline{x}} = \overline{A}\overline{x} + \overline{\Phi}(\overline{x}, u) + \overline{E} f_s \\ y_s = \overline{C}\overline{x} \end{cases} \tag{2.25}$$

where $\overline{x} = \begin{bmatrix} x \\ x_s \end{bmatrix}$, $\overline{A} = \begin{bmatrix} A & 0_{n \times p} \\ A_s C & -A_s \end{bmatrix}$, $\overline{\Phi}(\overline{x}, u) = \begin{bmatrix} \Phi(x, u) \\ 0_{p \times 1} \end{bmatrix}$, $\overline{E} = \begin{bmatrix} 0_{n \times s} \\ E_s \end{bmatrix}$, $\overline{C} = \begin{bmatrix} 0_{p \times n} & I_p \end{bmatrix}$.

In [20] it is shown that system 2.25 also satisfies the hypotheses 2.3 and 2.4, which means that the state observation and fault estimation is also possible for this one.

Fast fault estimation observer design

The fast fault estimation observer was developed to compensate the weakness of adaptive state observers to give precise estimates of time-varying faults. Its basic concept consists in using an adaptation law which can be qualified as a proportional derivative to improve the fault estimation dynamic. [20]
Let's state first the following hypothesis

Hypothesis 2.5. *the time derivative of the fault vector satisfies the following condition*

$$\left\|\dot{f}\right\| \leq \gamma \tag{2.26}$$

where γ is a known positive constant.

The fast fault estimation observer that corresponds to the system 2.13 is given by the equations [20]

$$\begin{cases} \dot{\hat{x}} = A\hat{x} + \Phi(\hat{x}, u) + E\hat{f} + L(y - C\hat{x}) \\ \dot{\hat{f}} = \Gamma F(\sigma(y - C\hat{x}) + \dot{y} - C\dot{x}) \end{cases} \tag{2.27}$$

where σ is a positive constant. From 2.13 and 2.27, the estimation error dynamics $\tilde{x}$ and $\tilde{f}$ are described by the following equations

$$\begin{cases} \dot{\tilde{x}} = (A - LC)\tilde{x} + \tilde{\Phi} + E\tilde{f} \\ \dot{\tilde{f}} = \dot{f} - \Gamma F(\sigma C\tilde{x} + C\dot{\tilde{x}}) \end{cases} \tag{2.28}$$

where $\tilde{\Phi} = \Phi(x, u) - \Phi(\hat{x}, u)$.
The time derivative of the output signal presents a serious issue for its evaluation when the output is submitted to noises. [20]
Because of this, the adaptive law (the second equation in 2.27) can be implemented in the following form

$$\begin{cases} \hat{f} = \Gamma F(w + y - C\hat{x}) \\ \dot{w} = \sigma(y - C\hat{x}) \end{cases} \tag{2.29}$$

The stability analysis in [20] has given the following theorem

Theorem 2.3.3. *[20] We consider the system 2.13 under hypotheses 2.1-2.5 and the observer 2.27.*
If there are two positive constants ϵ_1 and ϵ and two matrices $P \in \mathbb{R}^{n\times n}$ symmetric and positive definite and $F \in \mathbb{R}^{q\times p}$ such that

$$\begin{bmatrix} (A - LC)^T P + P(A - LC) + l_\Phi^2 \epsilon_1 I_n & P & \sigma^{-1}(A - LC)^T PE \\ * & -\epsilon_1 I_n & \sigma^{-1} PE \\ * & * & \sigma^{-1}(\epsilon I_n - 2E^T PE) \end{bmatrix} < 0 \tag{2.30}$$

$$E^T P = FC \tag{2.31}$$

then the errors $\tilde{x}$ and $\tilde{f}$ given by 2.28 converge to some neighborhood around the origin.In addition, if $\dot{f} = 0$, then $\tilde{x}$ and $\tilde{f}$ converge asymptotically to zero.

To compute the observer gains,the LMI problem to solve is as follows[20]

$$\begin{bmatrix} A^T P + PA - C^T M^T - MC + l_\Phi^2 \epsilon_1 I_n & P & \sigma^{-1}(PA - MC)^T \\ * & -\epsilon_1 I_n & \sigma^{-1} PE \\ * & * & \sigma^{-1}(\epsilon I_n - 2E^T PE) \end{bmatrix} < 0 \tag{2.32}$$

With $L = P^{-1}M$.

Conventional PI observer design

In addition to the proportional correction term, the PI observer uses an integral correction term which cancels the bias in the state estimation error caused by the model imperfections. [20]
The conventional PI observer that corresponds to the system 2.13 is given by [20]

$$\dot{\hat{x}} = A\hat{x} + \Phi(\hat{x}, u) + E\int_0^t L_2(y - C\hat{x})dt + L_1(y - C\hat{x}) \tag{2.33}$$

Taking $\hat{f} = \int_0^t L_2(y - C\hat{x})dt$, we can rewrite 2.33 into the following form

$$\begin{cases} \dot{\hat{x}} = A\hat{x} + \Phi(\hat{x}, u) + E\hat{f} + L_1(y - C\hat{x}) \\ \dot{\hat{f}} = L_2(y - C\hat{x}) \end{cases} \tag{2.34}$$

Let's put the observer 2.34 in the form

$$\dot{\hat{\mathcal{X}}} = \mathcal{A}\hat{\mathcal{X}} + \Phi(\hat{\mathcal{X}}, u) + \mathcal{L}(y - \mathcal{C}\hat{\mathcal{X}}) \tag{2.35}$$

where

$$\hat{\mathcal{X}} = \begin{bmatrix} \hat{x} \\ \hat{f} \end{bmatrix}, \mathcal{A} = \begin{bmatrix} A & E \\ 0_{q\times n} & 0_{q\times q} \end{bmatrix}, \mathcal{C} = \begin{bmatrix} C & 0_{p\times q} \end{bmatrix}, \Phi(\hat{\mathcal{X}}, u) = \begin{bmatrix} \Phi(\hat{x}, u) \\ 0_{q\times 1} \end{bmatrix}, \mathcal{L} = \begin{bmatrix} L_1 \\ L_2 \end{bmatrix}$$

Let $\tilde{\mathcal{X}} = \mathcal{X} - \hat{\mathcal{X}}$ where $\mathcal{X} = \begin{bmatrix} x^T & f^T \end{bmatrix}^T$ and suppose that $\dot{f} = 0$. The error dynamic equation $\tilde{\mathcal{X}}$ is obtained by subtracting 2.35 from 2.13:

$$\dot{\tilde{\mathcal{X}}} = (\mathcal{A} - \mathcal{L}\mathcal{C})\tilde{\mathcal{X}} + \tilde{\Phi} \tag{2.36}$$

where $\tilde{\Phi} = \Phi(\mathcal{X}, u) - \Phi(\hat{\mathcal{X}}, u)$. Subsequently, the synthesis of the observer 2.33 is only possible if the pair $(\mathcal{C}, \mathcal{A})$ is at least detectable. (**lemme2.3** in[20] gives a condition that ensures the detectability of the pair$(\mathcal{C}, \mathcal{A})$)
the following theorem ensures the stability of the observer 2.35.

Theorem 2.3.4. *[20] Let the system 2.13 under hypotheses 2.1 2.2 and 2.4 and the observer 2.35. For $\dot{f} = 0$, the estimation error of the augmented state $\tilde{\mathcal{X}}$ given by 2.36 is asymptotically stable if there are a real positive constant ϵ and two matrices $\mathcal{P} \in \mathbb{R}^{(n+q)\times(n+q)}$ symmetric and positive definite, and $\mathcal{M} \in \mathbb{R}^{(n+q)\times p}$ such that*

$$\begin{bmatrix} \mathcal{A}^T\mathcal{P} + \mathcal{P}\mathcal{A} - \mathcal{C}^T\mathcal{M}^T - \mathcal{C} + \epsilon l_\Phi^2 I_{n+q} & \mathcal{P} \\ * & -\epsilon I_{n+q} \end{bmatrix} < 0 \tag{2.37}$$

Once this problem solved, the observer gain is computed as follows

$$\mathcal{L} = \mathcal{P}^{-1}\mathcal{M} \tag{2.38}$$

PI H_∞ observer design

In this part, the H_∞ filtering has been combined with the PI observer to improve its performances when $\dot{f} \neq 0$. First, we state the following hypothesis

Hypothesis 2.6. *the function $\dot{f}$ has a finite energy,i.e.*

$$\int_0^\infty \dot{f}^T \dot{f} dt < \infty \tag{2.39}$$

We consider now the equation 2.36 which expresses the dynamic of the augmented estimation error. In the case where $\dot{f} \neq 0$, this equation becomes

$$\dot{\tilde{\mathcal{X}}} = (\mathcal{A} - \mathcal{L}\mathcal{C})\tilde{\mathcal{X}} + \tilde{\Phi} + \mathcal{E}\dot{f} \tag{2.40}$$

where $\mathcal{E} = \begin{bmatrix} 0_{q\times n} & I_q \end{bmatrix}^T$. The idea here, is to use the H_∞ filtering techniques to compute the observer gain $\mathcal{L}$ such that the following conditions are satisfied

$$\lim_{t\to\infty} \tilde{\mathcal{X}} = 0 \qquad \text{for} \quad \dot{f} = 0 \tag{2.41}$$

$$\int_0^\infty \tilde{\mathcal{X}}^T \mathcal{D} \tilde{\mathcal{X}} dt < \lambda \int_0^\infty \dot{f}^T \dot{f} dt \qquad \text{for} \quad \dot{f} \neq 0 \tag{2.42}$$

where λ is a positive constant and $\mathcal{D}$ a symmetric semi-positive definite matrix.

Theorem 2.3.5. *[20] Let the system 2.13 under hypotheses 2.1, 2.2 and 2.4 and the observer 2.35.*
If there are two real positive constants ϵ and λ and two matrices $\mathcal{P} \in \mathbb{R}^{(n+q)\times(n+q)}$ symmetric and positive definite, and $\mathcal{M} \in \mathbb{R}^{(n+q)\times p}$ such that

$$\begin{bmatrix} \mathcal{A}^T\mathcal{P} + \mathcal{P}\mathcal{A} - \mathcal{C}^T\mathcal{M}^T - \mathcal{M}\mathcal{C} + \epsilon l_\Phi^2 I_{n+q} + \mathcal{D} & \mathcal{P} & \mathcal{P}\mathcal{E} \\ * & -\epsilon I_{n+q} & 0_{(n+q)\times q} \\ * & * & -\lambda I_q \end{bmatrix} < 0 \tag{2.43}$$

where $\mathcal{D}$ is defined in accordance to 2.42, then the estimation error of the augmented state $\tilde{\mathcal{X}}$ given by 2.36 satisfies the conditions 2.41 and 2.42.

to gain an optimal precision in the estimation of x and f, the LMI problem 2.43 can be turned into the following LMI optimisation problem: [20]
Minimise λ such that

$$\begin{bmatrix} \mathcal{A}^T\mathcal{P} + \mathcal{P}\mathcal{A} - \mathcal{C}^T\mathcal{M}^T - \mathcal{M}\mathcal{C} + \epsilon l_\Phi^2 I_{n+q} + \mathcal{D} & \mathcal{P} & \mathcal{P}\mathcal{E} \\ * & -\epsilon I_{n+q} & 0_{(n+q)\times q} \\ * & * & -\lambda I_q \end{bmatrix} \tag{2.44}$$

2.3.5 Simulation example

Let's consider the flexible link arm 2.4 with an additive fault that corresponds to an abnormal viscous friction increase. The system satisfies the hypotheses 2.2-2.4. The system parameters values are: $J_m = 0.037(Kgm^2)$, $J_t = 0.093(Kgm^2)$, $k = 0.18(Nm/rad)$, $b = 0.0083(Nms/rad)$, $m = 0.21(Kg)$, $g = 9.81(m/s^2)$, $h = 0.15(m)$ and $k_\tau = 0.18(Nm/V)$.[20] The fundamental matrix of the system and the non-linear term are written in the following form [20]

$$A = \begin{bmatrix} 0 & 1 & 0 & 0 \\ -\frac{k}{J_m} & -\frac{b}{J_m} & \frac{k}{J_m} & 0 \\ 0 & 0 & -1 & 1 \\ \frac{k}{J_t} & 0 & -\frac{k}{J_t} & -1 \end{bmatrix}, \Phi(x,u) = \begin{bmatrix} 0 \\ \frac{k_\tau}{J_m}u \\ x_3 \\ \frac{-mgh}{J_t}\sin(x_3) + x_4 \end{bmatrix}$$

The observer gains computed in [20] are :

$$L = \begin{bmatrix} 1.1147 & -0 \\ -0.4321 & 1.7916 \\ -0 & 0.9284 \\ 1.9355 & -0.1921 \end{bmatrix}, F = \begin{bmatrix} 0 & -0.5426 \end{bmatrix}, \Gamma = 5$$

$$L = \begin{bmatrix} 1.7541 & 1.000 \\ -4.8649 & 3.8242 \\ 0.0000 & 0.9680 \\ 1.9355 & -0.4150 \end{bmatrix}, F = \begin{bmatrix} 0.0000 & -0.3776 \end{bmatrix}, \Gamma = 5, \sigma = 50$$

$$\mathcal{L} = \begin{bmatrix} 6.0856 & 0.9930 \\ -0.6767 & 29.0253 \\ -0.1668 & -0.7119 \\ 2.0227 & 2.1366 \\ -05349 & -15.6266 \end{bmatrix}$$

The simulation is run with following fault scenario

$$f = \begin{cases} 0 & \text{if } t < 5\text{s}, \\ 0.1 & \text{if } 5\text{s} \le t < 5.2\text{s}, \\ 0 & \text{if } 5.2\text{s} \le t < 7\text{s}, \\ 0.1 & \text{if } 7\text{s} \le t < 10\text{s}, \\ 0.1\sin(2t)cos((t-10)^2) & \text{if } 10\text{s} \le t. \end{cases}$$

The initial conditions are chosen to be $x = \begin{bmatrix} -0.5 & 0.5 & 0 & 0 \end{bmatrix}^T$.

The results obtained are:

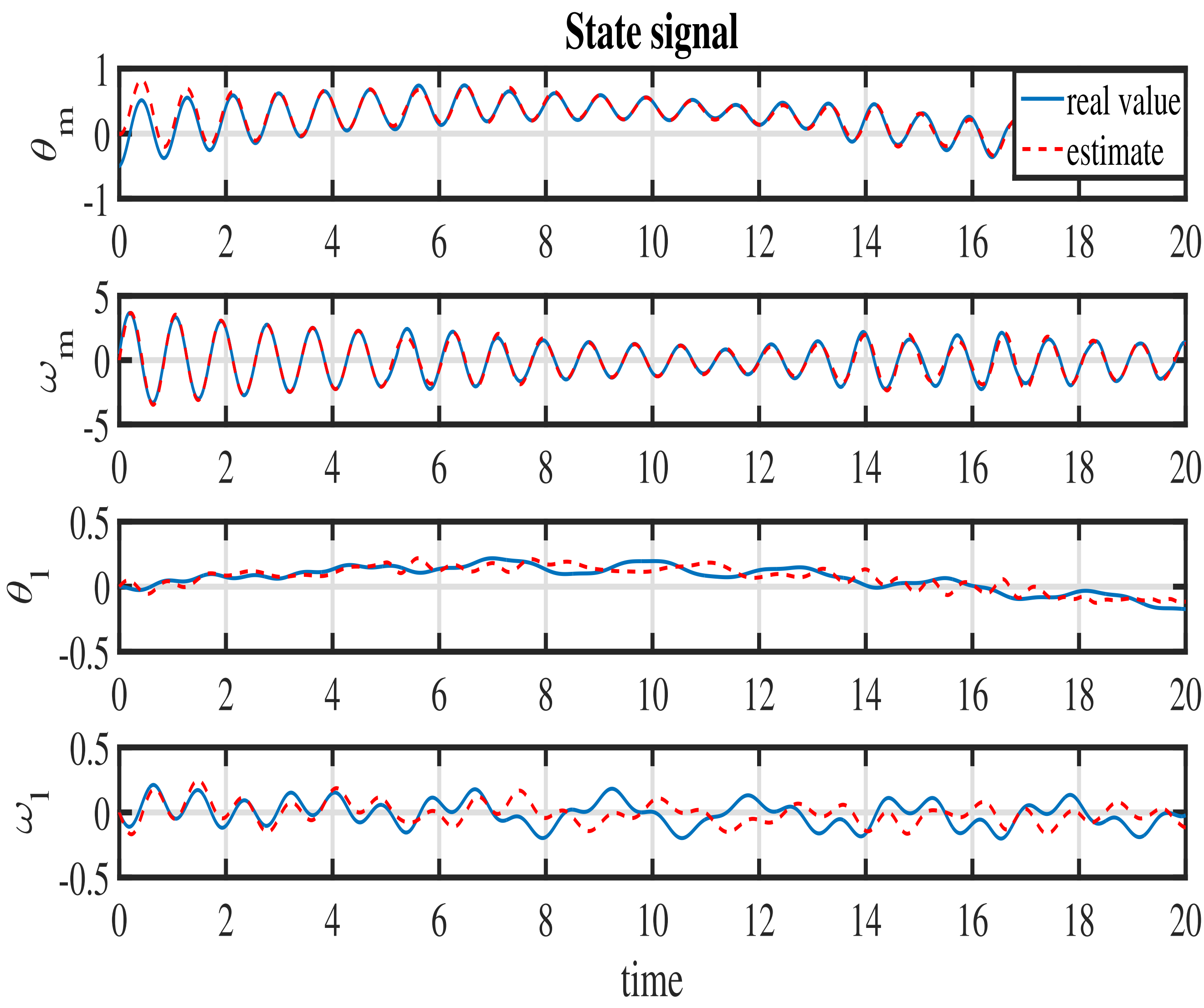

Figure 2.3: Conventional adaptive observer state estimation

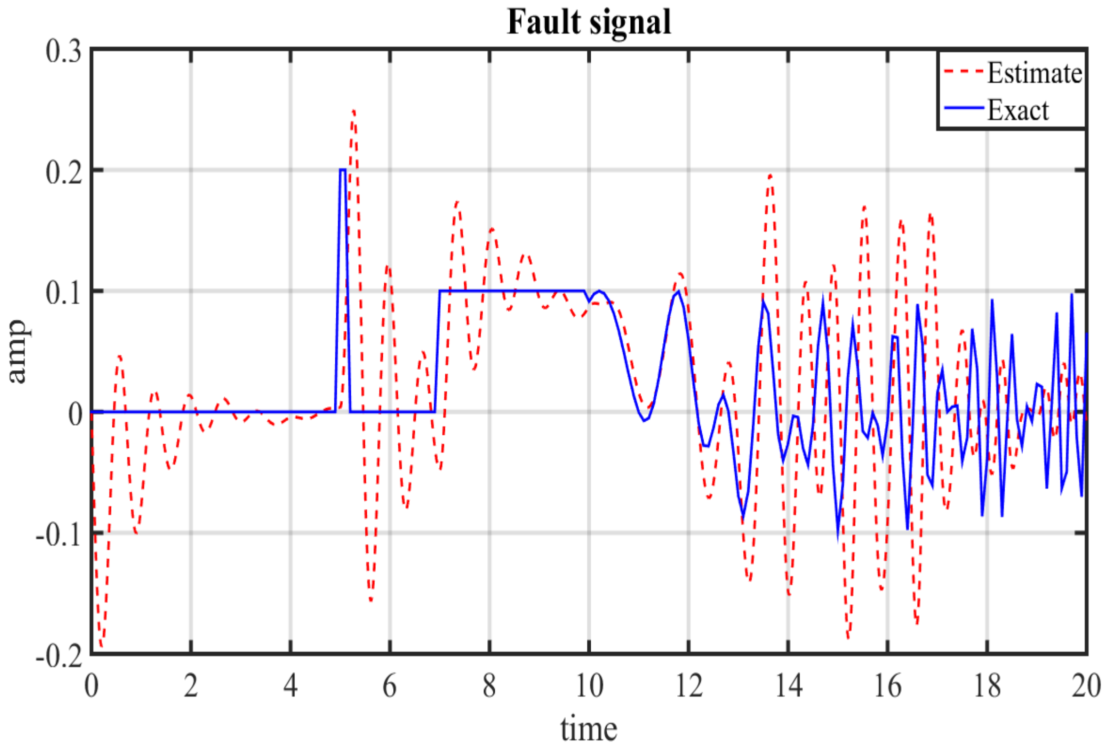

Figure 2.4: Conventional adaptive observer fault estimation

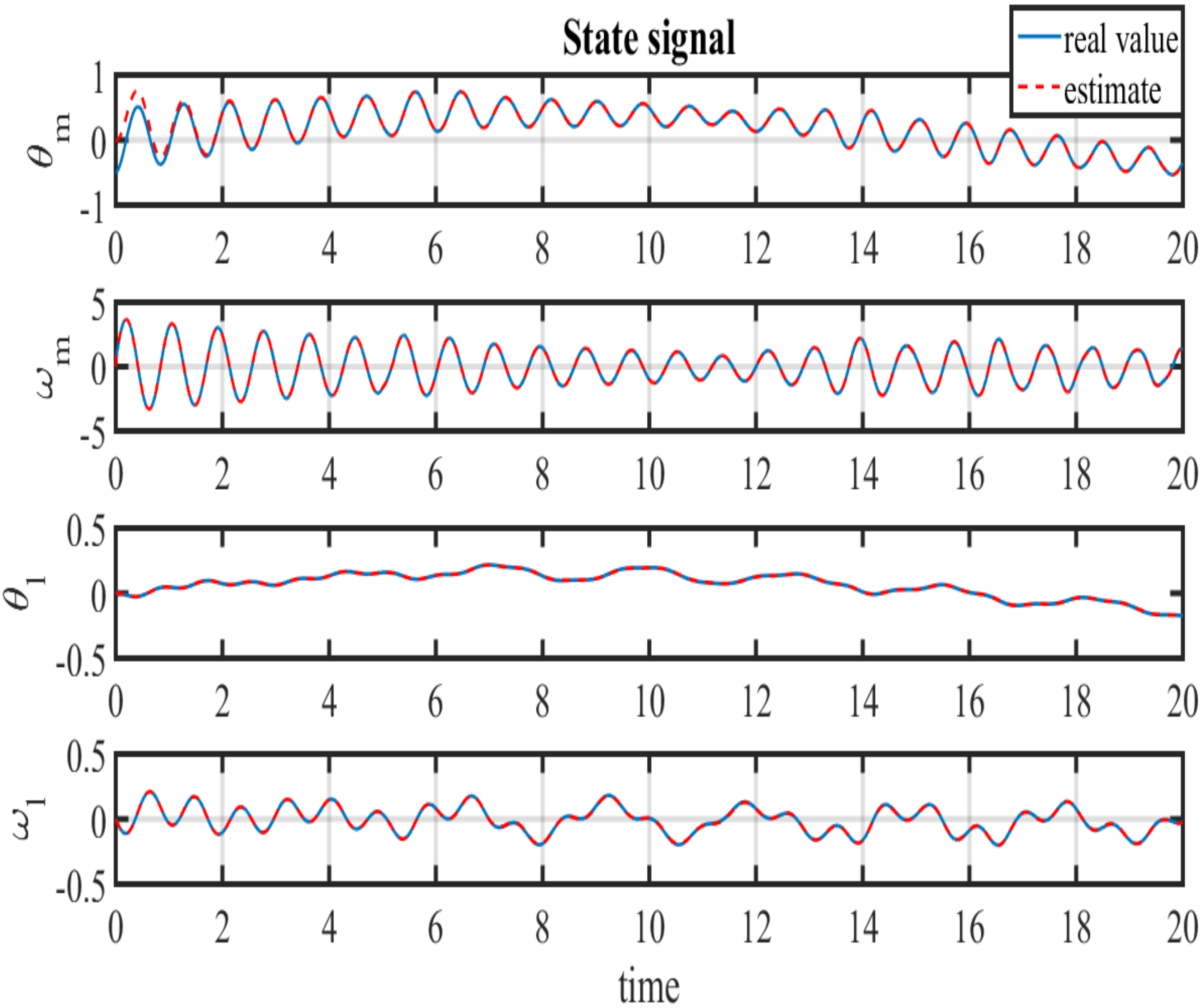

Figure 2.5: Fast fault estimation observer state estimation

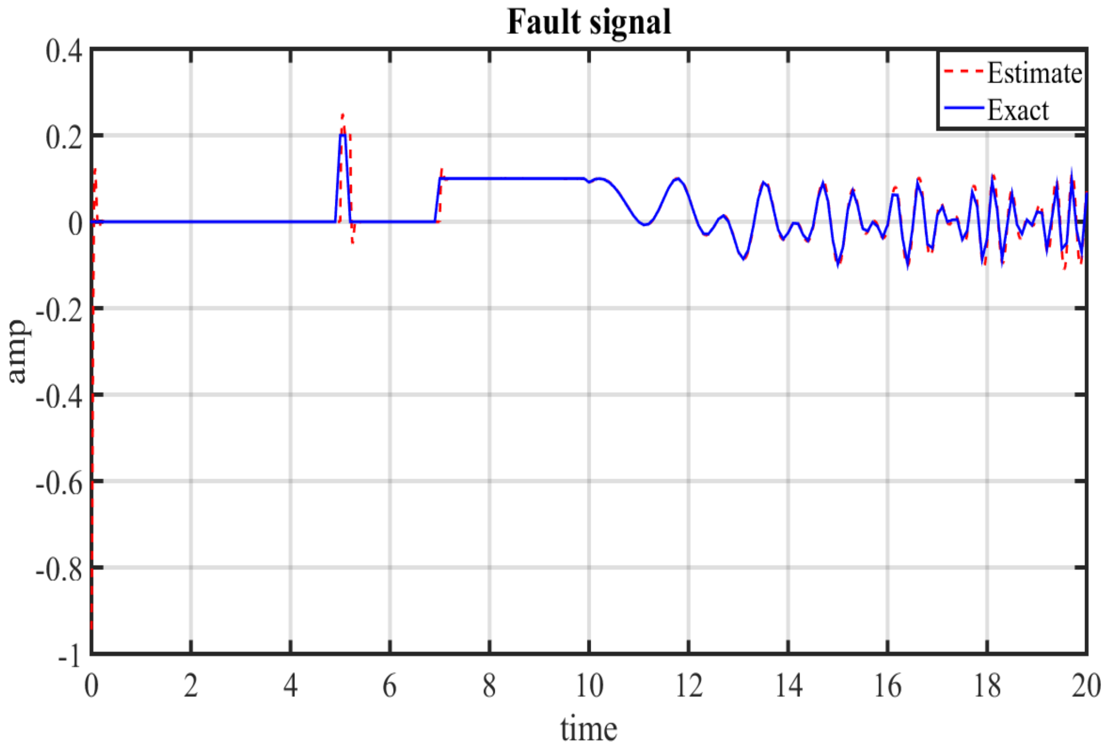

Figure 2.6: Fast fault estimation observer fault estimation

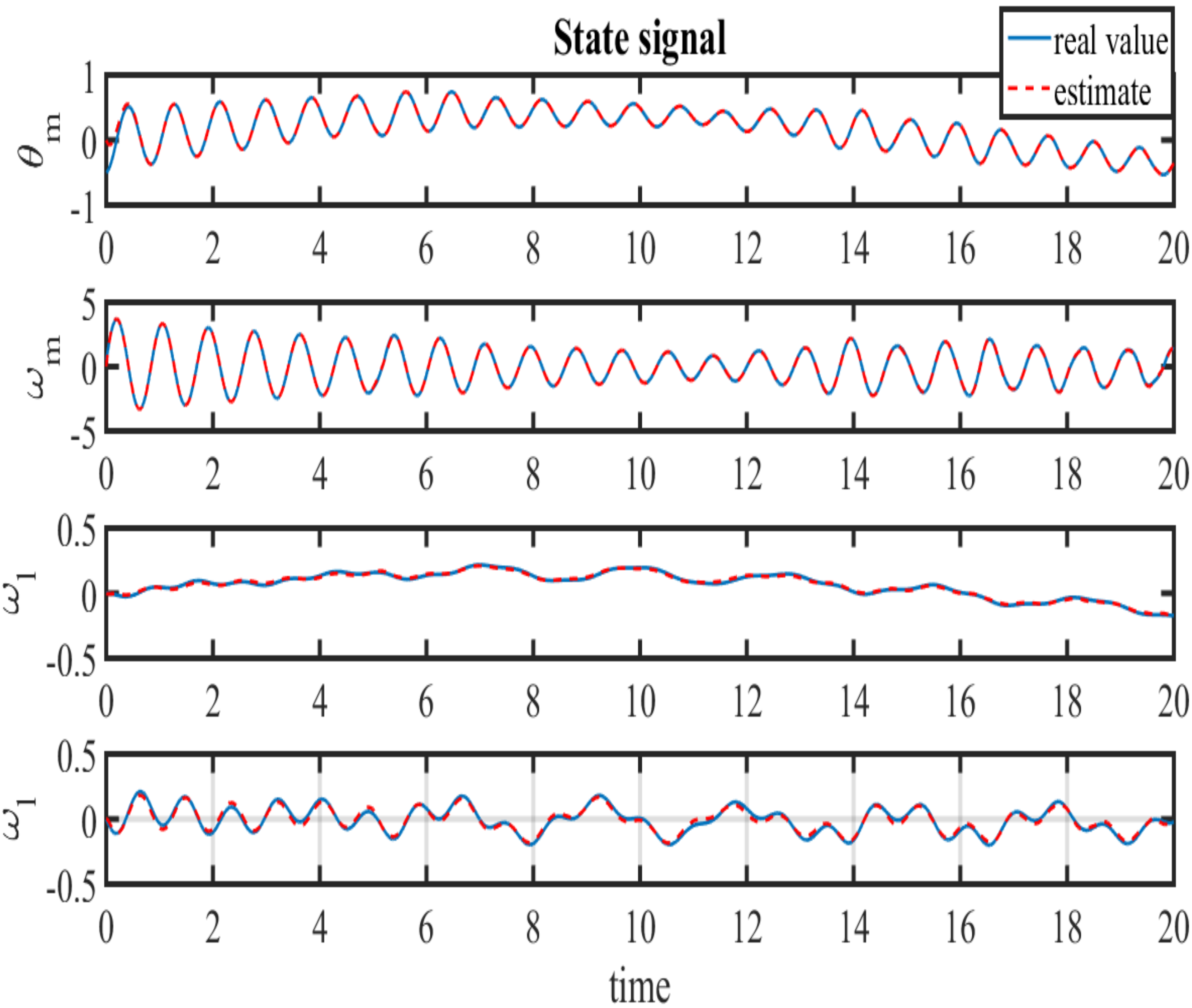

Figure 2.7: PI H_∞ observer state estimation

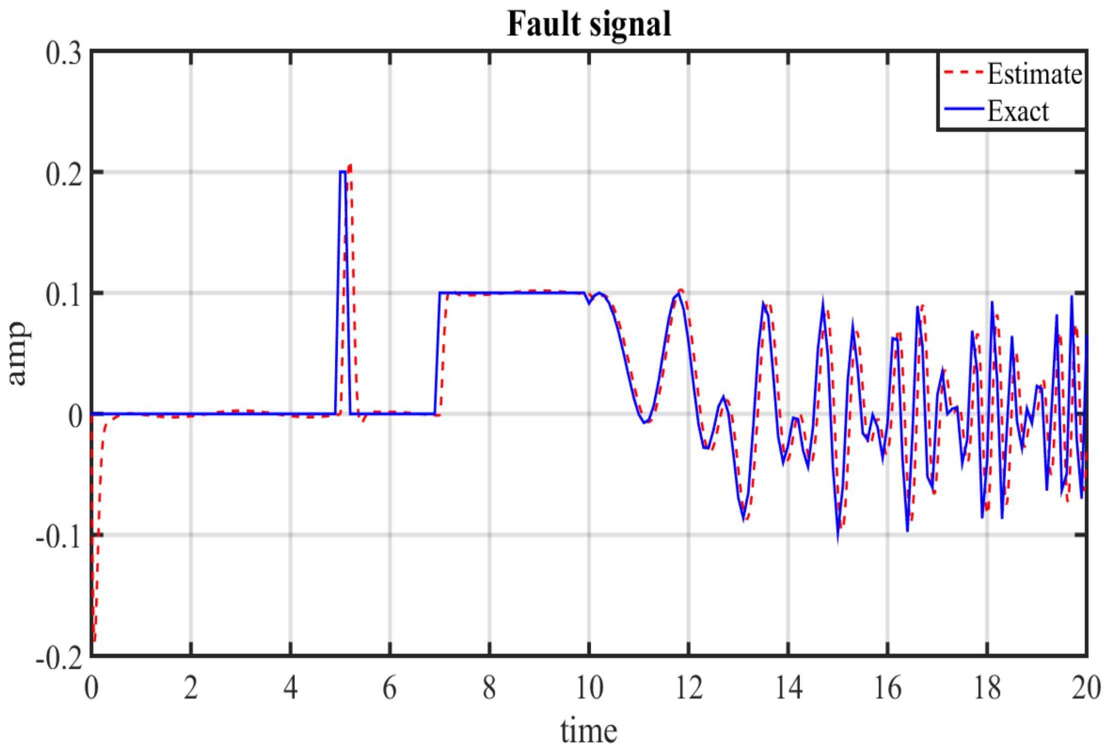

Figure 2.8: PI H_∞ observer fault estimation

2.4 Conclusion

This chapter gives an overview of observer based fault estimation and diagnosis.
First, we recalled definitions and notions related to model based fault diagnosis. We presented after that the adaptive nonlinear state observers for Lipschitzian systems. We ended this chapter by running a simulation example where we tested each observer on a nonlinear system.
Simulation results show that these observers represent an effective estimation strategy for fault diagnosis on the systems considered in this chapter.
To have similar observers to diagnose faults on time scale systems would be useful for any situation where time scale behavior results from a system component fault or sensor fault scenario likely to happen. For this reason we will try to generalize the fast fault observer and the PI observer to time scales in the next chapter.

CHAPTER 3

Time Scale Observer Design

3.1 Introduction

This chapter presents the filtering theory and design of observers for time scale systems.
At first, we will present the Kalman filter on time scales introduced in [6]. We'll add a fault estimation feature to this observer on the basis of what has been developed in the previous chapter (i.e. chapter 2) and extend the *Discrete* version of the Extended Kalman Filter to time scales.
After that, we study the observer based control for time scale systems and highlight the impact of graininess increase on systems robustness, we also discuss the LTR case for these systems.
At last, we will also extend the three adaptive observers introduced in the previous chapter (chapter 2) by extending theorems 2.3.3, 2.3.4 and 2.3.5 to the general arbitrary time scale case.

3.2 Kalman filter on time scales

In this section, we introduce the Kalman filter for linear systems on time scales.When the system is stochastic, the Kalman filter is an observer that estimates the system when it is corrupted by noisy measurements.

3.2.1 Time scale Kalman filter equations

We consider the linear stochastic system

$$\begin{cases} x^{\Delta}(t) = Ax(t) + Bu(t) + G\omega(t), \qquad x(t_0) = x_0, \\ y(t) = Cx(t) + v(t), \end{cases} \tag{3.1}$$

where $x \in \mathbb{R}^n$ represents the state, $u \in \mathbb{R}^m$ is a known input, $y \in \mathbb{R}^p$ represents the measurement, $\omega \in \mathbb{R}^l$ is the process noise, and $v \in \mathbb{R}^p$ is the measurement noise.
The state x is a nonstationary random variable with mean $\overline{x}$ and covariance $P_x = E\left[(x-\overline{x})(x-\overline{x})^T\right]$, the input u is deterministic, the output y is a non stationary random variable with mean $\overline{y}$ and covariance $P_y = E\left[(y-\overline{y})(y-\overline{y})^T\right]$, the process noise ω is a stationary white noise with mean 0 and covariance $E\left[\omega(t)\omega^T(s)\right] = Q\delta(t,s)$, the measurement noise v is a stationary white noise with mean 0 and covariance $E\left[v(t)v^T(s)\right] = R\delta(t,s)$.
x_0, ω and v are assumed to be mutually uncorrelated, $P(t_0) = P_0$, Q and R are all positive definite.
In this case it's important to find a filter that rejects the noise and retains the relevant data.
Therefore, we're looking for an accurate estimate of the true state in addition to the smallest possible mean square error. Which means finding an estimate $\hat{x}$ such that $\hat{x}$ satisfies

the observer equation

$$\hat{x}^{\Delta}(t) = A\hat{x}(t) + Bu(t) + K(t)\left[y(t) - C\hat{x}(t)\right], \qquad \hat{x}(t_0) = \overline{x}(t_0) \tag{3.2}$$

where $\overline{x}$ is the expected value of our true state and K represents the Kalman gain.
In this section the following hypotheses are made.

Hypothesis 3.1. *a. The true state and the estimate state belong to the same time scale.*

b. The state and measurement are Gaussian.

c. The state measurement is being updated in "real-time". In other words, there is a measurement at the next available point in the time scale.

d. The error covariance of our hybrid filter is found through the integrator just as it is for the Kalman-Bucy filter.

e. There exists a term $\delta(.,.)$ such that

$$\int_{t_0}^{t_f}\int_{t_0}^{t_f} x^T(\tau_1)Q\delta(\tau_1,\tau_2)x(\tau_2)\Delta\tau_1\Delta\tau_2 = \int_{t_0}^{t_f} x^T(\tau)Qx(\tau)\Delta\tau. \tag{3.3}$$

If x is the state of the system 3.1 and satisfies the hypotheses 3.1 and $\hat{x}$ solves 3.2, the state error $\tilde{x} = x - \hat{x}$ satisfies

$$\tilde{x}^{\Delta}(t) = M(t)\tilde{x}(t) + G\omega(t) - K(t)v(t), \tag{3.4}$$

where $M(t) = A - K(t)C$. (see **Lemma 3.11** in [6])
This leads to announce the the following theorem.

Theorem 3.2.1. *[6] The covariance of the solution of 3.4 is given by*

$$\begin{aligned} P(t) = e_M(t,t_0)\Bigg[P_0 + \int_{t_0}^{t} e_M(t_0,\sigma(\tau))GQG^T e_M^T(t_0,\sigma(\tau))\Delta\tau + \\ \int_{t_0}^{t} e_M(t_0,\sigma(\tau))K(\tau)RK^T(\tau)e_M^T(t_0,\sigma(\tau))\Delta\tau e_M^T(t,t_0). \end{aligned} \tag{3.5}$$

P given by 3.5 satisfies the following equation

$$P^{\Delta} = AP + (I+\mu A)PA^T + K\left[R + \mu CPC^T\right]K^T - K\left[CP + \mu CPA^T\right] - \left[\mu APC^T + PC^T\right]K^T + GQG^T.. \tag{3.6}$$

Definition 3.2.1. *[6] Assume that $R + \mu CPC^T > 0$. Then we define the Kalman gain by*

$$K(t) = (I + \mu(t)A)P(t)C^T(R + \mu(t)CP(t)C^T)^{-1}. \tag{3.7}$$

Now that the Kalman gain is in the form 3.7, it is possible to write the error propagation as a Riccati equation. [6]

Theorem 3.2.2. *[6] Assume that $R + \mu CPC^T > 0$ and define K by 3.7. Then P solves 3.5 if and only if*

$$P^{\Delta} = AP + (I + \mu A)PA^T - (I + \mu A)PC^T(R + \mu CPC^T)^{-1}CP(I + \mu A^T) + GQG^T. \quad (3.8)$$

Remark. *In [22] an other interesting contribution was provided to this topic. A Kalman filter has been developed where the measurement-update and time-update equations account for the size of the time step of a randomly generated time scale.*

3.2.2 Fault estimation feature

The purpose here is to design a Kalman filter that can diagnose faults in addition to the signal estimation and mean square error minimisation.
To design such a filter we go back to observers introduced the chapter 2, and try to adapt the proportional integral observer to time scales linear systems exposed to noises.
In, this part we consider the system 3.1 with some additive faults:

$$\begin{cases} x^{\Delta}(t) = Ax(t) + Bu(t) + Ef(t) + G\omega(t), \\ y(t) = Cx(t) + v(t), \end{cases} \quad (3.9)$$

where $f \in \mathbb{R}^q$ and $E \in \mathbb{R}^{n \times q}$. Let assume the following hypotheses about E and f.

Hypothesis 3.2. *The E matrix only contains rows of zeros and ones.*

Hypothesis 3.3. *The faults signals act in a low and limited frequency band.*

Hypothesis 3.4. *The fault signal to noise ratio is high enough to distinguish the faults impact from the noise impact.*

The hypothesis 3.4 is important as it allows to distinguish the faults effect from the noise effect on the measurements.
We can announce the following theorem.

Theorem 3.2.3. *Consider the system 3.9 and assume that hypotheses 3.2 to 3.4 hold. The state and fault signals can be accurately estimated by the observer*

$$\begin{cases} \hat{x}^{\Delta}(t) = A\hat{x}(t) + Bu(t) + E\hat{f}(t) + L_1(y(t) - C\hat{x}(t)), \\ \hat{f}^{\Delta}(t) = L_2(y(t) - C\hat{x}(t)), \end{cases} \quad (3.10)$$

where $\mathcal{K}(t) = \begin{bmatrix} L_1(t) \\ L_2(t) \end{bmatrix} = (I + \mu(t)\mathcal{A})P(t)\mathcal{C}^T(R + \mu(t)\mathcal{C}P(t)\mathcal{C}^T)^{-1}$,

$\mathcal{A} = \begin{bmatrix} A & E \\ 0 & 0 \end{bmatrix}$, $\mathcal{C} = \begin{bmatrix} C & 0 \end{bmatrix}$ *and* P *solves the equation 3.5.*

If the pair $[\mathcal{C}, \mathcal{A}]$ *is observable.*

Proof. Let's take the observer described by 2.34 and apply for the linear system 3.9 (in this case we take $\Phi(x, u) = Bu$) We obtain the equation 3.10. Let's consider now the augmented systems of both 3.9 and 3.10 we obtain

$$\begin{cases} \xi^\Delta = \mathcal{A}\xi + \mathcal{B}u + \mathcal{G}\Omega, \\ y = \mathcal{C}\xi + v, \end{cases}$$

and

$$\hat{\xi}^\Delta = \mathcal{A}\hat{\xi} + \mathcal{B}u + \mathcal{K}(t)(y - \mathcal{C}\hat{\xi})$$

where $\xi = \begin{bmatrix} x^T & f^T \end{bmatrix}^T$, $\hat{\xi} = \begin{bmatrix} \hat{x}^T & \hat{f}^T \end{bmatrix}^T$, $\mathcal{G} = \begin{bmatrix} G & 0 \\ 0 & 0 \end{bmatrix}$, $\Omega = \begin{bmatrix} \omega \\ 0 \end{bmatrix}$.

$\mathcal{A}$, $\mathcal{B}$, $\mathcal{C}$ and $\mathcal{K}$ are as stated in theorem 3.2.3. We can notice that the equation 3.2.2 is the same observer as 3.2 for the system 3.2.2.
Subsequently we deduce that theorems 3.4 and 3.2.2 are applicable to observer 3.2.2 provided the system 3.2.2 is observable. Moreover, we have chosen the observer 2.34 for its ability to reject noise easily. □

Remark. *Hypotheses 3.2 and 3.3 ensures that* $\tilde{f}^T\tilde{f}^\Delta$ *is negative.*

Let us find now some condition on the graininess μ that ensures the convergence of $\tilde{f}$ to the origin. Let's consider the Lyapunov function $V(t) = \frac{1}{2}\tilde{f}^T\tilde{f}$ where $\tilde{f} = f - \hat{f}$ and derive it using *iv*) and considering Hypothesis 3.3 (i.e. $f^\Delta \approx 0$) in theorem 1.2.1 and *iii*) in theorem 1.2.2 we obtain

$$V^\Delta(t) = \frac{1}{2}\left[-\hat{f}^{\Delta T}\tilde{f} - \tilde{f}^T\hat{f}^\Delta + \mu(t)\hat{f}^{\Delta T}\hat{f}^\Delta\right]. \tag{3.11}$$

A sufficient condition that guarantees the negativity of $V^\Delta(t)$ is

$$\mu(t) < \frac{2\tilde{f}^T\hat{f}^\Delta}{\hat{f}^{\Delta T}\hat{f}^\Delta}.$$

Remark. *If we assume that* $\left\|\hat{f}^\Delta\right\| > \lambda$ *and* $\left\|\tilde{f}\right\| < \gamma$ *then we'll obtain*

$$\mu(t) < \frac{\gamma}{\lambda}$$

From the remark above we deduce that the slower the fault estimation is, the more stable is the filter. In the case where $f^\Delta = 0$ the estimation doesn't vary in time which implies it cannot diverge even if the graininess takes very high values which is trivial.

3.3 Extended Kalman filter for time scale systems

The *Extended Kalman Filter* is the nonlinear version of the Kalman filter. It allows the estimation and prediction of observable states of non linear systems by linearizing around the different prediction points and applying the classical Kalman filter.
This filter is very famous and is largely applied in various fields to perform estimation and state prediction.For this reason, it would be appreciable to have a generalized version to time scale systems.
In this section we will generalize the *Discrete Time* Extended Kalman filter introduced in [30] to time scale systems and give a proof of its stochastic stability.

3.3.1 Time scale extended Kalman filter equations

We consider the non linear time scale stochastic system described by the following equation and observation model with additive noise

$$\begin{cases} x^{\Delta}(t) = f(x(t), u(t)) + G\omega(t), \\ y(t) = h(x(t)) + Dv(t), \end{cases} \tag{3.12}$$

where $x \in \mathbb{R}^n$ is the state vector, $u \in \mathbb{R}^m$ is the input signal, $y \in \mathbb{R}^p$ is the measured signal, $t \in \mathbb{T}$. The functions f and h are assumed to be C^1 class functions.
$\omega \in \mathbb{R}^l$ and $v \in \mathbb{R}^k$ are uncorrelated zero-mean white noise processes with identity covariance matrix. $G \in \mathbb{R}^{n\times l}$ and $D \in \mathbb{R}^{p\times k}$. We consider a constant initial condition x_0 with probability one.

Hypothesis 3.5. *the times scale $\mathbb{T}$ has a bounded graininess.*

We introduce the following state estimator for the system 3.12

$$\hat{x}^{\Delta} = f(\hat{x}, u) + K(t)(y - h(\hat{x})). \tag{3.13}$$

where the observer gain $K(t)$ is a matrix-valued stochastic process of size $p \times n$.
Because f and h are C^1-functions, they can be expanded via

$$f(x, u) - f(\hat{x}, u) = A_t(x - \hat{x}) + \varphi(x, \hat{x}, u), \tag{3.14}$$

and

$$h(x) - h(\hat{x}) = C_t(x - \hat{x}) + \chi(x, \hat{x}), \tag{3.15}$$

with a $n \times n$ matrix-valued stochastic process A_t and $p \times q$ matrix-valued stochastic process C_t given by

$$A_t = \frac{\partial f}{\partial x}(\hat{x}, u), \tag{3.16}$$

and

$$C_t = \frac{\partial h}{\partial x}(\hat{x}), \tag{3.17}$$

respectively.

Definition 3.3.1. *A time scale extended Kalman filter is given by the coupled equations:*

- *The delta differential equation 3.13 for the estimate.*
- *The linearization equations 3.16 and 3.17.*
- *the Riccati delta differential equation given by 3.2.2.*
- *The Kalman gain given by 3.7.*

Remark. *The usual choice for the matrices Q and R are the covariances for the corrupting noise terms in 3.12 i.e.*

$$Q = GG^T, \tag{3.18}$$

$$R = DD^T. \tag{3.19}$$

3.3.2 Error stochastic stability

In this part we will give the proof of the stochastic stability of the filter 3.13 estimation error.
To establish this proof we will base our proof on the work done in [30]. Actually, we will extend the proof already established for the discrete case to the general arbitrary time scale case.
We define the estimation error by

$$\zeta = x - \hat{x}. \tag{3.20}$$

Subtracting 3.13 from the state equation in 3.12 and using the measurement equation in 3.12 and 3.14-3.17 gives us the estimation error.

$$\zeta^{\Delta} = (A_t - K_t C_t)\zeta + r_t + s_t \tag{3.21}$$

where

$$r_t = \varphi(x, \hat{x}, u) - K_t \chi(x, \hat{x}) \tag{3.22}$$

$$s_t = Gw - K_t v \tag{3.23}$$

For the analysis of the error dynamics 3.21 we make use of the concept for the boundedness of stochastic processes.

Definition 3.3.2. *The stochastic process ζ is said to be exponentially bounded in mean square, if there are real numbers $\eta, \nu > 0$ and < 0 such that*

$$E\{\|\zeta\|^2\} \leq \eta \|\zeta_0\|^2 e^{\vartheta(t-t_0)} + \nu \tag{3.24}$$

for every $t \geq t_0$.

Remark. *The definition above is inspired from* ***Definition 2.1*** *in [30].*

Definition 3.3.3. *[30] The stochastic process is said to be bounded with probability one, if*

$$\sup_{t \geq t_0} \|\zeta\| < \infty \tag{3.25}$$

holds with probability one.

We introduce here our first lemma

Lemma 3.3.1. *Assume there is a stochastic process $V(\zeta)$ defined in a countable time scale $\mathbb{T}$ as well as real numbers $\underline{v}$, $\overline{v}$, $\lambda > 0$ and $0 < \alpha < 1$ such that*

$$\underline{v} \|\zeta\|^2 \leq V(\zeta) \leq \overline{v} \|\zeta\|^2 \tag{3.26}$$

and

$$E\{V^\sigma(\zeta^\sigma)|\zeta\} - V(\zeta) \leq \lambda - \alpha V(\zeta) \tag{3.27}$$

are fulfilled for every solution of 3.21. Then the stochastic process is bounded with probability one.

to see the proof of the discrete version of this lemma look at **lemma 2.1** in [30].
For isolated time scales we can make a bijection (a sort of mapping) between $\mathbb{T}$ and $\mathbb{N}$ which means that this lemma is always valid in this case.
The zero graininess case can be not taken into account because we're generalizing the discrete version of the Extended Kalman filter. Moreover, the zero graininess case takes us back to the continuous extended Kalman filter which stochastic stability is already established and demonstrated.
We can now state the theorem that gives us the filter stochastic stability.

Theorem 3.3.1. *Consider the non linear stochastic system given by 3.12 on a countable and bounded graininess time scale $\mathbb{T}$ and an extended Kalman filter as stated in 3.3.1. Let the following assumptions hold:*

1) *There are positive real numbers $\overline{a}, \overline{c}, \underline{p}, \overline{p} > 0$ such that the following bounds on various matrices are fulfilled for every $t > t_0$, $t \in \mathbb{T}$:*

$$\|A_t\| \leq \overline{a}, \tag{3.28}$$

$$\|C_t\| \leq \bar{c}, \tag{3.29}$$

$$\underline{p}I \leq P_t \leq \overline{p}I, \tag{3.30}$$

$$\underline{q}I \leq Q, \tag{3.31}$$

$$\underline{r}I \leq R. \tag{3.32}$$

2) A_t is regressive for every $t \geq t_0$.

3) There are positive numbers ϵ_φ, ϵ_χ, k_φ, $k_\chi > 0$ such that the nonlinear functions φ, χ in 3.22 are bounded via

$$\|\varphi(x, \hat{x}, u)\| \leq k_\varphi \|x - \hat{x}\|^2, \tag{3.33}$$

$$\|\chi(x, \hat{x})\| \leq k_\chi \|x - \hat{x}\|^2 \tag{3.34}$$

for $x, \hat{x} \in \mathbb{R}^n$ with $\|x - \hat{x}\| \leq \epsilon_\varphi$ and $\|x - \hat{x}\| \leq \epsilon_\chi$, respectively.

Then the estimation error ζ given by 3.20 is exponentially bounded in mean square and bounded with probability one, provided that the initial estimation error satisfies

$$\zeta_0 \leq \epsilon \tag{3.35}$$

and the covariance matrices of the noise terms are bounded via

$$GG^T \leq \delta I \tag{3.36}$$

$$DD^T \leq \delta I \tag{3.37}$$

for some δ,$\epsilon > 0$.

As in [30] the proof of this theorem is divided into several lemmas. These lemmas are the extension from the discrete case to time scale sets of the lemmas 3.1, 3.2 and 3.3 in [30].
We will introduce each lemma and give its proof, we will then demonstrate the Theorem 3.3.1.
Let's start with the first lemma.

Lemma 3.3.2. *Under the conditions of Theorem 3.3.1, there is a real number* $0 < \alpha < 1$ *such that* $\Pi_t = P_t^{-1}$ *satisfies the inequality*

$$[\,(I + \mu A_t) - \mu K_t C_t]^T \Pi_t^\sigma [\,(I + \mu A_t) - \mu K_t C_t] \leq (1 - \alpha)\Pi_t \tag{3.38}$$

for $t \geq t_0$ *with* K_t *given by 3.7.*

Proof. From 3.2.2, *iv*) in 1.2.1 and noticing that

$$(I + \mu A_t)P_t C_t^T (R + \mu C_t P_t C_t^T)^{-1} C_t P_t (I + \mu A_t)^T = (I + \mu A_t)P_t C_t^T K_t^T$$

we have

$$P_t^\sigma = P_t + \mu A_t P_t + \mu(I + \mu A_t)P_t A_t^T + \mu Q - \mu(I + \mu A_t)P_t C_t^T K_t^T,$$

The equation above can be written into the form

$$P_t^\sigma = (I + \mu A_t)P_t(I + \mu A_t)^T + \mu Q - \mu(I + \mu A_t)P_t C_t^T K_t^T, \tag{3.39}$$

Rearranging the terms yields

$$P_t^\sigma = [(I+\mu A_t)-\mu K_t C_t]P_t[(I+\mu A_t)-\mu K_t C_t]^T+\mu Q+\mu K_t C_t P_t[(I+\mu A_t)-\mu K_t C_t]^T \tag{3.40}$$

In the next step, we take care of the term $K_t C_t P_t[(I + \mu A_t) - \mu K_t C_t]^T$ on the right side of 3.40.
With 3.7 it can be verified that

$$(I + \mu A_t)^{-1}[(I + \mu A_t) - \mu K_t C_t]P_t = P_t - \mu P_t C_t^T (R + \mu C_t P_t C_t^T)^{-1} C_t P_t \tag{3.41}$$

is a symmetric matrix, and applying the matrix inversion lemma we obtain

$$(I + \mu A_t)^{-1}[(I + \mu A_t) - \mu K_t C_t]P_t = [P_t^{-1} + (\mu C_t^T)R^{-1}C_t]^{-1} > 0 \tag{3.42}$$

because $P_t^{-1} > 0$. Moreover, we have from 3.7 using $P_t > 0$ and $R > 0$

$$(I + \mu A_t)^{-1} K_t C_t = P_t C_t^T (R + \mu C_t P_t C_t^T)^{-1} C_t \geq 0 \tag{3.43}$$

combining 3.42 and 3.43 and using $P_t = P_t^T$ we establish that

$$\begin{gathered} K_t C_t P_t[(I + \mu A_t) - \mu K_t C_t]^T = \\ (I + \mu A_t)[(I + \mu A_t)^{-1} K_t C_t]\{(I + \mu A_t)^{-1}[(I + \mu A_t) - \mu K_t C_t]P_t\}^T (I + \mu A_t)^T \geq 0 \end{gathered}$$

holds and inserting into 3.40 leads to

$$P_t^\sigma \geq [(I + \mu A_t) - \mu K_t C_t]P_t[(I + \mu A_t) - \mu K_t C_t]^T + \mu Q \tag{3.44}$$

Inequality 3.42 implies that $[(I + \mu A_t) - \mu K_t C_t]$ exists and therefore we may write

$$P_t^\sigma \geq$$
$$[(I+\mu A_t)-\mu K_t C_t]\{P_t+[(I+\mu A_t)-\mu K_t C_t]^{-1}\mu Q[(I+\mu A_t)-\mu K_t C_t]^{-T}\}[(I+\mu A_t)-\mu K_t C_t]^T$$

From 3.7, 3.28-3.32 and $C_t P_t C_t^T \geq 0$ we have

$$\|K_t\| \leq (1+\overline{\mu a})\overline{pc}\frac{1}{\underline{r}} \tag{3.45}$$

Taking the inverse of both sides (this is allowed since $P_t \geq \underline{p}I$ and $(I+\mu A_t)-\mu K_t C_t$ are non singular), multiplying from left and right with $[(I+\mu A_t)-\mu K_t C_t]^T$ and $[(I+\mu A_t)-\mu K_t C_t]$, and using 3.30 we get finally with $\Pi_t = P_t^{-1}$

$$[(I+\mu A_t)-\mu K_t C_t]^T \Pi^\sigma [(I+\mu A_t)-\mu K_t C_t] \leq \left[1+\frac{\overline{\mu}\underline{q}}{\overline{p}\left[(1+\overline{\mu a})+\overline{\mu}(1+\overline{\mu a})\frac{\overline{p}.\overline{c}^2}{\underline{r}}\right]}\right]^{-1}\Pi_t$$

i.e. inequality 3.38 with $1-\alpha = 1/\left[1+\frac{\overline{\mu}\underline{q}}{\overline{p}\left[(1+\overline{\mu a})+\overline{\mu}(1+\overline{\mu a})\frac{\overline{p}.\overline{c}^2}{\underline{r}}\right]}\right]$ □

We introduce now our second lemma.

Lemma 3.3.3. *Let the conditions of theorem 3.3.1 be fulfilled, let $\Pi_t = P_t^{-1}$ and K_t, r_t be given by 3.7 and 3.22. Then there are positive real numbers $\epsilon', k_{nonl} > 0$ such that*

$$r_t^T \Pi_t [2(I+\mu A_t)-\mu K_t C_t](x-\hat{x})+r_t] \leq k_{nonl}\|x-\hat{x}\|^3 \tag{3.46}$$

holds for $\|x-\hat{x}\| \leq \epsilon'$

Proof. From 3.7, 3.28-3.32, 3.5 and $C_t P_t C_t^T > 0$ we have

$$\|K_t\| \leq (1+\overline{\mu a})\overline{pc}\frac{1}{\underline{r}}$$

and inserting into 3.22 yields

$$\|r_t\| \leq \|\varphi(x,\hat{x},u)\| + (1+\overline{\mu a})\overline{pc}\frac{1}{\underline{r}}\|\chi(x,\hat{x})\|. \tag{3.47}$$

Choosing $\epsilon' = min(\epsilon_\varphi, \epsilon_\chi)$ and using 3.33, 3.34 we obtain

$$\|r_t\| \leq k_\varphi \|x-\hat{x}\|^2 + (1+\overline{\mu a})\overline{pc}\frac{1}{\underline{r}}k_\chi\|x-\hat{x}\|^2 \tag{3.48}$$

for $\|x-\hat{x}\| \leq \epsilon'$ i.e.,

$$\|r_t\| \leq k'\|x-\hat{x}\|^2 \tag{3.49}$$

with

$$k' = k_\varphi + (1+\overline{\mu a})\overline{pc}\frac{1}{\underline{r}}k_\chi. \tag{3.50}$$

From 3.48 and 3.28-3.32 we get with $\Pi_t = P_t^{-1}$ for $\|x - \hat{x}\| \leq \epsilon'$

$$r_t^T \Pi_t \{2[(I + \mu A_t) - \mu K_t C_t](x - \hat{x}) + r_t\} \leq$$
$$k' \|x - \hat{x}\| \frac{1}{\underline{p}} \{2[(1 + \overline{\mu a}) + \overline{\mu}(1 + \overline{\mu a})\overline{pc}\frac{1}{\underline{r}}\overline{c}] \|x - \hat{x}\| + k'\epsilon' \|x - \hat{x}\|\}$$

we obtain 3.46 with

$$k_{nonl} = \frac{k'}{\underline{p}} \{2[(1 + \overline{\mu a}) + \overline{\mu}(1 + \overline{\mu a})\overline{pc}\frac{1}{\underline{r}}\overline{c}] + k'\epsilon'\}$$

□

Here comes the last lemma.

Lemma 3.3.4. *Let the conditions of Theorem 3.3.1 hold, let* $\Pi_t = P_t^{-1}$, *and* K_t, s_t *given by 3.7 and 3.23. Then there is a positive real number* $k_{noise} > 0$ *independent of* δ, *such that*

$$E\{s_t^T \Pi^\sigma s_t\} \leq k_{noise} \delta \tag{3.51}$$

holds.

Proof. Since v and ω are uncorrelated the expectation value of the cross terms containing both v and ω will vanish and we focus on the following terms:

$$s_t^T \Pi^\sigma s_t = \omega^T G^T \Pi^\sigma G \omega + v^T D^T K_t^T \Pi^\sigma K_t D v \tag{3.52}$$

From 3.7, 3.28:3.32 and $C_t P C_t^T > 0$ we have

$$\|K_t\| \leq (1 + \overline{\mu a})\overline{pc}\frac{1}{\underline{r}}$$

inserting into 3.52 and using 3.30 we get with $\Pi_t = P^{-1}$

$$s_t^T \Pi^\sigma s_t \leq \frac{1}{\underline{p}} \omega^T G^T G \omega + \frac{\overline{p}^2 \overline{c}^2}{\underline{p}\underline{r}^2}(1 + \overline{\mu a})^2 v^T D^T D v \tag{3.53}$$

Because both sides are of 3.53 are scalars, we may take the trace of the right-hand side of 3.53 without changing its value

$$s_t^T \Pi^\sigma s_t \leq \frac{1}{\underline{p}} \mathrm{tr}(\omega^T G^T G \omega) + \frac{(1 + \overline{\mu a})^2 \overline{c}^2 \overline{p}^2}{\underline{p}\underline{r}^2} \mathrm{tr}(v^T D^T D v) \tag{3.54}$$

Using the well-known matrix identity

$$\mathrm{tr}(\Gamma\Delta) = \Delta\Gamma$$

where Γ, Δ are such matrices that the above matrix multiplication and the trace operations make sense we get

$$s_t^T \Pi^\sigma s_t \leq \frac{1}{\underline{p}} \mathrm{tr}(G\omega\omega^T G^T) + \frac{(1+\overline{\mu a})^2 \overline{c}^2 \overline{p}^2}{\underline{p}\underline{r}^2} \mathrm{tr}(Dvv^T D^T) \tag{3.55}$$

Taking the mean value yields

$$E\{s_t^T \Pi^\sigma s_t\} \leq \frac{1}{\underline{p}} \mathrm{tr}(G\mathrm{E}\{\omega\omega^T\} G^T) + \frac{(1+\overline{\mu a})^2 \overline{c}^2 \overline{p}^2}{\underline{p}\underline{r}^2} \mathrm{tr}(D\mathrm{E}\{vv^T\} D^T) \tag{3.56}$$

where we have used D and G are deterministic matrices. Because v and ω are standard vector-valued white noise process, the conditions

$$\mathrm{E}\{vv^T\} = I \tag{3.57}$$

$$E\{\omega\omega^T\} = I \tag{3.58}$$

hold therefore we have

$$\mathrm{E}\{s_t^T \Pi^\sigma s_t\} \leq \frac{1}{\underline{p}} \mathrm{tr}(GG^T) + \frac{(1+\overline{\mu a})^2 \overline{c}^2 \overline{p}^2}{\underline{p}\underline{r}^2} \mathrm{tr}(DD^T) \tag{3.59}$$

Using 3.36 and 3.37 we get

$$\mathrm{E}\{GG^T\} \leq \delta \mathrm{tr}(I) = n\delta \tag{3.60}$$

$$\mathrm{E}\{DD^T\} \leq \delta \mathrm{tr}(I) = p\delta \tag{3.61}$$

where n and p are the number of the rows for G and D, respectively. Setting

$$k_{noise} = \frac{p}{\underline{q}} + \frac{(1+\overline{\mu a})^2 \overline{c}^2 \overline{p}^2 m}{\underline{p}\underline{r}^2} \tag{3.62}$$

if follows with 3.59 and 3.62 that

$$E\{s_t^T \Pi^\sigma s_t\} \leq k_{noise}\delta$$

yielding the desired inequality 3.51. □

Now that we have introduced and proved the extension of all the needed lemmas in [30], we can start the proof of the Theorem 3.3.1.
We choose

$$V(\zeta) = \zeta^T \Pi_t \zeta \tag{3.63}$$

with $\Pi = P^{-1}$, which exists since P_t is positive definite. From 3.30 we have

$$\frac{1}{\overline{p}} \|\zeta\|^2 \leq V(\zeta) \leq \frac{1}{\underline{p}} \|\zeta\|^2 \tag{3.64}$$

i.e., 3.26 with $\underline{\nu} = \frac{1}{\overline{p}}$ and $\overline{\nu} = \frac{1}{\underline{p}}$. To satisfy the requirements for an application of Lemma 3.3.1, we need an upper bound on $E\{V^\sigma(\zeta^\sigma)|\zeta\}$ as in 3.27. From 3.21 we have

$$V^\sigma(\zeta^\sigma) = \{\zeta[(I + \mu A_t) - \mu K_t C_t]^T + r_t^T + s_t^T\}\Pi^\sigma\{[(I + \mu A_t) - \mu K_t C_t]\zeta + r_t + s_t\}$$

And applying lemma 3.3.2 we obtain with 3.63

$$V^\sigma(\zeta^\sigma) \leq (1-\alpha)V(\zeta)+r_t^T\Pi^\sigma\{2[(I+\mu A_t)-\mu K_t C_t]\zeta+r_t\}+2s_t^T\Pi^\sigma\{[(I+\mu A_t)-\mu K_t C_t]\zeta+r_t\}+s_t^T\Pi^\sigma s_t \tag{3.65}$$

The conditional expectation $E\{V^\sigma(\zeta^\sigma)|\zeta\}$,the term $E\{s_t^T\Pi^\sigma\{[(I+\mu A_t)-\mu K_t C_t]\zeta+r_t\}|\zeta$ vanishes because neither Π^σ nor $A_t, C_t, K_t, r_t, \zeta_t$ depend on v or ω. The remaining terms are estimated via 3.3.3 and 3.3.4 yielding

$$E\{V^\sigma(\zeta^\sigma)|\zeta\} - V(\zeta) \leq -\alpha V(\zeta) + k_{nonl} \|\zeta\|^3 + k_{noise}\delta \tag{3.66}$$

for $\|\zeta\| < \epsilon'$. Defining

$$\epsilon = min(\epsilon', \frac{\alpha}{2\overline{p}k_{nonl}}) \tag{3.67}$$

we obtain with 3.63, 3.64 for $\|\zeta\| \leq \epsilon$

$$k_{nonl} \|\zeta\| \|\zeta\|^2 \leq \frac{\alpha}{2\overline{p}} \|\zeta\| \leq \frac{\alpha}{2} V(\zeta) \tag{3.68}$$

Inserting into 3.66 yields

$$E\{V^\sigma(\zeta^\sigma)|\zeta\} - V(\zeta) \leq -\frac{\alpha}{2} V(\zeta) + k_{noise}\delta \tag{3.69}$$

for $\|\zeta\| \leq \epsilon$. Therefore we're able to apply Lemma 3.3.1 with $\|\zeta_0\| \leq \epsilon$, $\underline{\nu} = \frac{1}{\overline{p}}$, $\overline{\nu} = \frac{1}{\underline{p}}$, and $\lambda = k_{noise}\delta$. When $\tilde{\epsilon} \leq \|\zeta\| \leq \epsilon$ with some $\tilde{\epsilon} < \epsilon$ the inequality 3.69 terms become negative and is fulfilled to guarantee the boundedness of the estimation error choosing

$$\delta = \frac{\alpha\tilde{\epsilon}^2}{2\overline{p}k_{noise}} \tag{3.70}$$

with some $\tilde{\epsilon} < \epsilon$ we have for $\|\zeta\| \geq \tilde{\epsilon}$

$$k_{noise}\delta \leq \frac{\alpha}{2\overline{p}} \|\zeta\|^2 \leq \frac{\alpha}{2} V(\zeta) \tag{3.71}$$

3.4 Observer based control on time scales

We discuss in this part the control of systems with a feedback based on observers to estimate the system state.
In [6] the observer based control has been discussed for the time scale LQG controller and a proof for the separation principle has been established. (see equation 31 page 435)
Let's consider a time scale linear system similar to 3.1 without process and measurement noises.

$$\begin{cases} x^{\Delta} = Ax + Bu, \quad x(t_0) = x_0 \\ y = Cx \end{cases} \tag{3.72}$$

with $x \in \mathbb{R}^n$, $A \in \mathbb{R}^{n\times n}$, $u \in \mathbb{R}^m$, $B \in \mathbb{R}^{n\times m}$, $y \in \mathbb{R}^p$ and $C \in \mathbb{R}^{p\times n}$. $t \in \mathbb{T}$.

Hypothesis 3.6. *the time scale $\mathbb{T}$ has a bounded graininess.*

We assume a time scale version of the famous Luenberger form observer.

$$\hat{x}^{\Delta} = A\hat{x} + Bu + L(y - C\hat{x}) \tag{3.73}$$

where $\hat{x}$ is the estimate and $L \in \mathbb{R}^{n\times p}$ is the observer gain. The estimation error $\tilde{x} = x - \hat{x}$ dynamic is described by the following equation

$$\tilde{x}^{\Delta} = (A - LC)\tilde{x} \tag{3.74}$$

We want to control the system 3.72 with a state feedback. Since we don't have a direct access to the state x we use the provided observer estimate $\hat{x}$.
This leads to the controlled system described by the equation

$$x^{\Delta} = Ax + B(-K\hat{x}) \tag{3.75}$$

where $K \in \mathbb{R}^{m\times n}$ is the feedback controller gain. (we assume $u = 0$ in 3.75)
adding and subtracting BKx to 3.75 and rearranging terms yields

$$x^{\Delta} = (A - BK)x + BK\tilde{x} \tag{3.76}$$

Considering the augmented state $\xi = \begin{bmatrix} x^T & \tilde{x}^T \end{bmatrix}^T$ we obtain the equation of the augmented system

$$\xi^{\Delta} = \begin{bmatrix} A - BK & BK \\ 0 & A - LC \end{bmatrix} \xi \tag{3.77}$$

The system 3.77 describes the separability principle of the state feedback controller and the Luenberger like observer. The observer and the controller can be designed separately and are independent of each other.
In addition, the hypothesis 3.6 and system 3.72 observability and controlability ensure system 3.77 stabilisability.
We can restrict the general form of controllers and observers with the above structure to the Kalman filter case and LQR case. It conducts us to the case discussed in [6].

3.5 LQG/LTR case

In this section we want to discuss the well known LTR issue.
LQG is based on the so-called principle of separation of control and estimation. The state-feedback controller LQR is optimal in the sense of a quadratic criterion, and the Kalman filter is the optimal state estimator in the presence of white noise disturbances. Taken together controller and filter give a control law which is optimal in the presence of white noise measurement and process noise.
Unfortunately the LQG controller lacks robustness due to systems uncertainties.[19]
To overcome this issue, the LQG/LTR controller has been designed to recover the robustness property of the LQG under the Kalman filter optimal state estimation.[7]
We will propose an LTR approach to overcome this issue for non zero graininess time scale systems. The controller and observer gains will be inspired from the delta operator formulation that has been developed in [26] and [25].
Indeed, the time scale theory is a generalization of the delta operator approach. subsequently, we will change the delta term in each gain equation (each LTR gain equation in [25] and [26]) by the graininess operator μ.
We will see later in a simulation that this approach seems to work well for the non zero graininess time scale case regarding to the system response obtained, unfortunately we won't give any proof for this new filter.
Generally the LQG/LTR controller design proofs rely on a frequency description of systems. To our knowledge, we do not have yet an effective frequency description of time-scale systems, which makes the evaluation of the filter capacity to recover the targeted robustness properties impossible. Subsequently, we cannot generalize the proofs based on the frequency description of systems.
the plant to be controlled is described by 3.1.

For this system the observer gain is given by

$$K_p = \frac{(I + \mu A)B[CB]^{-1}}{\mu} \tag{3.78}$$

And the feedback controller gain is given by

$$K_c = \frac{[CB]^{-1}C(I + \mu A)}{\mu} \tag{3.79}$$

Remark. *i) Some conditions need to be satisfied to be able to use this approach.*
Firstly, the system should have a number of outputs equal to the inputs.
Secondly, all the system zeros must be stable. [19]

ii) The gains given by 3.78 and 3.79 have no sense in the zero graininess case. However, this mustn't cancel the availability of this approach for the non zero graininess. An *extension can always be done to the continuous case by taking the continuous Loop Transfer Recovery controller in this case.*

3.6 Simulation examples

3.6.1 Kalman filter

We consider the spring-mass system described by the following equations

$$\begin{cases} \begin{bmatrix} x_1 \\ x_2 \end{bmatrix}^{\Delta} = \begin{bmatrix} 0 & 1 \\ -1 & -2 \end{bmatrix} \begin{bmatrix} x_1 \\ x_2 \end{bmatrix} + \begin{bmatrix} 0 \\ 1 \end{bmatrix} \omega, \\ \\ y = \begin{bmatrix} 1 & 0 \end{bmatrix} \begin{bmatrix} x_1 \\ x_2 \end{bmatrix} + v, \end{cases} \tag{3.80}$$

where x_1 represents the position of an object, x_2 is its velocity, y is the measurement, $\omega \approx N(0,1)$ is the process noise, and $v \approx N(0,2)$ represents the measurement noise. In applying the Kalman filter, it is assumed that the measurement are Gaussian with variances $\sigma_{x_1}^2 = 2$ and $\sigma_{x_2}^2 = 3$.
The system and filter initializations were
$x_0 = \begin{bmatrix} 1 \\ 1 \end{bmatrix}$, $\hat{x}_0 = \begin{bmatrix} 1 \\ 1 \end{bmatrix}$ and $P_0 = \begin{bmatrix} 2 & 0 \\ 0 & 3 \end{bmatrix}$.
The simulation is run on the time scales listed in 3.1.

$\mathbb{T}$	$\mu(t)$	$\sigma(t)$
$2\mathbb{Z}$	2	$t+2$
$\mathbb{H}_n$	$\frac{1}{n+1}$	$\mathbb{H}_{n+1}$
$\mathbb{P}_{a,b}$	$\mu(\mathbb{P}_{a,b})$	$\sigma(\mathbb{P}_{a,b})$
$\mathbb{N}^{\frac{1}{2}}$	$\frac{1}{\sqrt{t+1}-\sqrt{t}}$	$\sqrt{t+1}$

Table 3.1: Time scales considered for simulation

where $\mu(\mathbb{P}_{a,b}) = \begin{cases} 0, & t \in \cup_{k=0}^{\infty}[kc, kc+a) \\ b, & t \in \cup_{k=0}^{\infty}\{kc+a\} \\ c = a+b \end{cases}$ and $\sigma(\mathbb{P}_{a,b}) = \begin{cases} t, & t \in \cup_{k=0}^{\infty}[kc, kc+a) \\ t+b & t \in \cup_{k=0}^{\infty}\{kc+a\} \end{cases}$

The simulations have given the following results

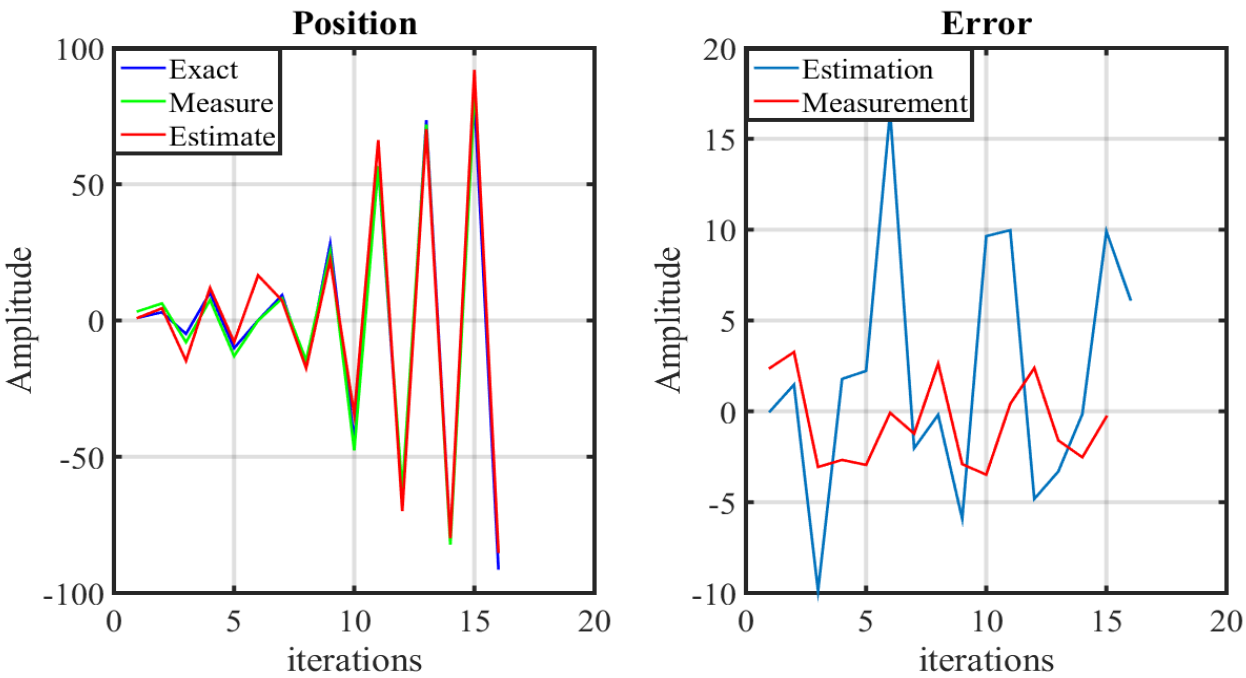

Figure 3.1: Time scale Kalman filter simulation for $\mathbb{T} = 2\mathbb{Z}$.

We can see that the estimation error is superior to the measurement error when $\mu(t) = 2$.

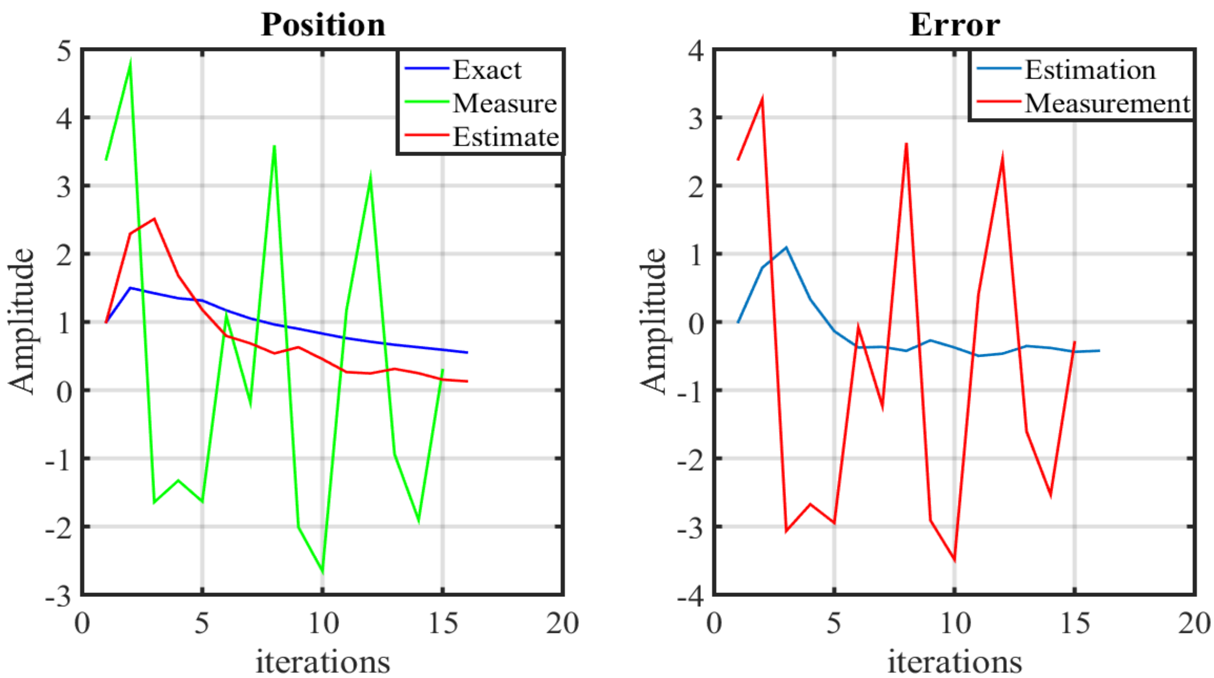

Figure 3.2: Time scale Kalman filter simulation for $\mathbb{T} = \mathbb{H}_n$.

For this case, the estimation error is smaller.(notice that the graininess is very small here)

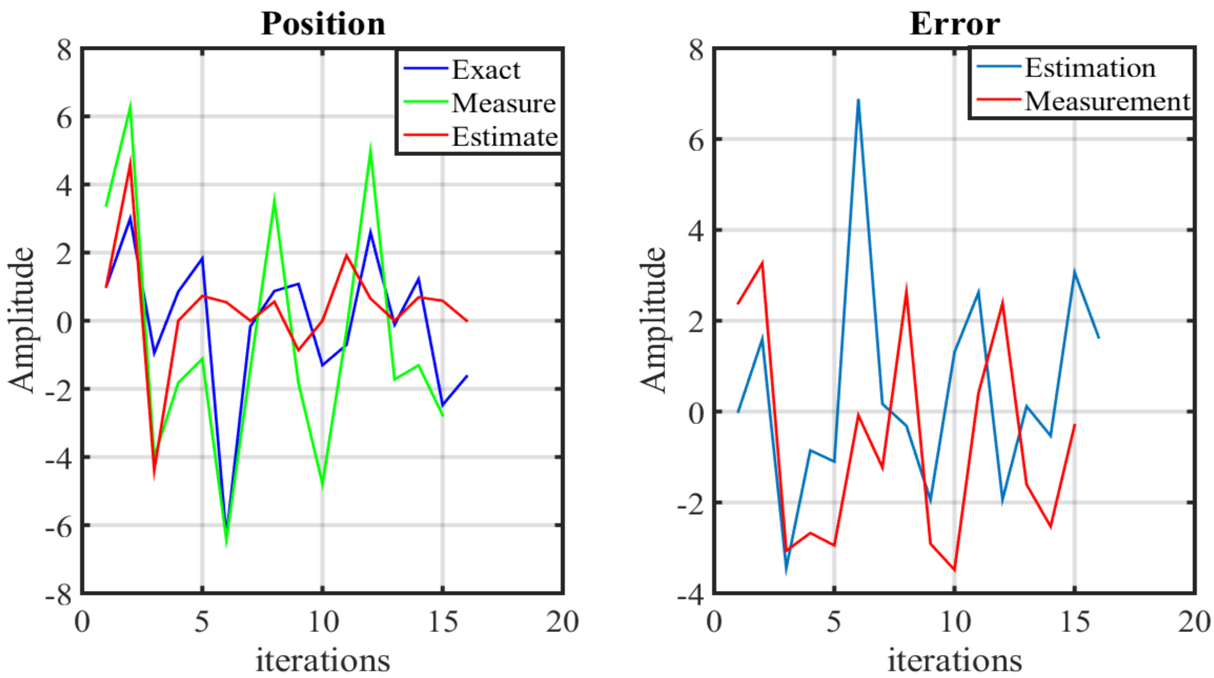

Figure 3.3: Time scale Kalman filter simulation for $\mathbb{T} = \mathbb{P}_{12}$.

The estimation error is high for high graininess values and lessen when the graininess decreases.

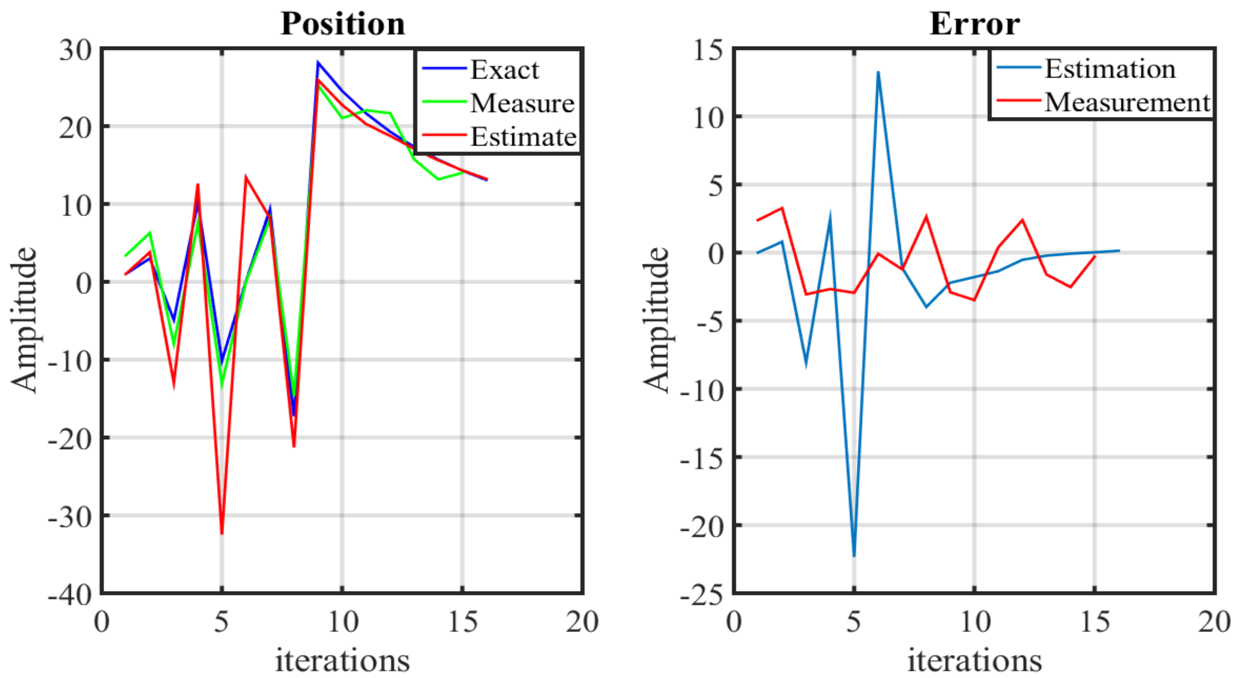

Figure 3.4: Time scale Kalman filter simulation for $\mathbb{T} = 2\mathbb{Z}$ for $t \leq 8$ and $\mathbb{T} = \mathbb{H}_n$ for $t > 8$.

In the figure above, we observe that the estimation error decreases with the graininess.

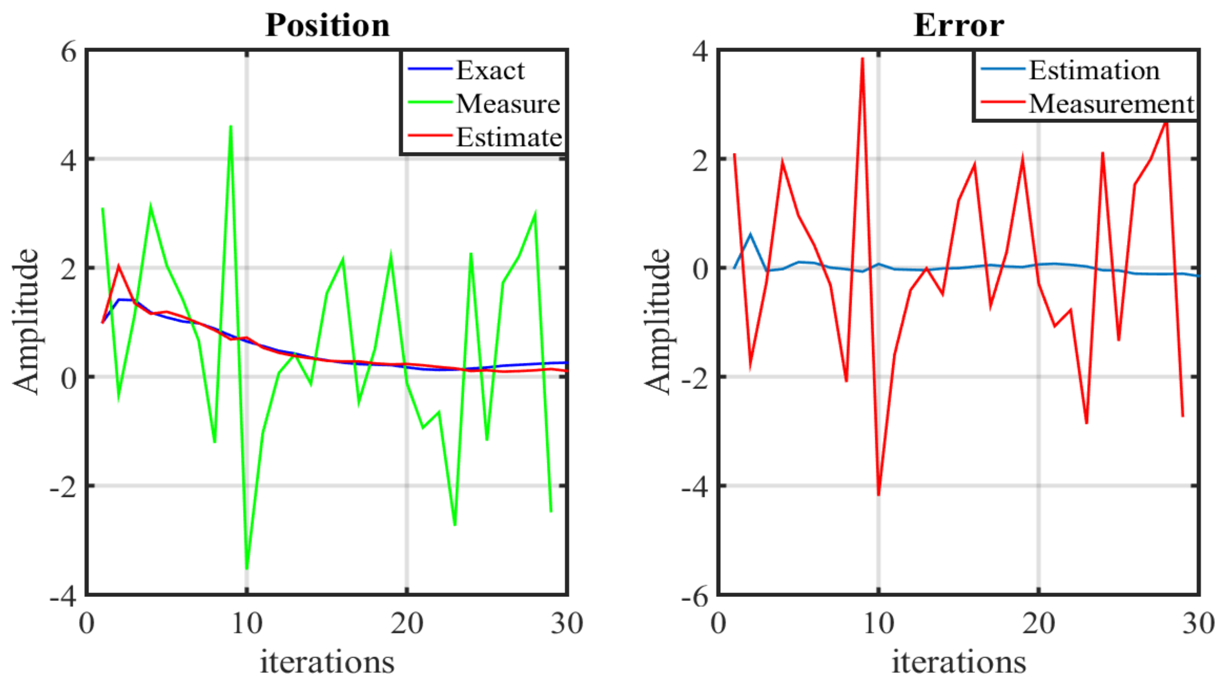

Figure 3.5: Time scale Kalman filter simulation for $\mathbb{T} = \mathbb{N}^{\frac{1}{2}}$.

The observer behaves very well here, the estimation error is close to the origin. in this case, the graininess is small.

Fault estimation case:

In this scenario, we add some faults to the mass-spring system 3.80 and perform the simulations.

The simulation will be done on time scales $2\mathbb{Z}$, $\mathbb{H}_n$, $\mathbb{N}^{\frac{1}{2}}$ and a union of these three time scales.

the fault signal experiences two phases. The first one is a step signal. During the second phase it oscillates.

The simulation have given the results below.

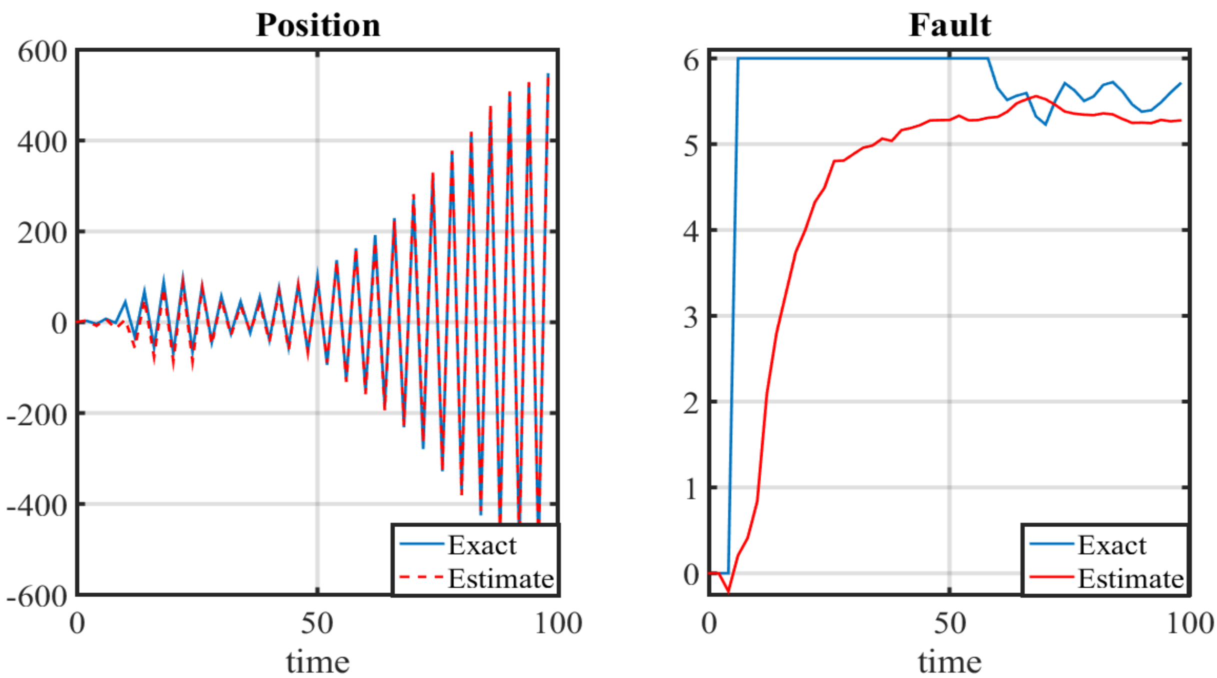

Figure 3.6: Time scale Kalman filter with fault estimation feature for $\mathbb{T} = 2\mathbb{Z}$.

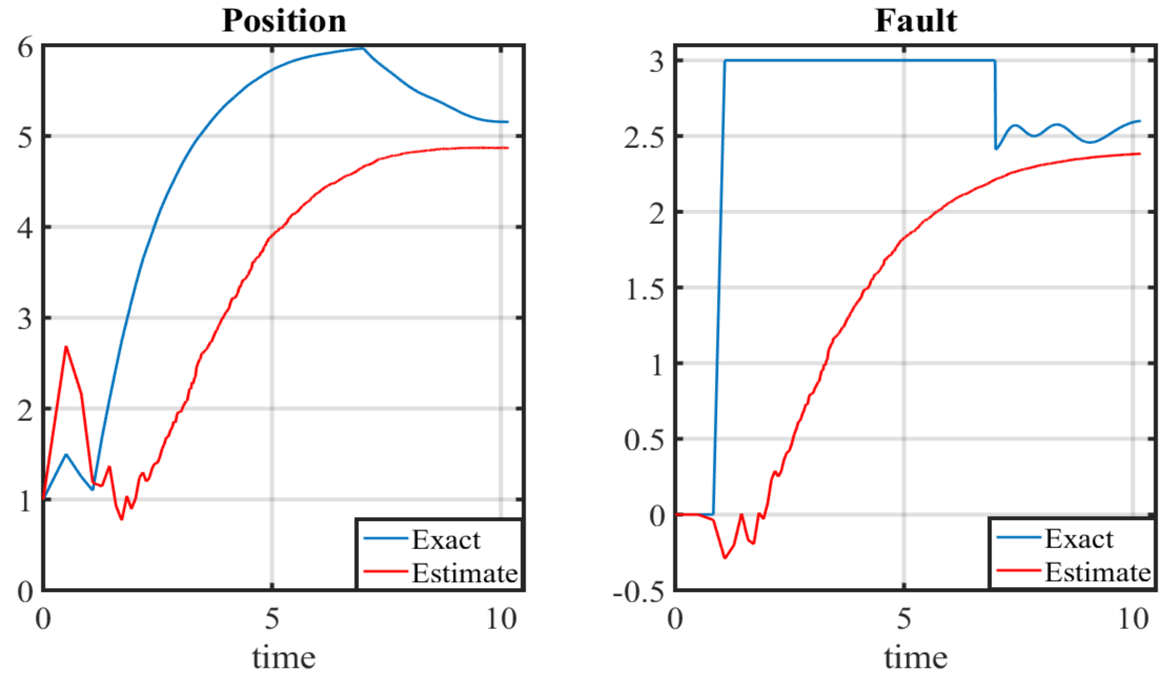

Figure 3.7: Time scale Kalman filter with fault estimation feature for $\mathbb{T} = \mathbb{H}_n$.

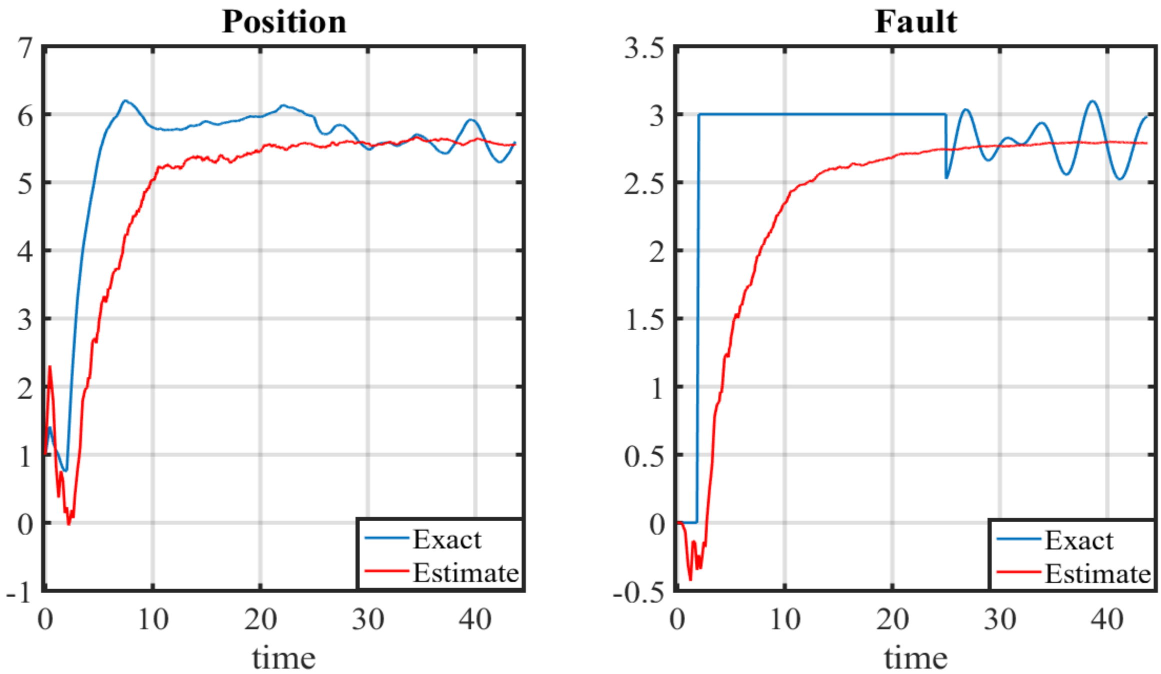

Figure 3.8: Time scale Kalman filter with fault estimation feature for $\mathbb{T} = \mathbb{N}^{\frac{1}{2}}$.

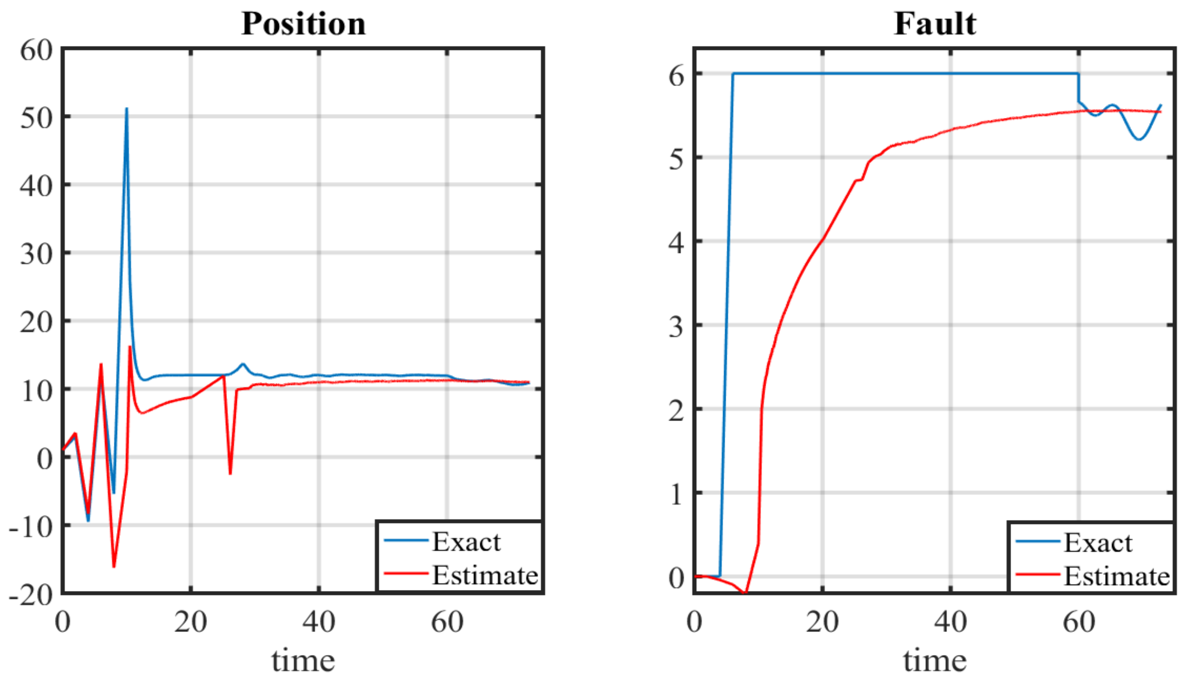

Figure 3.9: Time scale Kalman filter with fault estimation feature for $\mathbb{T} = 2\mathbb{Z}\ \mathbb{H}_n\ \mathbb{N}^{\frac{1}{2}}$.

Comments on results

The Riccati and the gain equations change depending on the time scale, subsequently the gain will get impacted following the time scale on which the system evolves.
From figure 3.1 to figure 3.5 we have plot the true position, the measurements, the estimates and the estimation error with the measurement error to have an idea of the filter effectiveness.
The time scale Kalman filter seems to work well in certain time scales but not all of them, even though the estimation error appears to be bounded in all cases.
Actually, the estimation error drops when the graininess operator $\mu(t)$ is small. On the other hand, we observe that the error gets larger when the graininess stretches.
According to theorem 1.4.2, we can state that this behavior is expected from the theory since the larger the graininess is, the harder becomes the estimation error stabilisation. Moreover, if we look at the graininess as a delay, it conducts the estimation error to increase as a consequence of the delays impact on the error stability.
From figure 3.6 to 3.8 we have plot the position with its estimate and measurements. We have also plot the fault signal that occurs to the system with its estimate.
The filter succeeds to approximate the fault on each time scale. When the fault oscillates the filter fails to identify the oscillatory behavior of the fault signal.
The fault estimation dynamic is extremely slow, this slowness suppress the capacity of the filter to shape accurately time varying fault signals, especially when they have an im-

portant oscillatory behavior like in the simulation. Nevertheless, we have seen that this slowness ensures the fault estimation error stability. Since the fault estimation isn't accurate the state estimation looses accuracy even in small graininess time scales. However, this phenomenon doesn't deteriorate the global stability of the state estimation.

3.6.2 Extended Kalman filter

The extended Kalman filter will be tested on a time scale system inspired from 2.4. (Basically we replace the classical derivative by its Hilger version)
We added process and measurement noises. Both are zero mean processes with respectively the deviations 30 and 40.
The time scale on which the system has been run is characterized by a random graininess with some gaps. Time is given in seconds while the different angles are in radians.
We obtained the following results

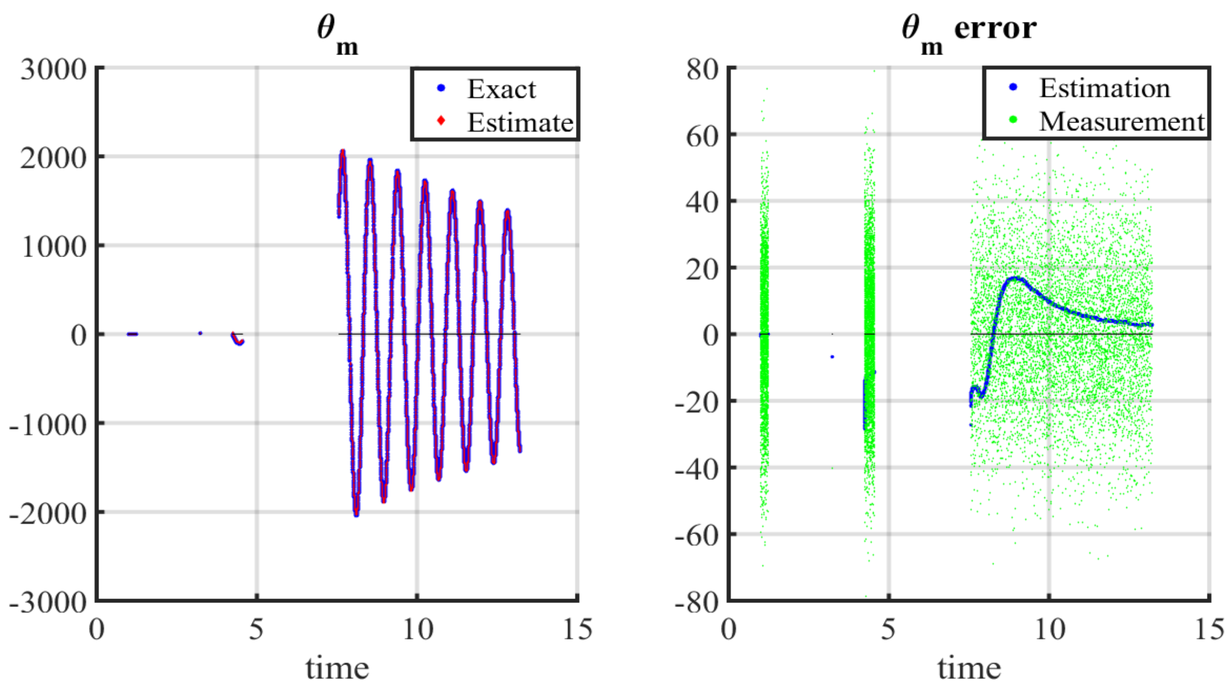

Figure 3.10: Time scale extended Kalman filter motor shaft angle estimation and its estimation error.

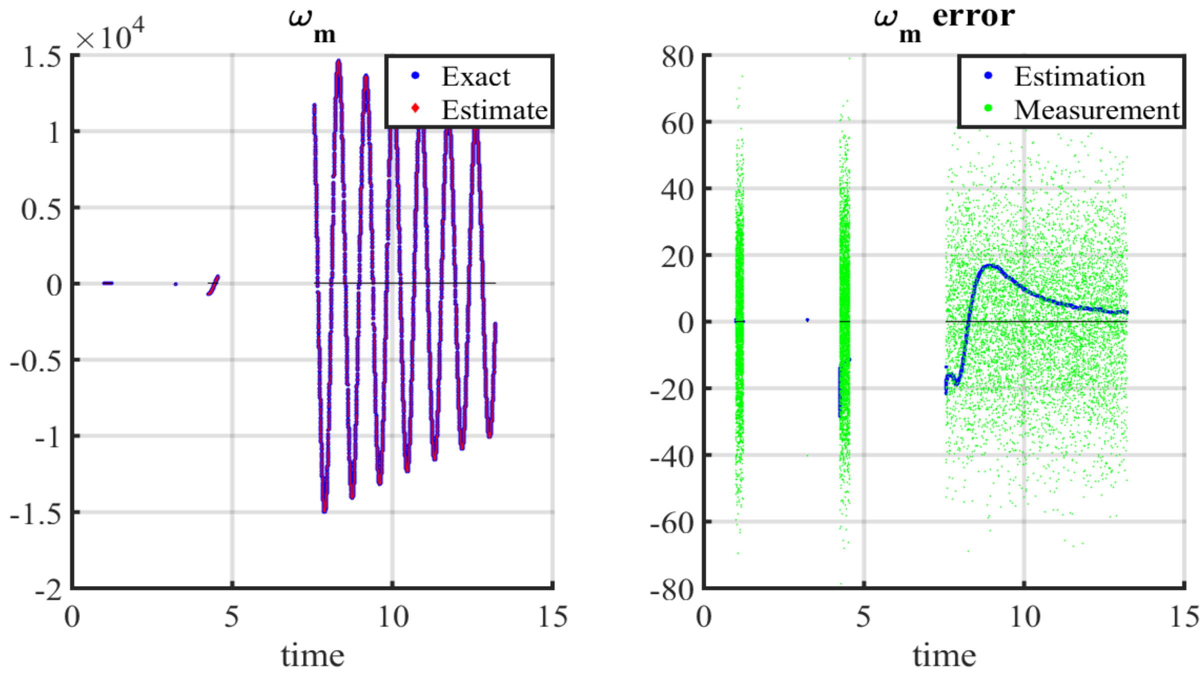

Figure 3.11: Time scale extended Kalman filter motor shaft angular velocity estimation and its estimation error

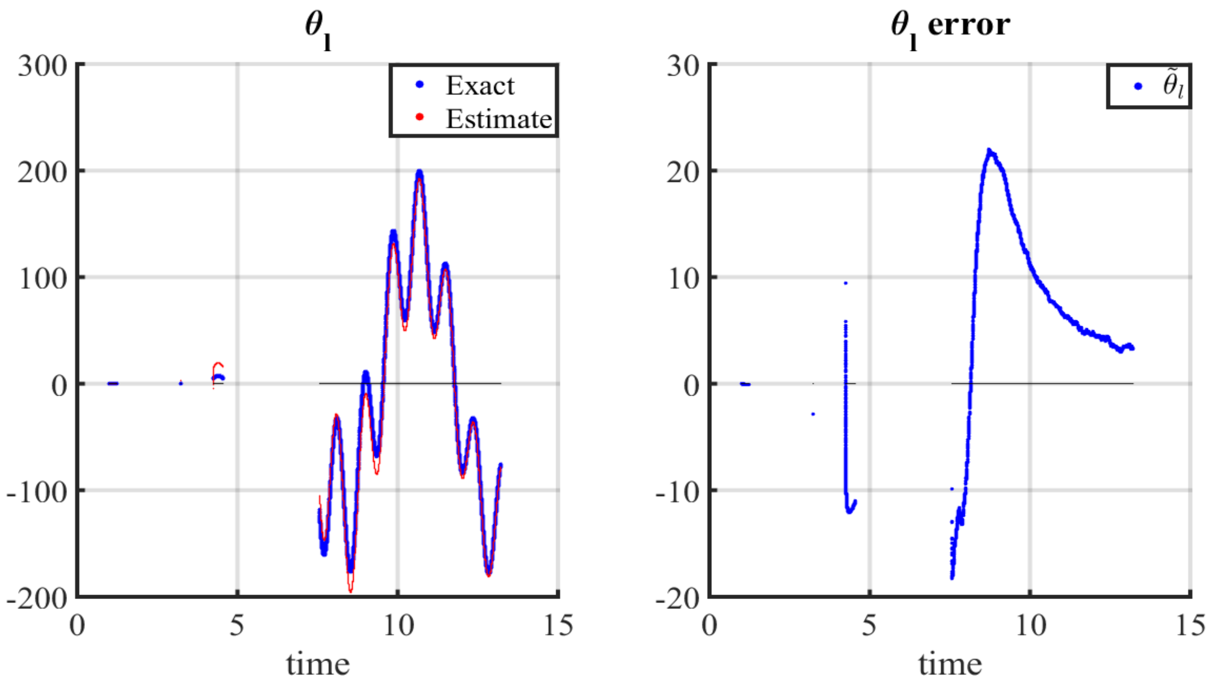

Figure 3.12: Time scale extended Kalman filter rod angle estimation and its estimation error.

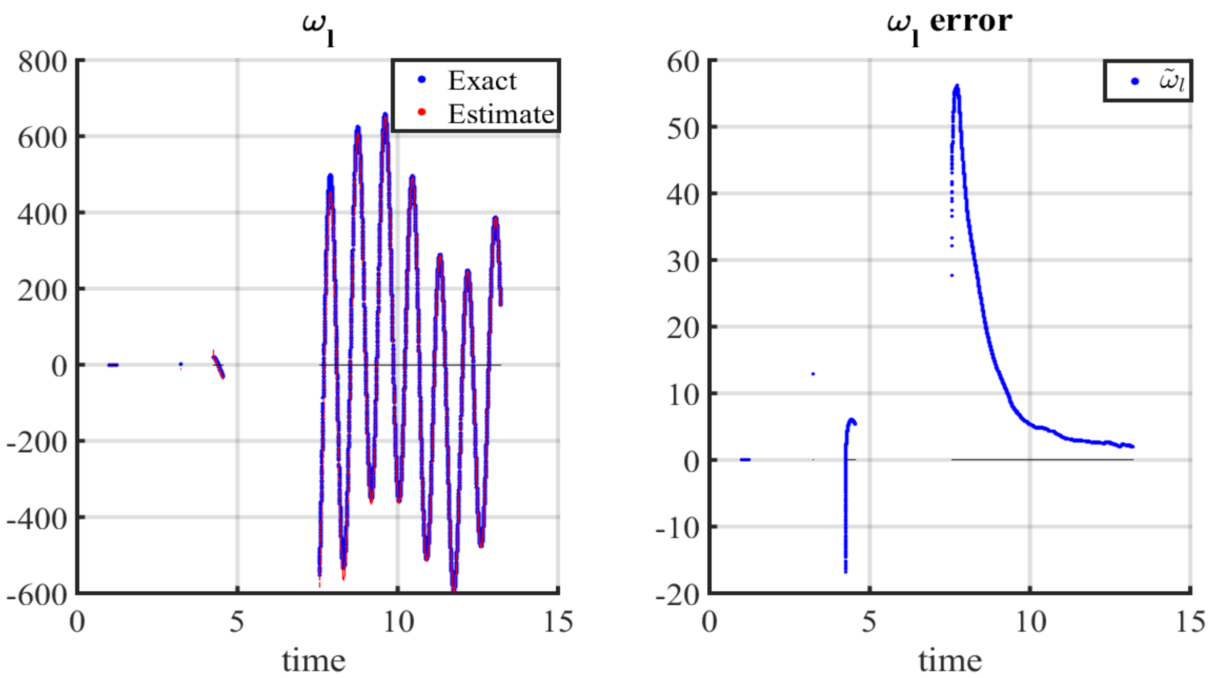

Figure 3.13: Time scale extended Kalman filter Rod angular velocity estimation and its estimation error.

Comments on results

We have plot the motor shaft and rod angular positions with their estimations and the estimation error with the time scale.
For this simulation we have deliberately chosen small graininess values (unless the gaps) to avoid the system instability.
The time scale extended Kalman filter behaves globally well. It has inherited same dynamical performances as the time scale Kalman filter from which it's inspired. The estimation error is bounded but it increases when the graininess reaches higher values even if in this simulation the estimation error is always under the measurement error even when the graininess increases.

3.6.3 Observer based control

We run a simulation of the linearization of the inverted pendulum presented in [18], the system is shown in figure 3.14. This system is stabilized with a pole placement.

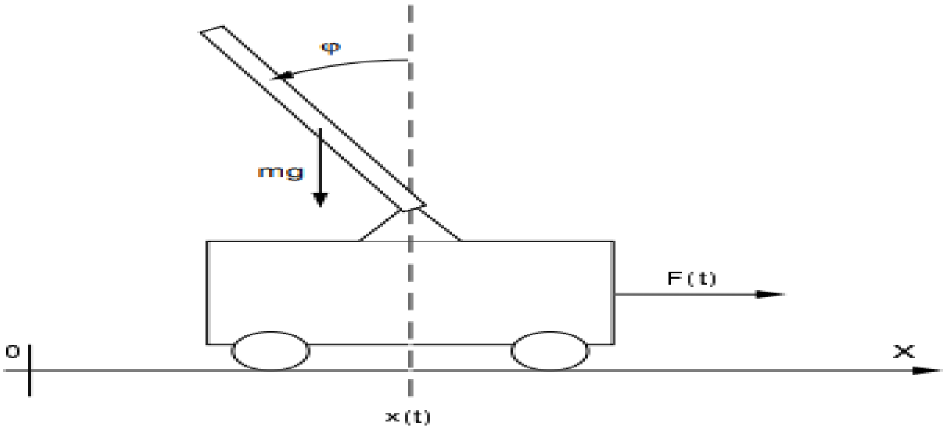

Figure 3.14: Inverted Pendulum.

the equations that govern the system dynamic are

$$\ddot{\varphi}(t) = \frac{3g}{2L_b}\varphi(t) - \frac{f_b}{4J_b}\dot{\varphi}(t) + \frac{3}{2L_b}\ddot{x}(t) \tag{3.81}$$

$$\ddot{x}(t) = -\frac{f_{cc}}{m_{cc}+m_b}\dot{x}(t) + \frac{m_b L_b/2}{m_{cc}+m_b}\ddot{\varphi}(t) + \frac{1}{m_{cc}+m_b}F(t) \tag{3.82}$$

Where m_b is the pendulum mass, m_{cc} is the cart mass, L_b is the pendulum length and J_b is its inertial momentum. f_{cc} and f_b are the friction forces that the system is subjected to. The state space representation of this system is presented in [18], we consider the following time scale system which is derived from this model.

$$\begin{bmatrix} \varphi^{\Delta}(t) \\ \varphi^{\Delta^2}(t) \\ x^{\Delta}(t) \\ x^{\Delta^2}(t) \end{bmatrix} = \begin{bmatrix} 0 & 1 & 0 & 0 \\ 40.4 & -0.217 & 0 & -1.54 \\ 0 & 0 & 0 & 1 \\ 0.959 & -0.005 & 0 & -0.411 \end{bmatrix} \begin{bmatrix} \varphi(t) \\ \varphi^{\Delta}(t) \\ x(t) \\ x^{\Delta}(t) \end{bmatrix} + \begin{bmatrix} 0 \\ 50.0 \\ 0 \\ 13.3 \end{bmatrix} u(t) \tag{3.83}$$

The system outputs are the pendulum angle $\varphi(t)$ (given in radians (rad)) and the cart position $x(t)$ (given in meters (m)). this system is stabilisable using the observer based control in accordance with theorem 1.4.3.
Parameters values are given in [18] table 3 page7.
The time scale on which the simulation has been run has been practically generated. This time set is a successive union of continuous time set and discrete time sets. Figure 3.15 gives an idea of this time scale general structure. This time scale is interesting because it gathers high and small graininess cases with different time scale density transitions. Time here is given in seconds (s).
We design a state feedback controller for this system with the purpose of stabilising it.

```
T=[t(1:15),t(16:20),t(21:'31':62),t(63:66)...,
 t(67:74),t(75:80),t(81:82),t(83:85)...,
 t(86:'127':'132,133,134'),t(135:153)...,
 t(154:172),t(173:203)...,
 t(204:'210,211':'219,220,221,222,223')...,
 t(224:237),t(238:272),t(273:284)...,
 t(285:'289':'292':'294,295':'298,299':'301':308)...,
 t(309:332),t(333:'359':361),t(362:366)...,
 t('367,368':'370,371':372),t(373:384)...,
 t(385:400),t(401:428),t(429:'468':'470')...,
 t(471:497),t(498:521),t(522:535)...,
 t(536:'542,543':'545'),t(546:551),t(552:566)...,
 t(567:580),t(581:589),t(590:594),t(595:596)...,
 t(597:600)]
```

Figure 3.15: Practically generated time scale set.

$$u(t) = -K.x(t) = -\begin{bmatrix} K_{\varphi} & K_{\varphi^{\Delta}} & K_x & K_{x^{\Delta}} \end{bmatrix} \begin{bmatrix} \varphi(t) \\ \varphi^{\Delta}(t) \\ x(t) \\ x^{\Delta}(t) \end{bmatrix}. \tag{3.84}$$

We place the poles of the system in the stability region that is relative to this time scale following what has been stated in theorem 1.4.2.
The maximum value of this time scale graininess is $\overline{\mu} = 5$. It conducts us to impose the following Hilger plane poles to the system $p = [-0.15, -0.1, -0.13, -0.17]$. Using the cylindrical transformation (see equation 1.3 in definition 1.2.13) we impose the following eigen values to the system $eig = [-0.1055, -0.0787, -0.09559, -0.1145]$. the simulation has given the following results

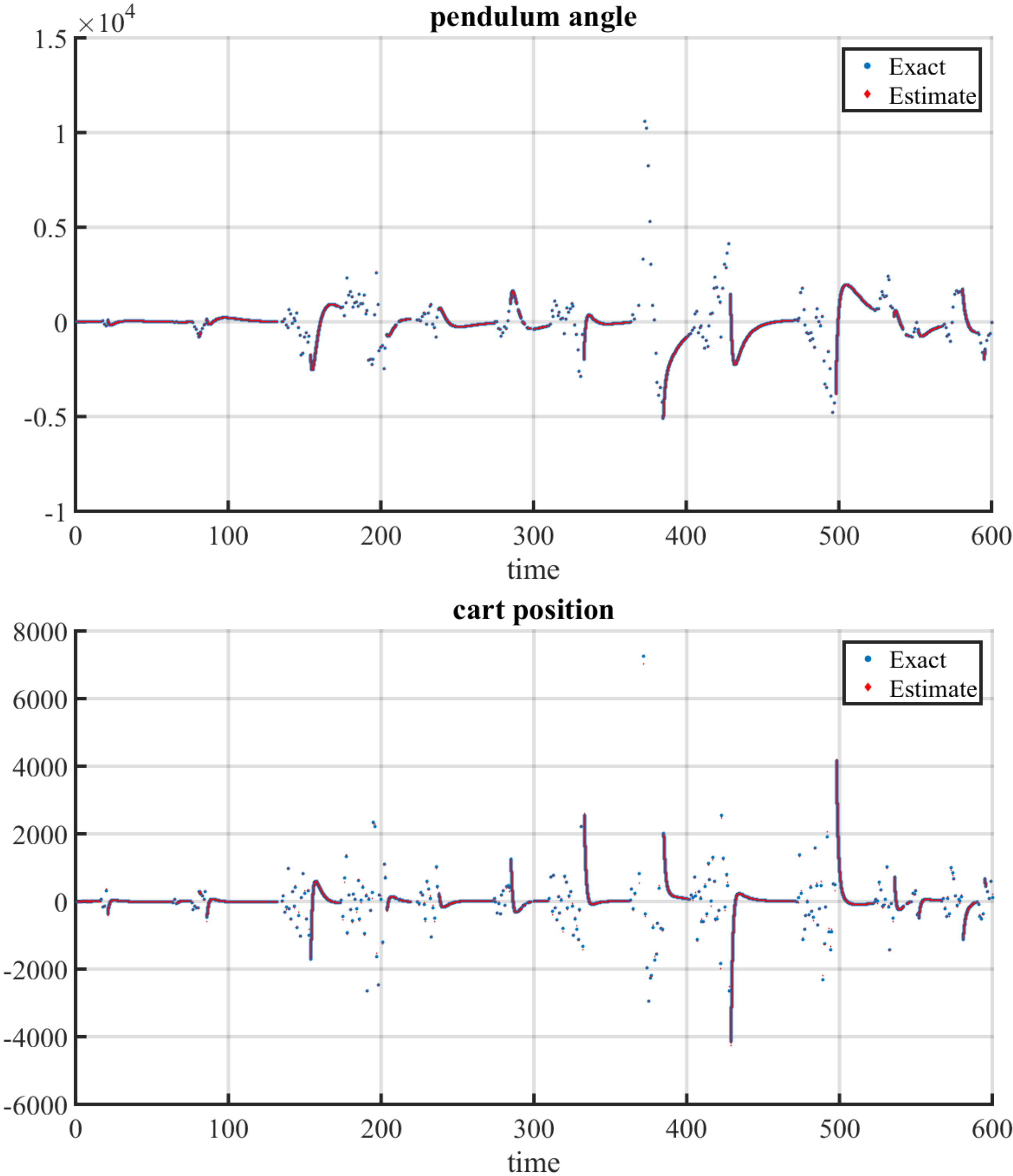

Figure 3.16: Observer based control simulation in noisy scenario

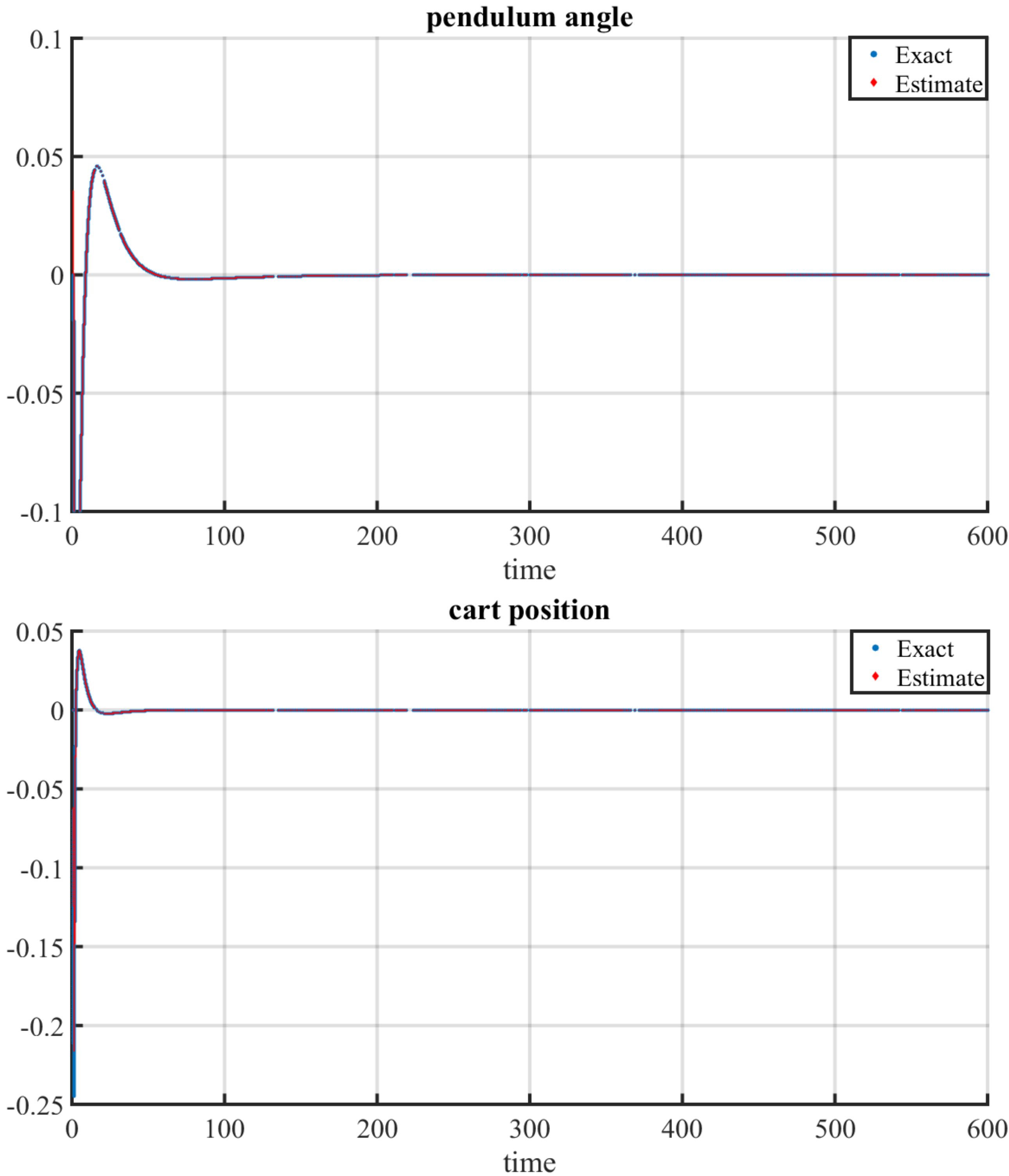

Figure 3.17: Observer based control simulation in non noisy scenario

Comments on results

In this simulation, we have driven the eigenvalues to the stability region as mentioned previously. The reference for output signals is the origin.
First, the observer based control succeed to stabilise the system in this time scale in both scenarios.
When the graininess increases both output signals deviate from their reference in the noisy scenario. However, the signals are bounded in the totality of the time scale on which the simulation is run.
According to theorem 1.4, the system states should be uniformly exponentially stable which is not the case in this simulation.
The stability has been deteriorated by the impact of the noise on the system. These noises drive system poles out of the stability region of the Hilger complex plane that shrinks under high graininess values.
We deduce from this simulation that high graininess values badly impact time scale systems robustness and constitute a threat to their stability. It also induces an increase in the noise impact on the system stability.
If this deduction is correct, the suppression of noises should drive the system to converge exponentially to its reference. This phenomenon is observed in the figure 3.17.

3.6.4 LQG/LTR

In this part we consider an altered version of the system 3.83.
In this case we turn the B matrix to

$$B = \begin{bmatrix} 50 & 0 \\ 0 & 0 \\ 0 & 13 \\ 0 & 0 \end{bmatrix}$$

The system here is submitted to process and measurement noises with zero mean and respectively the deviations $Q = 6$ and $R = 0.2$. We also induce a variation of system parameters to assess the controllers robustness, we alter the state matrix parameters by 0.5%.
We define the following criteria

$$J = \int_0^\infty (x^T M x + u^T N u) dt \qquad (3.85)$$

where $M = \begin{bmatrix} 10 & 0 & 0 & 0 \\ 0 & 0 & 0 & 0 \\ 0 & 0 & 30 & 0 \\ 0 & 0 & 0 & 0 \end{bmatrix}$ and $N = \begin{bmatrix} 1 & 0 \\ 0 & 1 \end{bmatrix}$.

We have two possible control strategies to design our controller using LTR approach.

case1: $\begin{cases} K_p = (I + \mu(t)A)PC^T(R + \mu(t)CPC^T)^{-1}. \\ K_c = \frac{[CB]^{-1}C(I+\mu(t)A)}{\mu(t)}. \end{cases}$

where Q and R are system noises deviation matrices. K_c and K_p are controller and observer gains respectively.

case2: $\begin{cases} K_p = \frac{(I+\mu(t)A)B[CB]^{-1}}{\mu(t)}. \\ K_c = (N + \mu(t)B^T S^\sigma B)^{-1} B^T S^\sigma (I + \mu(t)A). \end{cases}$

where S solves 1.5.

the time scale envisaged in this simulation is the union of uniform discrete and other non-uniform sets with a larger graininess.

$\mathbb{T} = [\mathbb{Z}, 1, 1.5, 3, 1, 2.5, 1, 1.5, 2.9, \mathbb{Z}, 2, 1, 1.4, 2.8, 1.4, 6, 1.03, \mathbb{Z}, 2, 3.4, 1.9, 6, 1.8, 0.8, \mathbb{Z}]$.

The simulations have given the following results ($ref = [150, 300]$)

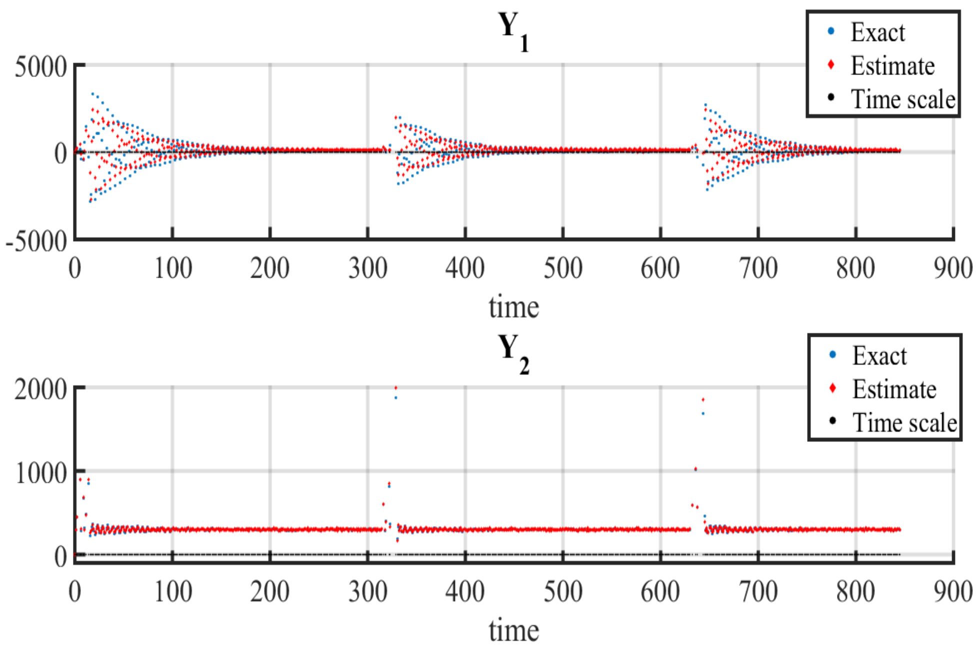

Figure 3.18: LTR controller case1 simulation

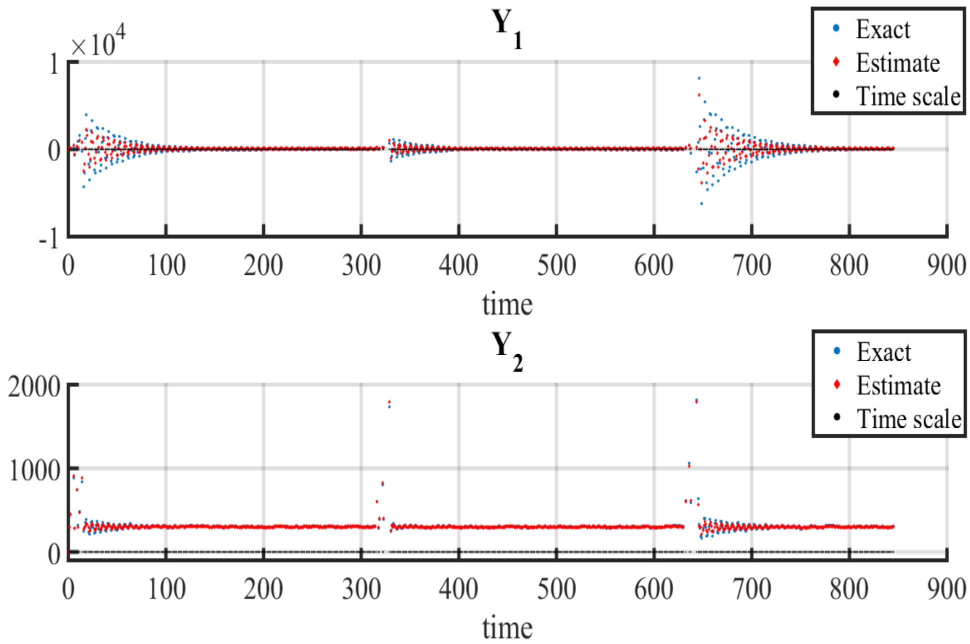

Figure 3.19: LTR controller case2 simulation

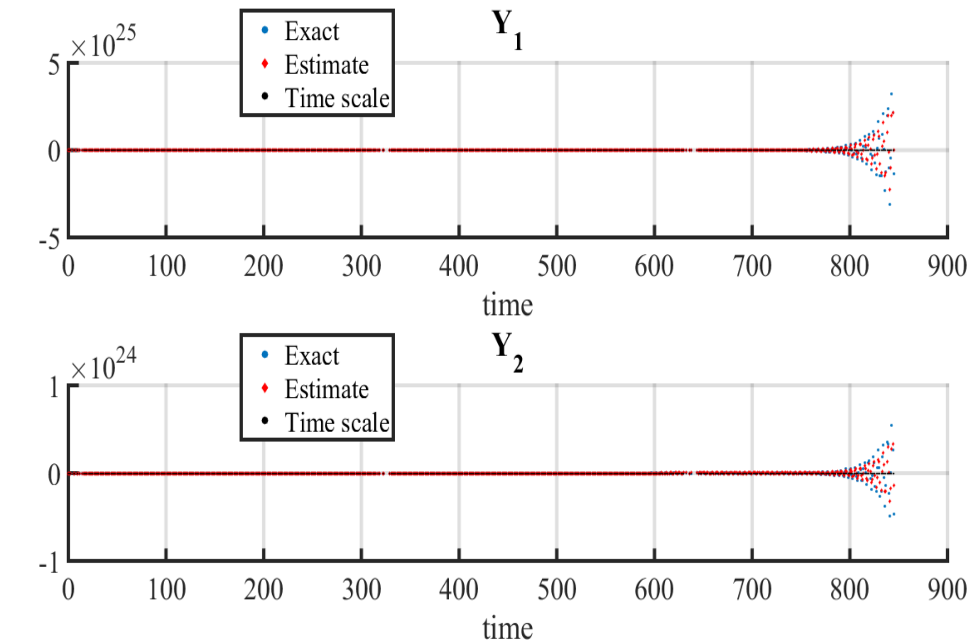

Figure 3.20: LQG case controller simulation

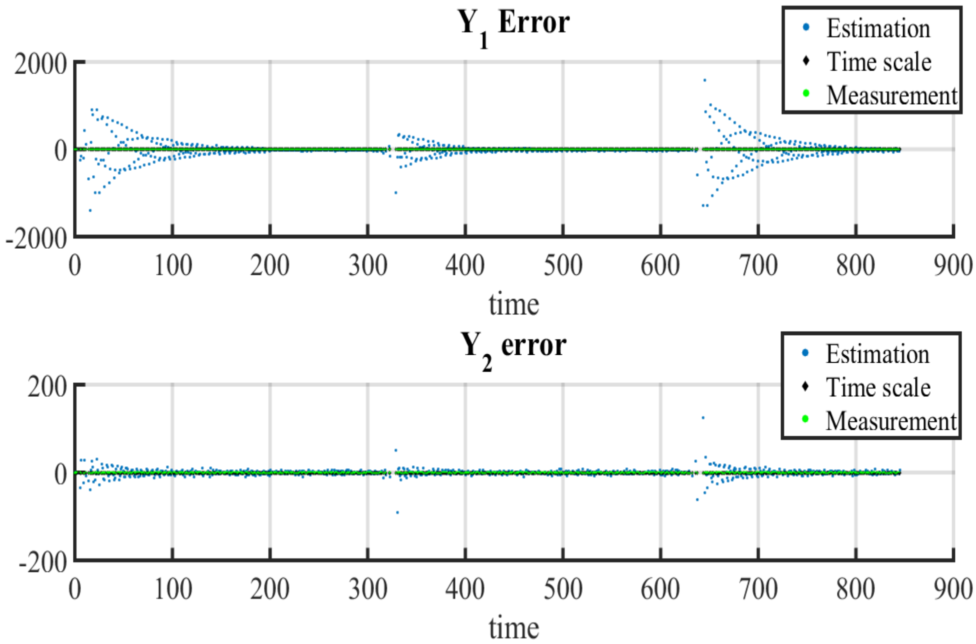

Figure 3.21: LTR controller case1 estimation error

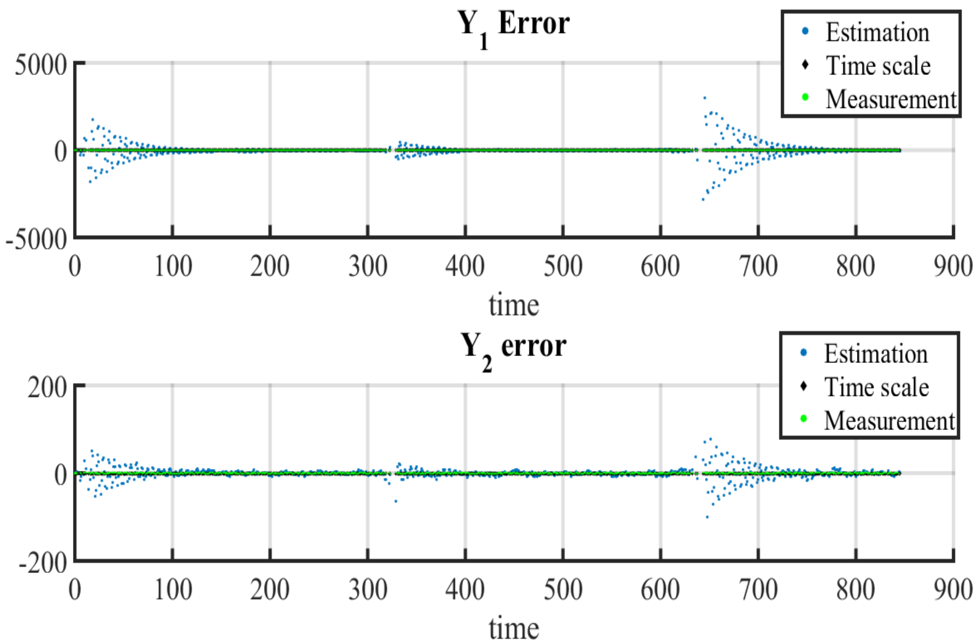

Figure 3.22: LTR controller case2 estimation error

Comments on results

From figure 3.15 and figure 3.16 we can see that both LTR approaches give interesting results.
This controller succeed to recover the targeted robustness properties in this simulation while the LQG fails to stabilise the system.
Regarding to the estimation error, the first case LTR controller gives better estimation performances than the second case.

3.7 Adaptive non linear fault estimation observers

The purpose of this section is to generalize the non linear adaptive observers introduced in chapter 2 to time scale systems. We will do that by giving a generalization of theorems 2.3.3, 2.3.4 and 2.3.5 to time scale systems.
First we start by considering the lipschitzian nonlinear time scale system described by equations

$$\begin{cases} x(t)^{\Delta} = Ax(t) + \Phi(x(t), u(t)) + Ef(t), \\ y(t) = Cx(t), \end{cases} \tag{3.86}$$

where $x \in \mathbb{R}^n$ is the state vector, $u \in \mathbb{R}^m$ the input vector, $y \in \mathbb{R}^p$ the output vector, $\Phi : \mathbb{R}^n \times \mathbb{R}^m \to \mathbb{R}^n$ is a known nonlinear function, $f \in \mathbb{R}^q$ an unknown vector that models faults effect on the system which is to identify. $A \in \mathbb{R}^{n \times n}$, $B \in \mathbb{R}^m$, $E \in \mathbb{R}^{n \times q}$ and $C \in \mathbb{R}^{n \times p}$ are constant matrices with $rank(C) = p$ and $rank(E) = q$. t belongs to some bounded graininess time scale $\mathbb{T}$.
The pair (C, A) is supposed to be observable and the non linear function $\Phi(x, u)$ doesn't alter the system observability.
Moreover all hypotheses 2.1-2.5 are admitted to be satisfied. We introduce now some useful relations. (Young inequality)

Lemma 3.7.1. *[1] for all non strictly positive reals a and b and all strictly positive reals p and q such that $\frac{1}{p} + \frac{1}{q} = 1$ the following inequality always holds*

$$ab \leq \frac{a^p}{p} + \frac{b^q}{q}.$$

A frequent case of the Young inequality is

Lemma 3.7.2. *[1] For all reals a and b and all reals $\epsilon > 0$ the following inequality holds*

$$ab \leq \frac{a^2}{2\epsilon} + \frac{\epsilon b^2}{2}.$$

in the case where a and b are vectors, the inequality above becomes

$$a^T b \leq \frac{\|a\|^2}{2\epsilon} + \frac{\epsilon \|b\|^2}{2} \tag{3.87}$$

3.7.1 Fast fault estimation observer

First, we start by stating the time scale equivalent of the hypothesis 2.5.

Hypothesis 3.7. *The delta derivative of the faults vector satisfies the following condition*

$$\|f^\Delta\| \leq \gamma. \tag{3.88}$$

where γ is a known positive constant.

The fast fault estimation observer that corresponds to system 3.86 is given by equations

$$\begin{cases} \hat{x}^\Delta = A\hat{x} + \Phi(\hat{x}, u) + E\hat{f} + L(y - C\hat{x}), \\ \hat{f}^\Delta = \Gamma F(\sigma \times (y - C\hat{x}) + y^\Delta - C\hat{x}^\Delta), \end{cases} \tag{3.89}$$

where σ is a positive constant. From 3.86 and 3.89, we deduce the estimation errors dynamics $\tilde{x}$ and $\tilde{f}$ that are governed by equations

$$\begin{cases} \tilde{x}^\Delta = (A - LC)\tilde{x} + \tilde{\Phi} + E\tilde{f}, \\ \tilde{f}^\Delta = f^\Delta - \Gamma F(\sigma C\tilde{x} + C\tilde{x}^\Delta), \end{cases} \tag{3.90}$$

where $\tilde{\Phi} = \Phi(x, u) - \Phi(\hat{x}, u)$.
To overcome the derivative evaluation issue, we can rewrite the second equation in 3.89 in the form

$$\begin{cases} \hat{f} = \Gamma F(w + y - C\hat{x}, \\ w^\Delta = \sigma \times (y - C\hat{x}). \end{cases} \tag{3.91}$$

The following theorem ensures the observer stability

Theorem 3.7.1. *We consider the system 3.86 and the observer 3.89.*
If there exist five positive constants ϵ, ϵ_1, ϵ_2, ϵ_3 and ϵ_4 and two matrices $P \in \mathbb{R}^{n\times n}$ positive definite and symmetric and $F \in \mathbb{R}^{q\times p}$ such that

$$\begin{bmatrix} Q_{11} & Q_{22} & Q_{13} \\ * & Q_{22} & Q_{23} \\ * & * & Q_{33} \end{bmatrix} < 0. \tag{3.92}$$

$$FC = E^T P[I + \mu(A - LC)]. \tag{3.93}$$

with $Q_{11} = [(A-LC)^T P[I+\mu(A-LC)]+P(A-LC)+l_\Phi^2\epsilon_1 I - \frac{\mu}{\sigma\epsilon_2}(\sigma I + A - LC)^T[I+\mu(A-LC)^T]P[I+\mu(A-LC)](\sigma I + A - LC) + \frac{\mu}{\sigma}[\sigma I + (A-LC)]^T C^T F^T \Gamma F C[\sigma I + (A-LC)]$.

$Q_{12} = [I+\mu(A-LC)^T]P + \frac{\mu}{\sigma}[\sigma I + (A-LC)]C^T F^T \Gamma F C$.

$Q_{13} = -\frac{1}{\sigma}(A-LC)^T[I+\mu(A-LC)]^T PE + \frac{\mu}{\sigma}[(\sigma I + A - LC)]^T C^T F^T \Gamma F C E$.

$Q_{22} = -\epsilon_1 I + \mu P - \frac{\mu}{\sigma\epsilon_3}[I+\mu(A-LC)]^T PP[I+\mu(A-LC)] + \frac{\mu}{\sigma}C^T F^T \Gamma F C$.

$Q_{23} = -\frac{1}{\sigma}[I+\mu(A-LC)]^T PE + \mu PE + \frac{\mu}{\sigma}C^T F^T \Gamma F C E$.

$Q_{33} = \frac{\epsilon}{\sigma}I - 2E^T(I+\mu(A-LC)]PE + \mu E^T PE - \frac{\mu}{\epsilon_4}E^T[I+\mu(A-LC)]^T PP[I+\mu(A-LC)E + \frac{\mu}{\sigma}E^T C^T F^T \Gamma F C E$.

Then the errors $\tilde{x}$ *and* $\tilde{f}$ *given by 3.90 converge to some neighborhood of the origin. Moreover, if* $f^\Delta = 0$ *then* $\tilde{x}$ *and* $\tilde{f}$ *converge asymptotically to zero.*

Proof. To prove this theorem, we consider the following Lyapunov function

$$V = \tilde{x}^T P \tilde{x} + \frac{1}{\sigma}\tilde{f}^T \Gamma^{-1}\tilde{f}. \tag{3.94}$$

Using *iii*) in theorem 1.2.2 and *iv*) in theorem 1.2.1 we obtain

$$V^\Delta = \tilde{x}^{\Delta T} P \tilde{x} + \frac{1}{\sigma}\tilde{f}^{\Delta T}\Gamma^{-1}\tilde{f} + \tilde{x}^{\sigma T} P \tilde{x}^\Delta + \frac{1}{\sigma}\tilde{f}^{\sigma T}\Gamma^{-1}\tilde{f}^\Delta. \tag{3.95}$$

Developing each term, using equation 3.97 and rearranging them yields

$V^\Delta = \tilde{x}^T[(A-LC)^T P + P(A-LC) + \mu(A-LC)^T P(A-LC)]\tilde{x} + 2\tilde{x}^T P\tilde{\Phi} + \frac{2}{\sigma}\tilde{f}^T\Gamma^{-1}f^\Delta - \frac{2}{\sigma}\tilde{f}^T E^T P[I+\mu(A-LC)]\tilde{x}^\Delta + 2\mu\tilde{x}^T(A-LC)^T P\tilde{\Phi} + 2\mu\tilde{\Phi}^T PE\tilde{f} + \mu\tilde{\Phi}^T P\tilde{\Phi} + \mu\tilde{f}^T E^T PE\tilde{f} + \frac{\mu}{\sigma}f^{\Delta T}\Gamma^{-1}f^\Delta - \frac{2\mu}{\sigma}f^{\Delta T}E^T P[I+\mu(A-LC)](\sigma\tilde{x} + \tilde{x}^\Delta) + \frac{\mu}{\sigma}(\sigma C\tilde{x} + C\tilde{x}^\Delta)^T F^T \Gamma F(\sigma C\tilde{x} + C\tilde{x}^\Delta)$.

On the other hand, from the Lipschitz condition 2.9, we obtain

$$l_\Phi^2\epsilon_1\tilde{x}^T\tilde{x} - \epsilon_1\tilde{\Phi}^T\tilde{\Phi} \geq 0. \tag{3.96}$$

where ϵ_1 is a positive constant. Now we add the left part of inequality 3.96 to the right part of the equation above.

$V^\Delta \leq \tilde{x}^T[(A-LC)^T P[I+\mu(A-LC)]\tilde{x} + 2\tilde{x}^T[I+\mu(A-LC)^T P\tilde{\Phi} + l_\Phi^2\epsilon_1\tilde{x}^T\tilde{x} - \epsilon_1\tilde{\Phi}^T\tilde{\Phi} + \frac{2}{\sigma}\tilde{f}^T\Gamma^{-1}f^\Delta + 2\mu\tilde{\Phi}^T PE\tilde{f} + \mu\tilde{\Phi}^T P\tilde{\Phi} - \frac{2}{\sigma}\tilde{f}^T E^T P[I+\mu(A-LC)][(A-LC)\tilde{x} + \tilde{\Phi} + E\tilde{f}] + \mu\tilde{f}^T E^T PE\tilde{f} + \frac{\mu}{\sigma}f^{\Delta T}\Gamma^{-1}f^\Delta + \frac{\mu}{\sigma}(\sigma C\tilde{x} + C\tilde{x}^\Delta)^T F^T\Gamma F(\sigma C\tilde{x} + C[(A-LC)\tilde{x} + \tilde{\Phi} + E\tilde{f}]) - \frac{2\mu}{\sigma}f^{\Delta T}E^T P[I+\mu(A-LC)](\sigma\tilde{x} + (A-LC)\tilde{x} + \tilde{\Phi} + E\tilde{f})$.

Applying the young inequality to the terms $\frac{2}{\sigma}\tilde{f}^T\Gamma^{-1}f^\Delta$, $\frac{2\mu}{\sigma}f^{\Delta T}E^T P[I+\mu(A-LC)][\sigma\tilde{x} + (A-LC)\tilde{x}]$, $\frac{2\mu}{\sigma}f^{\Delta T}E^T P[I+\mu(A-LC)]\tilde{\Phi}$ and $\frac{2\mu}{\sigma}f^{\Delta T}E^T P[I+\mu(A-LC)]E\tilde{f}$ yields

$V^\Delta \leq \tilde{x}^T[(A-LC)^T P[I+\mu(A-LC)] + P(A-LC)]\tilde{x} + 2\tilde{x}^T[I+\mu(A-LC)^T P\tilde{\Phi} + l_\Phi^2\epsilon_1\tilde{x}^T\tilde{x} -$

$\epsilon_1\tilde{\Phi}^T\tilde{\Phi} + \frac{\epsilon}{\sigma}\tilde{f}^T\tilde{f} + \frac{1}{\sigma\epsilon}f^{\Delta T}\Gamma^{-1T}\Gamma^{-1}f^{\Delta} - \frac{2}{\sigma}\tilde{f}^T E^T P[I + \mu(A - LC)](A - LC)\tilde{x} - \frac{2}{\sigma}\tilde{f}^T E^T P[I + \mu(A - LC)]\tilde{\Phi} - \frac{2}{\sigma}\tilde{f}^T E^T P[I + \mu(A - LC)]E\tilde{f} + 2\mu\tilde{\Phi}^T PE\tilde{f} + \mu\tilde{\Phi}^T P\tilde{\Phi} + \mu\tilde{f}^T E^T PE\tilde{f} + \frac{\mu}{\sigma}f^{\Delta T}\Gamma^{-1}f^{\Delta} + \frac{\mu}{\sigma}[\sigma\tilde{x} + (A - LC)\tilde{x} + \tilde{\Phi} + E\tilde{f}]^T C^T F^T \Gamma FC[\sigma\tilde{x} + (A - LC)\tilde{x} + \tilde{\Phi} + E\tilde{f}] - \frac{\mu\epsilon_2}{\sigma}f^{\Delta T}E^T E f^{\Delta} - \frac{\mu}{\sigma\epsilon_2}\tilde{x}^T(\sigma I + A - LC)^T[I + \mu(A - LC)]^T PP[I + \mu(A - LC)](\sigma I + A - LC)\tilde{x} - \frac{\mu\epsilon_3}{\sigma}f^{\Delta T}E^T E f^{\Delta} - \frac{\mu}{\sigma\epsilon_3}\tilde{\Phi}^T[I + \mu(A - LC)]^T PP[I + \mu(A - LC)]\tilde{\Phi} - \frac{\mu\epsilon_4}{\sigma}f^{\Delta T}E^T E f^{\Delta} - \frac{\mu}{\sigma\epsilon_4}\tilde{f}^T E^T[I + \mu(A - LC)]^T PP[I + \mu(A - LC)]E\tilde{f}.$

After rearranging terms again the inequality above can be rewritten into the form

$$V^{\Delta} \leq \chi^T \begin{bmatrix} Q_{11} & Q_{22} & Q_{33} \\ * & Q_{22} & Q_{23} \\ * & * & Q_{33} \end{bmatrix} \chi + f^{\Delta T}[\frac{\Gamma^{-1T}\Gamma^{-1}}{\sigma\epsilon} + \frac{\mu}{\sigma}\Gamma^{-1} - \frac{\mu\epsilon_2}{\sigma}E^T E - \frac{\mu\epsilon_3}{\sigma}E^T E - \frac{\mu\epsilon_4}{\sigma}E^T E]f^{\Delta}.$$

where $\chi = \begin{bmatrix} \tilde{x} \\ \tilde{\Phi} \\ \tilde{f} \end{bmatrix}$ and $Q_{ij\in\{1,2,3\}^2}$ are as stated in theorem 3.7.1.

If Hypothesis 3.7 is satisfied and taking $\begin{bmatrix} Q_{11} & Q_{12} & Q_{13} \\ * & Q_{22} & Q_{23} \\ * & * & Q_{33} \end{bmatrix} = Z$ and $[\frac{\Gamma^{-1T}\Gamma^{-1}}{\epsilon} + \mu\Gamma^{-1} - \mu\epsilon_2 E^T E - \mu\epsilon_3 E^T E - \mu\epsilon_4 E^T E] = R$ leads to

$$V^{\Delta} \leq -\lambda_{min}(-Z)\left\|\chi\right\|^2 + \frac{1}{\sigma}\gamma^2\lambda_{max}(R). \tag{3.97}$$

It means that errors $\tilde{x}$ and $\tilde{f}$ converge to some neighborhood around the origin if inequality 3.92 is satisfied.
In the case where $f^{\Delta} = 0$, the errors $\tilde{x}$ and $\tilde{f}$ converge asymptotically to zero. □

3.7.2 Proportional integral observer

The conventional PI observer that corresponds to the system 3.86 is given by

$$\hat{x}^{\Delta} = A\hat{x} + \Phi(\hat{x}, u) + E\int_0^t L_2(y - C\hat{x})\Delta t + L_1(y - C\hat{x}). \tag{3.98}$$

Setting $\hat{f} = \int_0^t L_2(y - C\hat{x})\Delta t$, we can rewrite 3.98 into the form

$$\begin{cases} \hat{x}^{\Delta} = A\hat{x} + \Phi(\hat{x}, u) + E\hat{f} + L_1(y - C\hat{x}). \\ \hat{f}^{\Delta} = L_2(y - C\hat{x}). \end{cases} \tag{3.99}$$

To simplify the stability analysis of this observer we set it into the form

$$\hat{\mathcal{X}}^{\Delta} = \mathcal{A}\hat{\mathcal{X}} + \Phi(\hat{\mathcal{X}}, u) + \mathcal{L}(y - \mathcal{C}\hat{\mathcal{X}}). \tag{3.100}$$

where $\hat{\mathcal{X}} = \begin{bmatrix} \hat{x} \\ \hat{f} \end{bmatrix}$, $\mathcal{A} = \begin{bmatrix} A & E \\ 0_{q\times n} & 0_{q\times q} \end{bmatrix}$, $\mathcal{C} = \begin{bmatrix} C & 0_{p\times q} \end{bmatrix}$, $\Phi(\mathcal{X}, \hat{u}) = \begin{bmatrix} \Phi(\hat{x}, u) \\ 0_{q\times 1} \end{bmatrix}$, $\mathcal{L} = \begin{bmatrix} L_1 \\ L_2 \end{bmatrix}$.

Let $\tilde{\mathcal{X}} = \mathcal{X} - \hat{\mathcal{X}}$ where $\mathcal{X} = \begin{bmatrix} x^T & f^T \end{bmatrix}^T$ and assuming that $f^\Delta = 0$. The estimation error dynamic equation is given by

$$\tilde{\mathcal{X}}^\Delta = (\mathcal{A} - \mathcal{L}\mathcal{C})\tilde{\mathcal{X}} + \tilde{\Phi}. \tag{3.101}$$

where $\tilde{\Phi} = \Phi(\mathcal{X}, u) - \Phi(\hat{\mathcal{X}}, u)$.
Notice that the observability condition must always be satisfied to design this observer.
We announce the following theorem now

Theorem 3.7.2. *Let the system 3.86 and the observer 3.99. For $f^\Delta = 0$, the estimation error of the augmented state $\tilde{\mathcal{X}}$ given by 3.101 is asymptotically stable if there exist a positive constant ϵ and two matrices $\mathcal{P} \in \mathbb{R}^{(n+q)\times(n+q)}$ symmetric and positive definite, and $\mathcal{M} \in \mathbb{R}^{(n+q)\times p}$ such that*

$$\begin{bmatrix} Q_{11} & Q_{12} \\ * & -\epsilon I + \mu\mathcal{P} \end{bmatrix} < 0. \tag{3.102}$$

where $Q_{11} = \mathcal{A}^T\mathcal{P} - \mathcal{C}^T\mathcal{M}^T + \mathcal{P}\mathcal{A} - \mathcal{M}\mathcal{C} + l_\Phi^2\epsilon I + \mu\mathcal{A}^T P\mathcal{A} - \mu\mathcal{A}^T\mathcal{M}\mathcal{C} - \mu\mathcal{C}^T\mathcal{M}^T\mathcal{A} + \mu\mathcal{C}^T\mathcal{M}^T\mathcal{P}^{-1}\mathcal{M}\mathcal{C}$.

$Q_{12} = \mathcal{P} + \mu(\mathcal{A}^T\mathcal{P} - \mathcal{C}^T\mathcal{M}^T)$.

The observer gain is computed as follows

$$\mathcal{L} = \mathcal{P}^{-1}\mathcal{M}. \tag{3.103}$$

Proof. Let's consider the Lyapunov function

$$V = \tilde{\mathcal{X}}^T\mathcal{P}\tilde{\mathcal{X}}. \tag{3.104}$$

The delta derivative of V is

$$V^\Delta = \tilde{\mathcal{X}}^{\Delta T}\mathcal{P}\tilde{\mathcal{X}} + \tilde{\mathcal{X}}^{\sigma T}\mathcal{P}\tilde{\mathcal{X}}^\Delta. \tag{3.105}$$

Developing each term in 3.105 and rearranging them yields

$V^\Delta = \tilde{\mathcal{X}}^T[(\mathcal{A}-\mathcal{L}\mathcal{C})^T\mathcal{P}+[I+\mu(\mathcal{A}-\mathcal{L}\mathcal{C})]^T\mathcal{P}(\mathcal{A}-\mathcal{L}\mathcal{C})]\tilde{\mathcal{X}}+2\tilde{\mathcal{X}}^T[I+\mu(\mathcal{A}-\mathcal{L}\mathcal{C})]^T\mathcal{P}\tilde{\Phi}+\mu\tilde{\Phi}^T\mathcal{P}\tilde{\Phi}$.

From Lipschitz condition (i.e.$l_\Phi^2\epsilon\tilde{\mathcal{X}}^T\tilde{\mathcal{X}} - \epsilon\tilde{\Phi}^T\tilde{\Phi} \geq 0$) we have

$V^\Delta \leq \tilde{\mathcal{X}}^T[(\mathcal{A} - \mathcal{L}\mathcal{C})^T\mathcal{P} + [I + \mu(\mathcal{A} - \mathcal{L}\mathcal{C})]^T\mathcal{P}(\mathcal{A} - \mathcal{L}\mathcal{C})]\tilde{\mathcal{X}} + 2\tilde{\mathcal{X}}^T[I + \mu(\mathcal{A} - \mathcal{L}\mathcal{C})]^T\mathcal{P}\tilde{\Phi} + \mu\tilde{\Phi}^T\mathcal{P}\tilde{\Phi} + l_\Phi^2\epsilon\tilde{\mathcal{X}}^T\tilde{\mathcal{X}} - \epsilon\tilde{\Phi}^T\tilde{\Phi}$.

Now using the substitution $\mathcal{L} = \mathcal{P}^{-1}\mathcal{M}$, V^{Δ} satisfies

$$V^{\Delta} \leq \xi^T \mathcal{Z} \xi, \tag{3.106}$$

where

$$\xi = \begin{bmatrix} \tilde{\mathcal{X}}^T & \tilde{\Phi}^T \end{bmatrix}^T, \tag{3.107}$$

and

$$\mathcal{Z} = \begin{bmatrix} Q_{11} & Q_{12} \\ * & -\epsilon I + \mu \mathcal{P} \end{bmatrix}. \tag{3.108}$$

where Q_{11} and Q_{12} are as stated in theorem 3.7.2.
It's obvious now that if condition 3.102 is satisfied $\tilde{\mathcal{X}}$ tends asymptotically to zero. □

3.7.3 PI H_∞ observer

In this subsection we adapt the H_∞ filtering with the PI observer to time scales with the purpose to enhance its performances when $f^{\Delta} \neq 0$.
First we start by announcing a time scale version of the 2.6.

Hypothesis 3.8. *the function f^{Δ} has a finite energy,i.e.,*

$$\int_0^{\infty} f^{\Delta T} f^{\Delta} \Delta t < \infty. \tag{3.109}$$

We reconsider the equation 3.101 for the case $f^{\Delta} \neq 0$

$$\tilde{\mathcal{X}}^{\Delta} = (\mathcal{A} - \mathcal{L}\mathcal{C})\tilde{\mathcal{X}} + \tilde{\Phi} + \mathcal{E} f^{\Delta}, \tag{3.110}$$

where $\mathcal{E} = \begin{bmatrix} 0_{q \times n} & I \end{bmatrix}^T$. We want the observer gain $\mathcal{L}$ to satisfy the conditions

$$\begin{cases} \lim\limits_{t \to \infty} \tilde{\mathcal{X}} = 0 & \text{for} \quad f^{\Delta} = 0, \\ \displaystyle\int_0^{\infty} \tilde{\mathcal{X}}^T \mathcal{D} \tilde{\mathcal{X}} \Delta t < \lambda \int_0^{\infty} f^{\Delta T} f^{\Delta} \Delta t & \text{for} \quad f^{\Delta} \neq 0. \end{cases} \tag{3.111}$$

where λ is a positive constant and $\mathcal{D}$ a symmetric semi positive definite matrix .
We announce now the theorem that ensures the H_∞ filter stability.

Theorem 3.7.3. *Let the system 3.86 and the observer 3.99. If there exist two real positive constants ϵ and λ and two matrices $\mathcal{P} \in \mathbb{R}^{(n+q)\times(n+q)}$ symmetric and positive definite, and $\mathcal{M} \in \mathbb{R}^{(n+q)\times p}$ such that*

$$\begin{bmatrix} Q_{11} & Q_{12} & Q_{13} \\ * & Q_{22} & Q_{23} \\ * & * & Q_{33} \end{bmatrix} < 0, \tag{3.112}$$

where $Q_{11} = \mathcal{A}^T\mathcal{P} - \mathcal{C}^T\mathcal{M}^T + \mathcal{P}\mathcal{A} - \mathcal{M}\mathcal{C} + \epsilon l_\Phi^2 + \mathcal{D} + \mu(\mathcal{A}^T\mathcal{P}\mathcal{A} - \mathcal{C}^T\mathcal{M}^T\mathcal{A} - \mathcal{A}^T\mathcal{M}\mathcal{C} + \mathcal{C}^T\mathcal{M}^T\mathcal{P}^{-1}\mathcal{M}\mathcal{C})$.

$Q_{12} = \mathcal{P} + \mu(\mathcal{A}^T\mathcal{P} - \mathcal{C}^T\mathcal{M}^T)$.
$Q_{13} = \mathcal{P}\mathcal{E} + \mu(\mathcal{A}^T\mathcal{P}\mathcal{E} - \mathcal{C}^T\mathcal{M}^T\mathcal{E})$.

$Q_{22} = -\epsilon I + \mu\mathcal{P}$, $Q_{23} = 2\mu\mathcal{P}\mathcal{E}$ *and* $Q_{33} = -\lambda I + \mu\mathcal{E}^T\mathcal{E}$.

And $\mathcal{D}$ *is defined such that it satisfies 3.111.*
Then, the estimation error of the augmented state $\tilde{\mathcal{X}}$ *satisfies the conditions in 3.111.*

Proof. Considering the Lyapunov function $V = \tilde{\mathcal{X}}^T\mathcal{P}\tilde{\mathcal{X}}$ and following the same steps in the proof of Theorem 3.7.2 when $f^\Delta \neq 0$ we obtain the inequality

$$V^\Delta \leq \xi^T\mathcal{Z}\xi + 2\xi^T\mathcal{P}\mathcal{E}f^\Delta, \tag{3.113}$$

where ξ and $\mathcal{Z}$ are defined by 3.107 and 3.108 respectively.
We consider now the criteria

$$J = \tilde{\mathcal{X}}^T\mathcal{D}\tilde{\mathcal{X}} - \lambda f^{\Delta T}f^\Delta + V^\Delta. \tag{3.114}$$

Inequality 3.113 implies

$$J \leq \tilde{\mathcal{X}}^T\mathcal{D}\tilde{\mathcal{X}} - \lambda f^{\Delta T}f^\Delta + \xi^T\mathcal{Z}\xi + 2\xi^T\mathcal{P}\mathcal{E}f^\Delta. \tag{3.115}$$

If we replace ξ and $\mathcal{Z}$ by their expressions we obtain

$$J \leq \begin{bmatrix} \tilde{\mathcal{X}} \\ \tilde{\Phi} \\ f^\Delta \end{bmatrix}^T \begin{bmatrix} Q_{11} & Q_{12} & Q_{13} \\ * & Q_{22} & Q_{23} \\ * & * & Q_{33} \end{bmatrix} \begin{bmatrix} \tilde{\mathcal{X}} \\ \tilde{\Phi} \\ f^\Delta \end{bmatrix}. \tag{3.116}$$

where $Q_{ij\in\{1,2,3\}^2}$ are defined as stated in 3.7.3. If the inequality 3.112 is satisfied thus $J < 0$ and subsequently

$$\int_0^\infty J\Delta t = \int_0^\infty (\tilde{\mathcal{X}}^T\mathcal{D}\tilde{\mathcal{X}} - \lambda f^{\Delta T}f^\Delta)\Delta t + V(\infty) - V(0) < 0. \tag{3.117}$$

Under zero initial conditions $V(0) = 0$, the inequality 3.117 implies

$$\int_0^\infty \tilde{\mathcal{X}}^T\mathcal{D}\tilde{\mathcal{X}}\Delta t < \lambda \int_0^\infty f^{\Delta T}f^\Delta\Delta t. \tag{3.118}$$

Moreover, if $f^\Delta = 0$, it's obvious that $J < 0$ implies $V^\Delta < 0$ and subsequently the asymptotic stability of $\tilde{\mathcal{X}}$ towards the origin. □

3.7.4 Simulation

We run a simulation for the system 2.4 on a time scale with random graininess.
the fault scenario is the same as in the chapter 2.
the simulations have given the following results

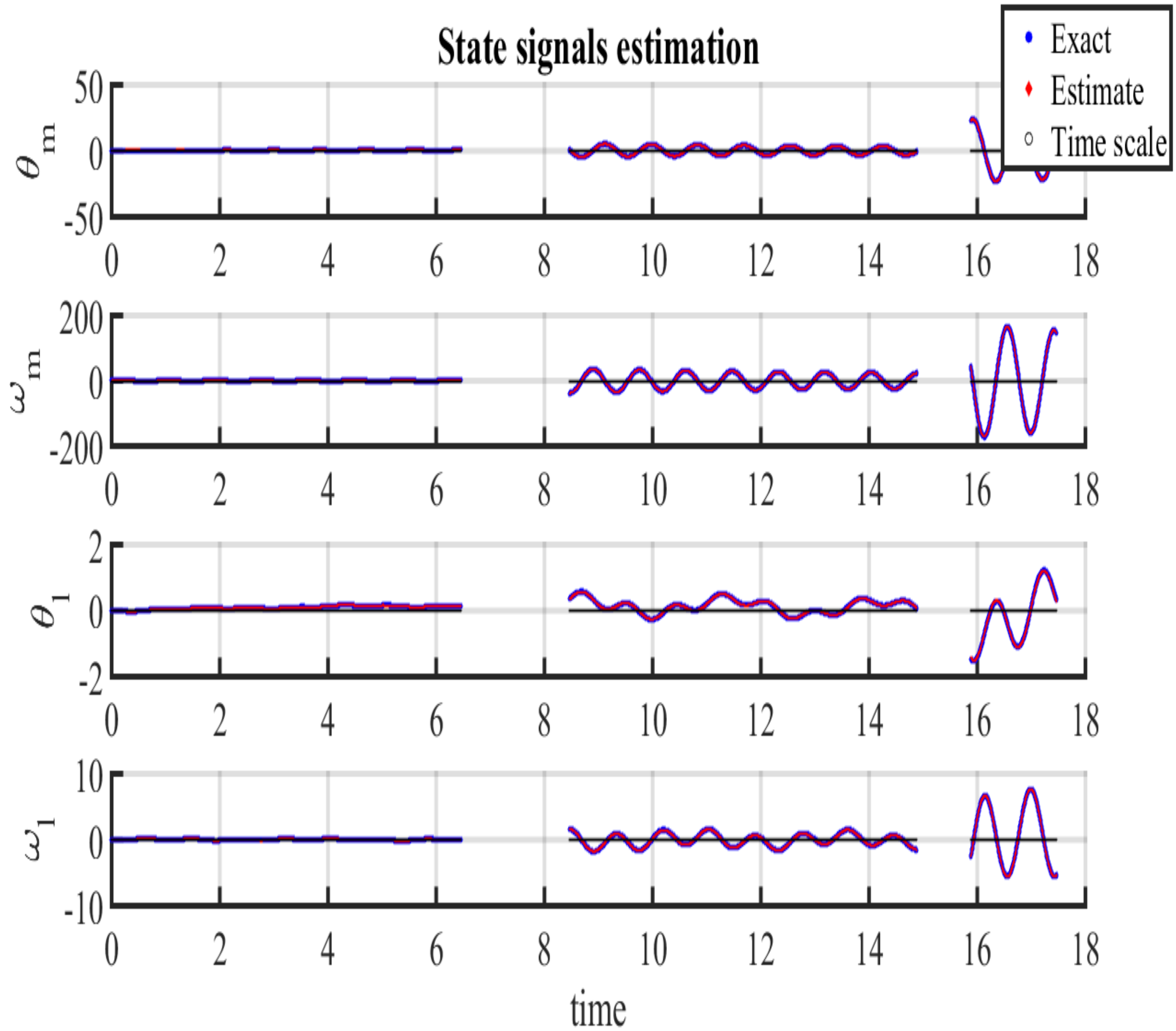

Figure 3.23: Time scale fast fault estimation observer state estimation.

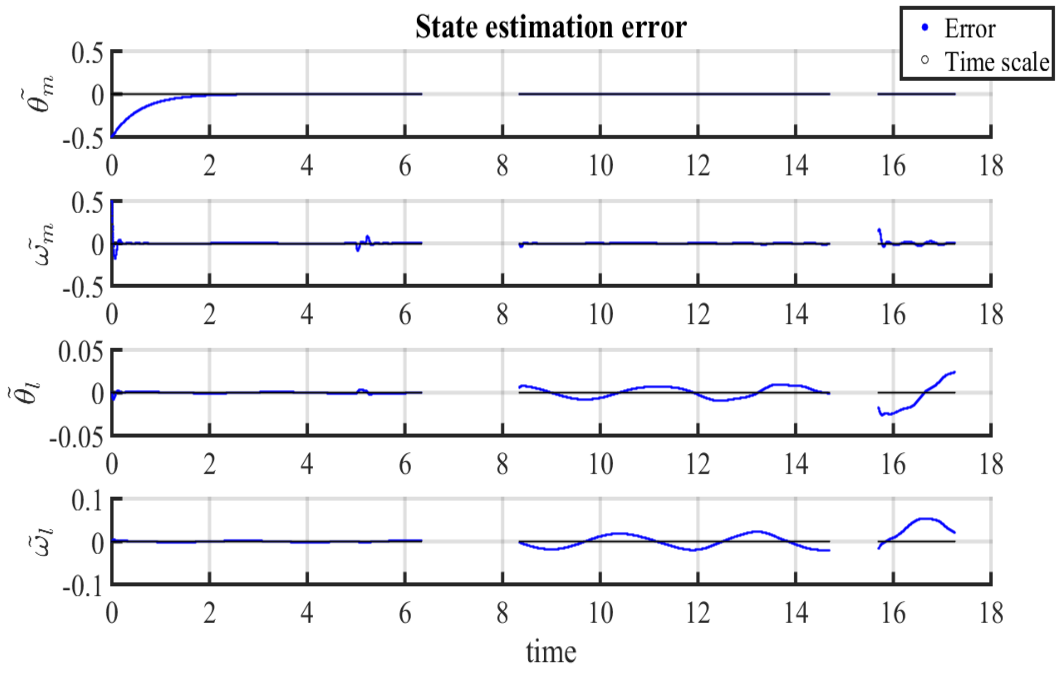

Figure 3.24: Time scale fast fault estimation observer state estimation error

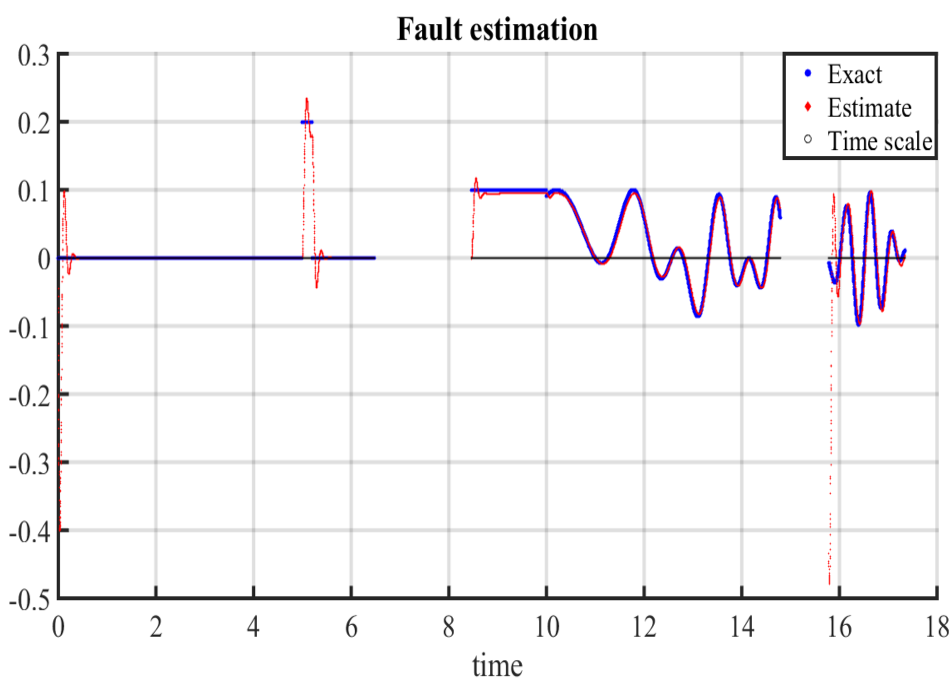

Figure 3.25: Time scale fast fault estimation observer fault estimation.

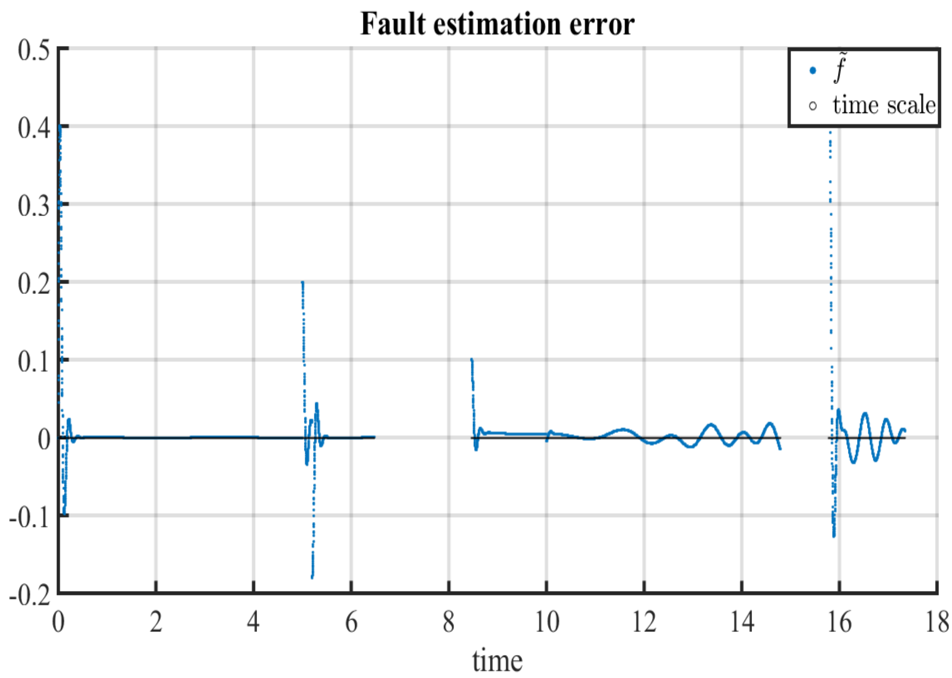

Figure 3.26: Time scale fast fault estimation observer fault estimation error.

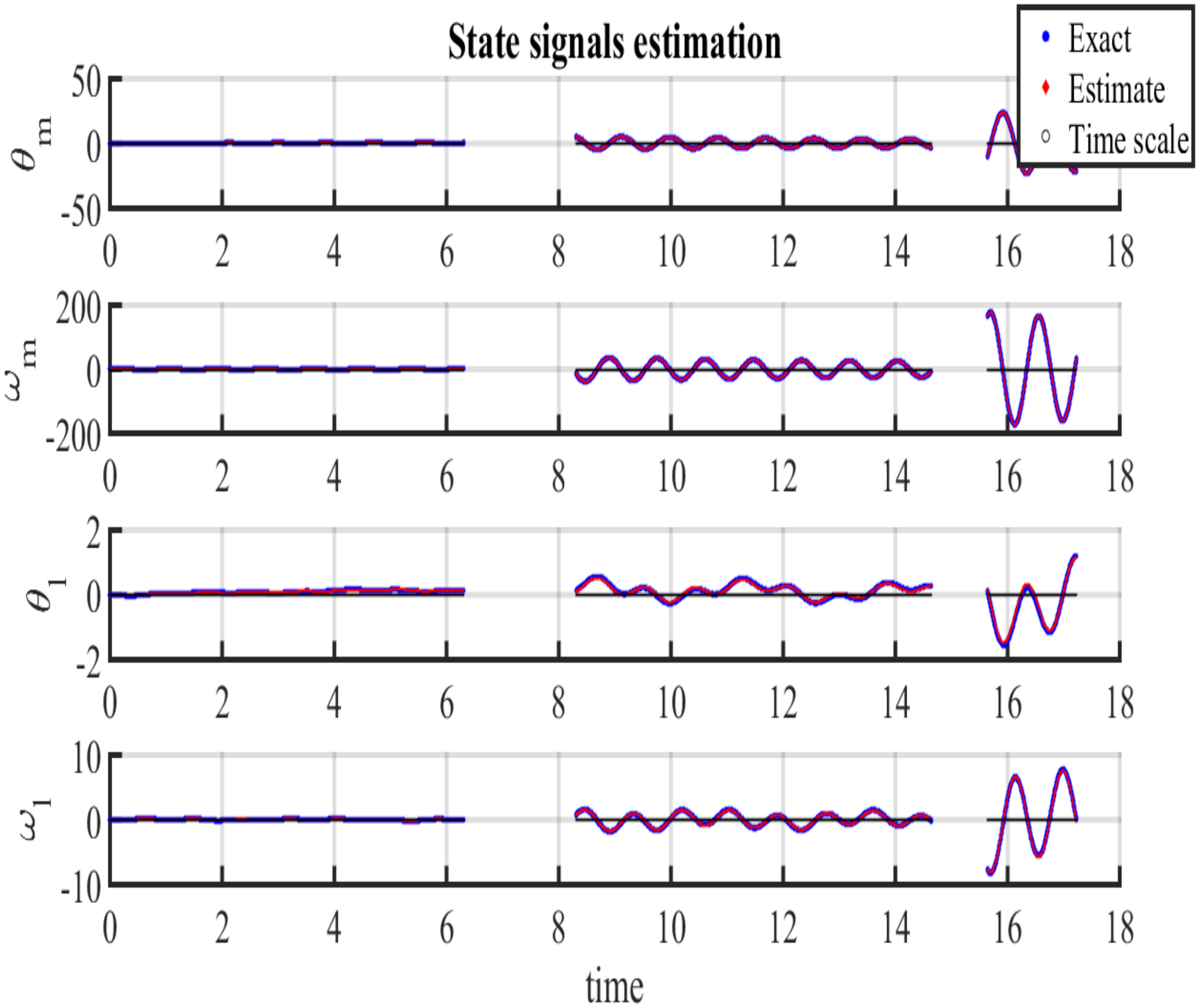

Figure 3.27: Time scale PI H_∞ observer state estimation.

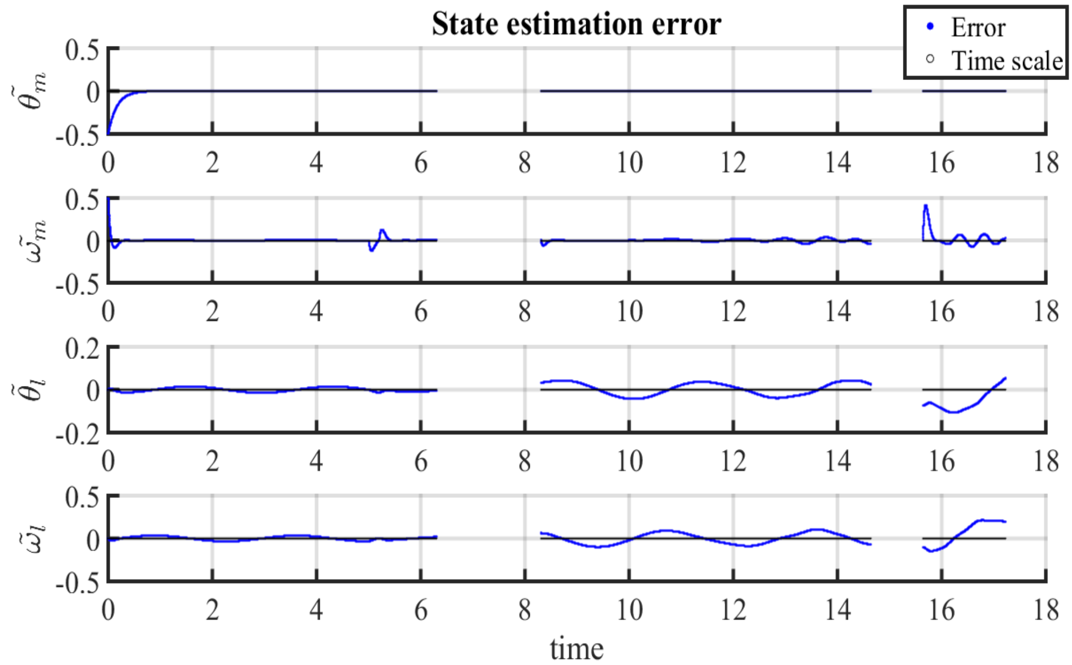

Figure 3.28: Time scale PI H_∞ observer state estimation error

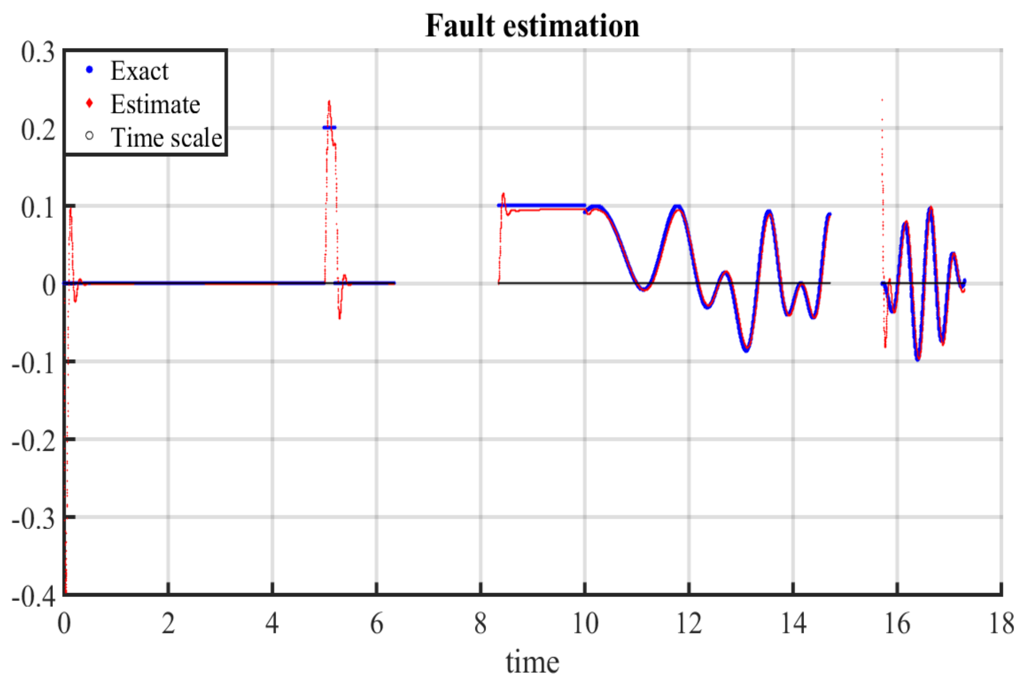

Figure 3.29: Time scale PI H_∞ observer fault estimation.

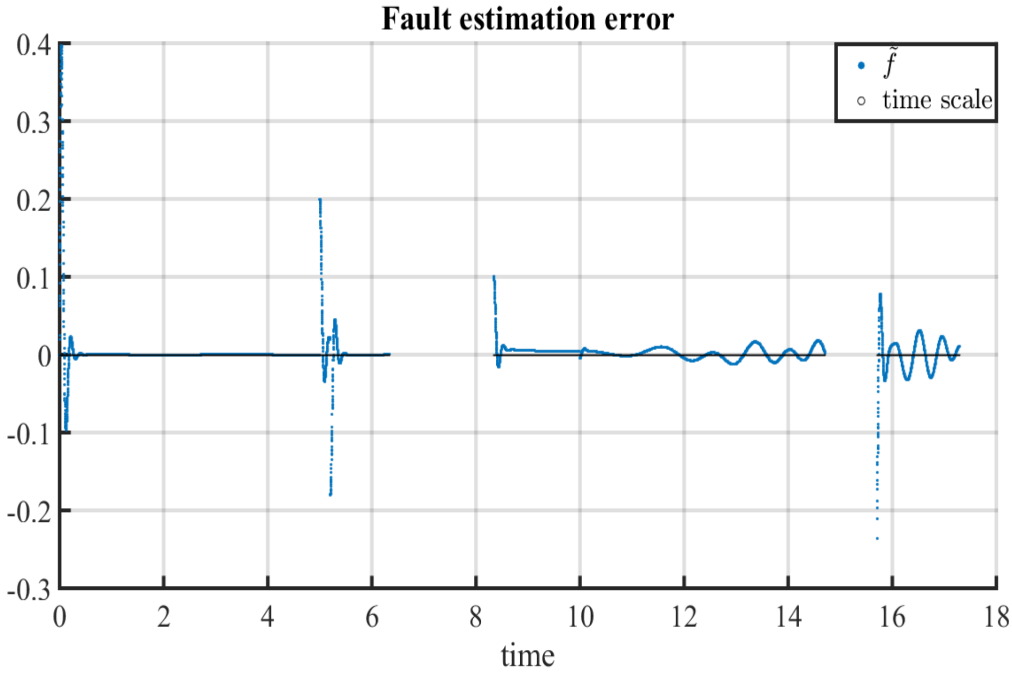

Figure 3.30: Time scale PI H_∞ observer fault estimation error.

Comments on results

In this simulation, we have chosen gains similar to the ones used in the chapter 2.
This choice is related to the fact that the graininess of the time scale is very small (to guarantee the system stability during the simulation), following this we can satisfy the conditions stated in theorems 3.7.2 and 3.7.1 by considering a continuous time scale which allows us to use the previous gains.
the simulation in both cases has given good results, the observers identify the fault signal accurately and perform the state estimation with high efficiency.
It's interesting to notice that the gaps don't deteriorate the state estimation quality as it is the case for the Kalman filter. The fault estimation doesn't even deviate from the fault signal after high graininess values when the fault signal is steady.
On the other hand, when the fault varies the same previously observed phenomenon for the time scale Kalman filter happens. The estimation error picks when the graininess reaches higher values.
The time scale fast fault estimation observer converges asymptotically when the fault signal delta derivative is equal to zero as it's expected from theorem 3.7.1.
The Proportional integral observer designed with H_∞ filtering technique has a satisfying performance in the fault varying case even if we notice a small phase shift in the fault estimation.

3.8 Conclusion

In this chapter, we have introduced observers newly designed for time scale systems.
These observers have shown interesting behaviors during simulations.
The estimation accuracy appeared to depend on the nature of the observer and the structure of the time scale on which the system evolves.
Indeed, the time scale Kalman filter introduced in [6] and its non linear extended version are affected by the time scale structure. Large graininess induce larger estimation error especially in noisy scenarios where system robustness is deteriorated under large graininess because of stability region narrowness.
It would be useful to study deeper this phenomenon in the future works to find a way to overcome this issue or at least limit the impact of the graininess on the estimation error.
The adaptive non linear fault estimation observers didn't experience this issue but the calculations to find gains that would satisfy the conditions established in theorems related to each observer are complicated.
It is possible to establish a formulation as a LMI optimisation problem to solve for each value of μ by extending what has been developed in [20] to the general time scale case. However, this approach need a more detailed study to find necessary conditions on the time scale structure that would ease these calculations and decrease its numerical and computational complexity.

CHAPTER 4

Application to the Radar Target Tracking

4.1 Introduction

In the present chapter, we will apply the new time scale extended Kalman filter as a filtering technique for the radar target tracking.
The target tracking is a wide domain which objective is to track the movements of a given mobile in a space defined by the perception area of different sensors [12]. In our case, we will only focus on the tracking using radars.
During the previous decades, for meany strategic reasons this domain attracted the attention of many researchers around the world, and this led to the emergence of several techniques and algorithms to estimate a target trajectory.
Many scenarios of target tracking such that jamming, saturation or passive detection induce a non uniformity of the measurements, which makes the time scale analysis tools really relevant here.
First, we will introduce the generalities around the target tracking using Kalman filter algorithms, after that we will adapt those algorithms to the general time scale case and we will conclude with some simulations.

4.2 Generalities around the target tracking

In this this section, we introduce a simplified version of models that describe a body trajectory in the horizontal plane. we will then derive the discrete state equations from it to the maneuvering target case and non maneuvering one.
After that, we'll talk briefly about the classical filtering estimation techniques using the EKF.

4.2.1 Model of target trajectories

To model the trajectory of a target, we can state that whatever the complexity of this trajectory, we can always describe it with a succession of line segments, circle arcs, elliptical arcs...etc...[9]
From the statement above, we can determine the trajectory followed by a target at some instant t by determining the different canonical trajectories followed by the target during this time. [11] In our study we restrain ourselves to the line segments and we describe the target evolution by the evolution of its (x, y) coordinates through time.
If $\vec{F}_t$ is the sum of all the forces that act on the body at an instant t, we obtain by the second dynamic fundamental relation

$$m\frac{d^2}{dt^2}\begin{bmatrix}x(t)\\y(t)\end{bmatrix} = \vec{F}_t, \tag{4.1}$$

where m is the mass of the targeted body. The forces are reduced to air friction and other external disturbances when the body isn't in a maneuver phase.
When it produces an acceleration to maneuver (engines thrust), the net force $\vec{F}_t$ is also the result of this action.

Non maneuvering target

Non maneuvering targets can be described by very simple models.
Generally these bodies have mainly a rectilinear motion at constant speed. This movement is characterized by the equations [11]

$$\begin{cases} s = (t_k - t_{k-1})v + s_0, \\ v = \frac{ds}{dt} = \dot{s}, \end{cases} \tag{4.2}$$

where s is the crossed distance, v is the velocity and $(t_k - t_{k-1})$ is the time difference.
In discrete time, these equations become [11]

$$\begin{cases} s(k) = (t_k - t_{k-1})v(k-1) + s(k-1), \\ v(k) = v(k-1), \end{cases} \tag{4.3}$$

Inspiring ourselves from the model described by the equation 3.3 in [11], we can write an augmented version of this model for the plane

$$\begin{cases} x_1(k) = x_1(k-1) + Tx_2(k-1), \\ x_2(k) = x_2(k-1), \\ x_3(k) = x_3(k-1) + Tx_4(k-1), \\ x_4(k) = x_4(k-1), \end{cases} \tag{4.4}$$

where $\begin{cases} x_1(k) = s_x(k) & x_2(k) = v_x(k) \\ x_3(k) = s_y(k) & x_4(k) = v_y(k) \end{cases}$ and $T = t_k - t_{k-1}$.
Naturally, the systems are subjected to noises thus we have the following discrete state model

$$x_k = Ax_{k-1} + \omega, \tag{4.5}$$

where $x = \left[x_1 x_2 x_3 x_4\right]^T$, $A = \begin{bmatrix} 1 & T & 0 & 0 \\ 0 & 1 & 0 & 0 \\ 0 & 0 & 1 & T \\ 0 & 0 & 0 & 1 \end{bmatrix}$ and ω is a process noise with zero mean and covariance matrix $Q = \sigma_Q^2 \begin{bmatrix} \frac{T^2}{2} & T & 0 & 0 \\ 0 & T & 0 & 0 \\ 0 & 0 & \frac{T^2}{2} & T \\ 0 & 0 & 0 & T \end{bmatrix}$.

Maneuvering target

Now we add to the system 4.3 a third term that represents the acceleration of the body.

$$\begin{cases} s = (t_k - t_{k-1})v + s_0, \\ v = \frac{ds}{dt} = \dot{s} = (t_k - t_{k-1})a + v_0, \\ a = \frac{dv}{dt} = \dot{v}, \end{cases}$$

where a is the acceleration of the body. We deduce from the equations above the discrete time description

$$\begin{cases} s(k) = (t_k - t_{k-1})v(k-1) + s(k-1), \\ v(k) = (t_k - t_{k-1})a(k-1) + v(k-1), \\ a(k) = u. \end{cases} \tag{4.6}$$

u here is an input signal that controls the body acceleration. This leads to a system of equations equivalent to 4.4

$$\begin{cases} x_1(k) = x_1(k-1) + Tx_2(k-1) + \frac{T^2}{2}x_3(k-1), \\ x_2(k) = x_2(k-1) + Tx_3(k-1), \\ x_3(k) = u_x, \\ x_4(k) = x_4(k-1) + Tx_5(k-1) + \frac{T^2}{2}x_6(k-1), \\ x_5(k) = x_5(k-1) + Tx_6(k-1), \\ x_6(k) = u_y, \end{cases} \tag{4.7}$$

where $\begin{cases} x_1(k) = s_x(k) \quad x_2(k) = v_x(k) \\ x_3(k) = a_x(k) \\ x_4(k) = s_y(k) \quad x_5(k) = v_y(k) \\ x_6(k) = a_y(k) \end{cases}$

The equations above lead to the following state model

$$x_k = Ax_{k-1} + Bu + \omega. \tag{4.8}$$

Where $x = \begin{bmatrix} x_1 & x_2 & x_3 & x_4 \end{bmatrix}^T$, $A = \begin{bmatrix} 1 & T & \frac{T^2}{2} & 0_{1\times3} \\ 0 & 1 & T & 0_{1\times3} \\ 0 & 0 & 1 & 0_{1\times3} \\ 0_{1\times3} & 1 & T & \frac{T^2}{2} \\ 0_{1\times3} & 0 & 1 & T \\ 0_{1\times3} & 0 & 0 & 1 \end{bmatrix}$, $B = \begin{bmatrix} 0 & 0 \\ 0 & 0 \\ 1 & 0 \\ 0 & 0 \\ 0 & 0 \\ 0 & 1 \end{bmatrix}$, and $u = \begin{bmatrix} u_x \\ u_y \end{bmatrix}$

4.2.2 Measurement equation

The radar sends an impulse signal in a given direction. This signal propagates in all directions by forming spherical waves. After ΔT the signal reaches the target, this time is proportional to the target distance. A part of this signal is reflected by the target and after the same time ΔT, the reflected wave reaches the radar, which after processing the received signal gives an estimation of the distance between the radar and the target and the angle formed by the radar aim axis and a reference axis. (the measurement process is described with more details in [12])
Such a radar performs the tracking by distance and angle measurements. These measurements are described by the following equation [11]

$$y_k = h(x_k) = \begin{bmatrix} \sqrt{s_x(k)^2 + s_y(k)^2} \\ atan(\frac{s_y(k)}{s_x(k)}). \end{bmatrix} \tag{4.9}$$

Obviously, the measurements are corrupted with noises. Taking into account 4.9 and these noises leads to the following measurement equation

$$y = h(x) + v, \tag{4.10}$$

where x is the process state vector and the measurement noise v is a gaussian white noise with the covariance matrix $R = \begin{bmatrix} \sigma_d & 0 \\ 0 & \sigma_\phi \end{bmatrix}$.

4.2.3 Radar tracking using EKF

Regarding to the non linearities that characterize the measurement equation, we apply the extended Kalman filter by locally linearizing the model around the estimation points and applying the Kalman filter to determine the correction gain.
The set of EKF equations for the target tracking are given in [12]

$$\begin{cases} \hat{x}_k^- = f(\hat{x}_{k-1}, u_{k-1,0}) \\ P_k^- = A_k P_{k-1} A_k^T + Q_{k-1} \\ K_k = P_k^- C_k^T (C_k P_k^- C_k^T + R_k)^{-1} \\ \hat{x}_k = \hat{x}_k^- + K_k(y_k - h(\hat{x}_k^-)) \\ P_k = (I + K_k C_k) P_k^- \end{cases} \tag{4.11}$$

where C and A are given by 3.17 and 3.16 respectively. P is obtained by solving 3.8 for the case $\mu(t) = 1$.

Remark. *In our simulation we will take the input control signal u equal to zero in the filter algorithm. As we're performing a tracking simulation, we don't have access to this signal.*

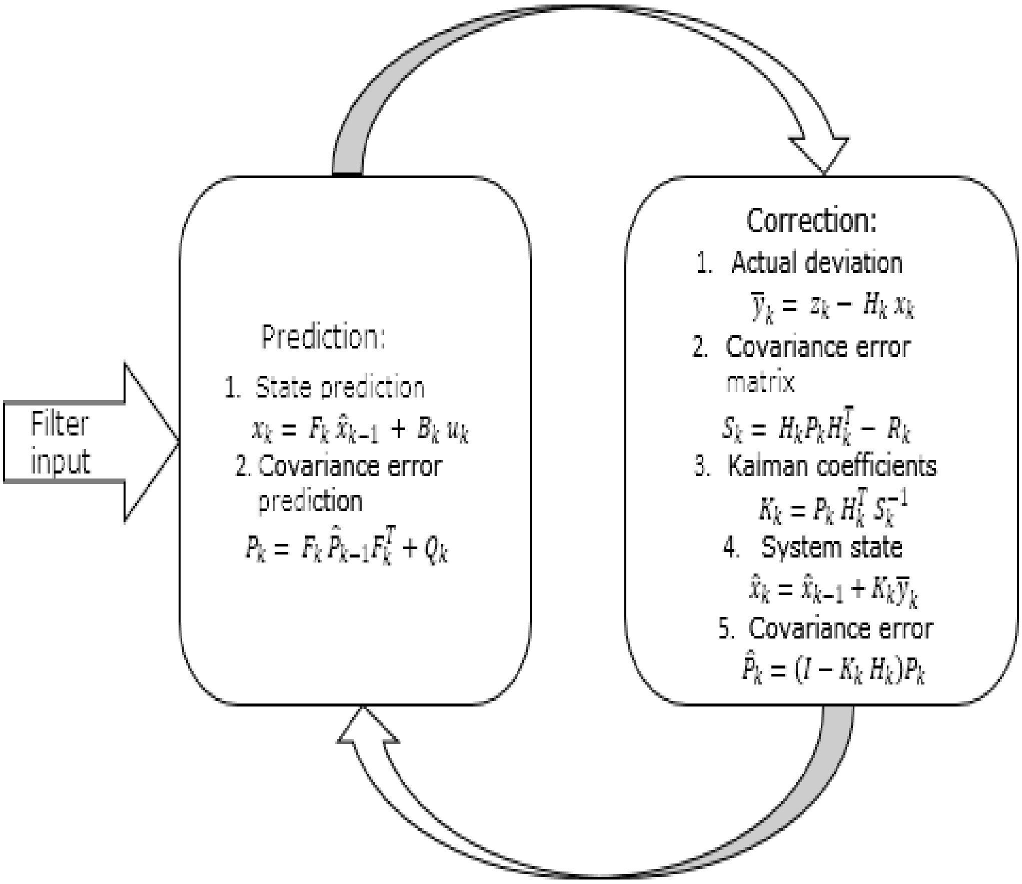

Figure 4.1: Kalman filter algorithm scheme. [28]

Remark. *In general, the Kalman filter is not sufficient enough to estimate the dynamic of a maneuvering target to track it.*
In these conditions, special maneuver detection devices incorporated in the tracking system are used to be able to follow the trajectories of the targets with precision. [12]
To lighten this issue, we will give to the control signal u impulse values.

4.3 Simulation

In the simulations, we generate a trajectory using the difference equation 4.6 for a body in that evolves in the (x, y) plane.
After that we generate radar measurements using the radar measurement equation 4.9.
In our scenario, we partially loose the target position at some instants. We will use both classical and time scale extended Kalman filters to perform the target tracking.

Remark. *In the matlab code, we replace some values of the measurements vector by NaN to indicate that we lost the target at this instant.*

Remark. *When the value of y is equal to NaN, in the classical EKF estimation we simply estimate the position using the equation $\hat{x}_k = A\hat{x}_{k-1}$, we remove the correction term since we do not have any measurement.*
In this simulation the parameters are taken as follows:
$\sigma_d = \sqrt{2}$, $\sigma_\phi = \sqrt{\frac{\pi}{1800}}$, $\sigma_Q = \sqrt{2}$, $X_0 = [3, 40, 4, 20]^T$ *for the non maneuvering case and* $\sigma_d = \sqrt{50}$, $\sigma_\phi = \sqrt{\frac{\pi}{1800}}$, $\sigma_Q = \sqrt{2}$,$X_0 = [1500, 0, 0.1, 180, 1, -0.5]^T$, *for the maneuvering case.*

Remark. *the graininess operator is increased by the sampling period each time the measure is replaced by NaN.*
example: when $y = [NaN, NaN, NaN]$ we have $\mu = 4T_e$. where T_e is the sampling period.
Time is given in seconds (s) and distances are given in meters (m) for both maneuvering and non maneuvering cases.

Remark. *For the non maneuvering case we use a predictive version of the discrete extended Kalman filter. each time we don't have a measurement we remove the correction term of the filter and we replace the filter equation by $\hat{x}_{k+1} = f(x_{k+1}, 0)$.*

Figure 4.2: Linear trajectory and measurements generation.

Non maneuvering case:

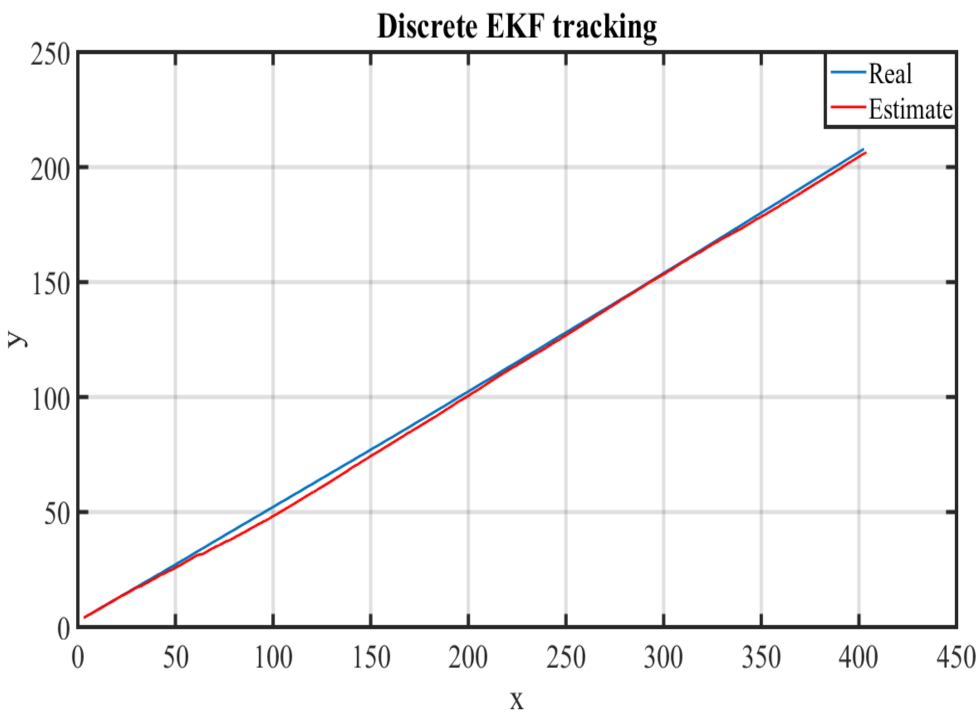

Figure 4.3: Target tracking using discrete EKF.

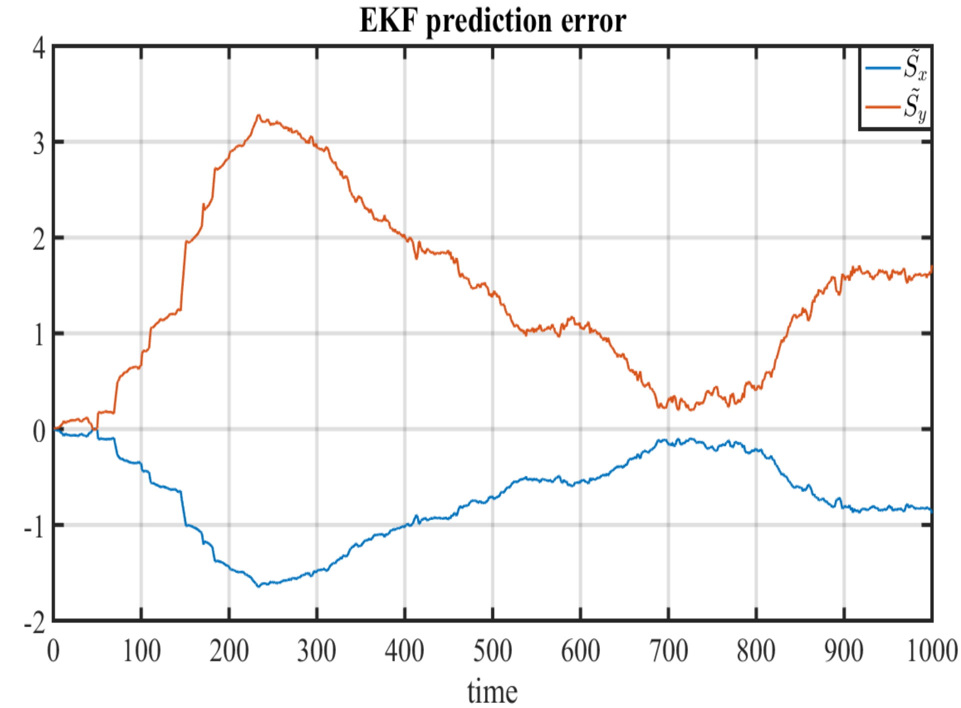

Figure 4.4: Discrete extended Kalman filter targes position estimation error.

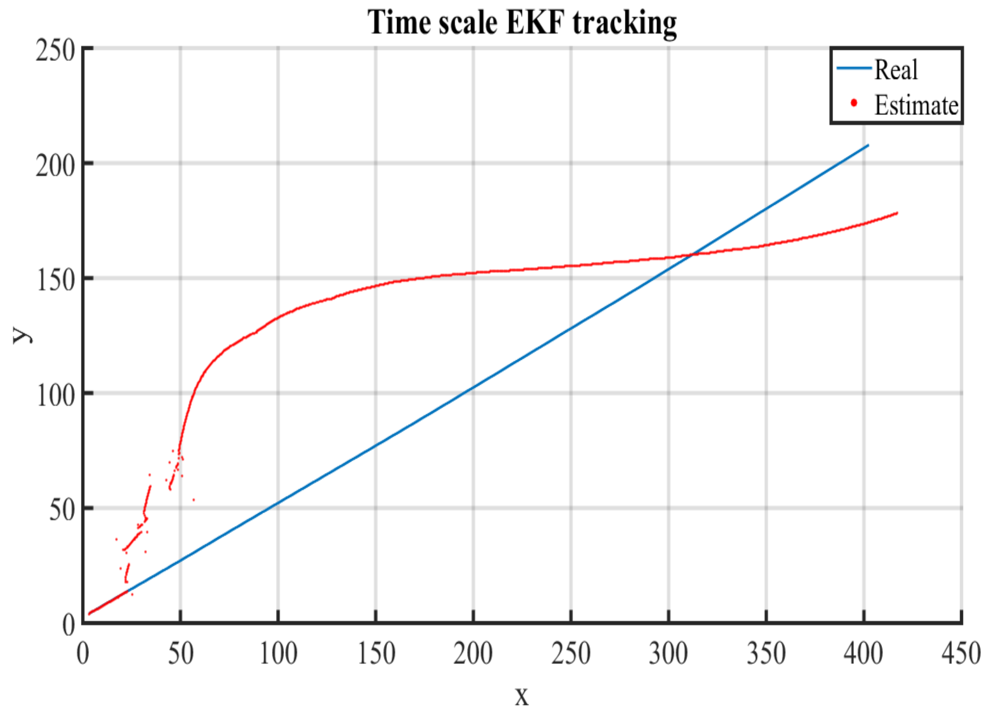

Figure 4.5: Target tracking using time scale extended Kalman filter.

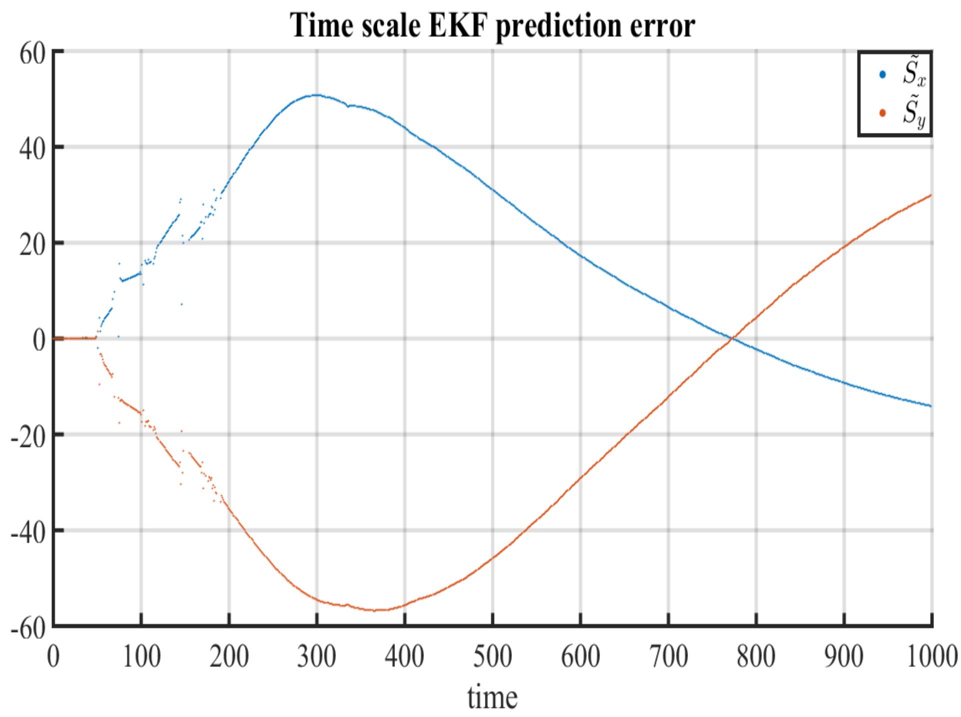

Figure 4.6: Time scale extended Kalman filter target position estimation error.

Maneuvering case:

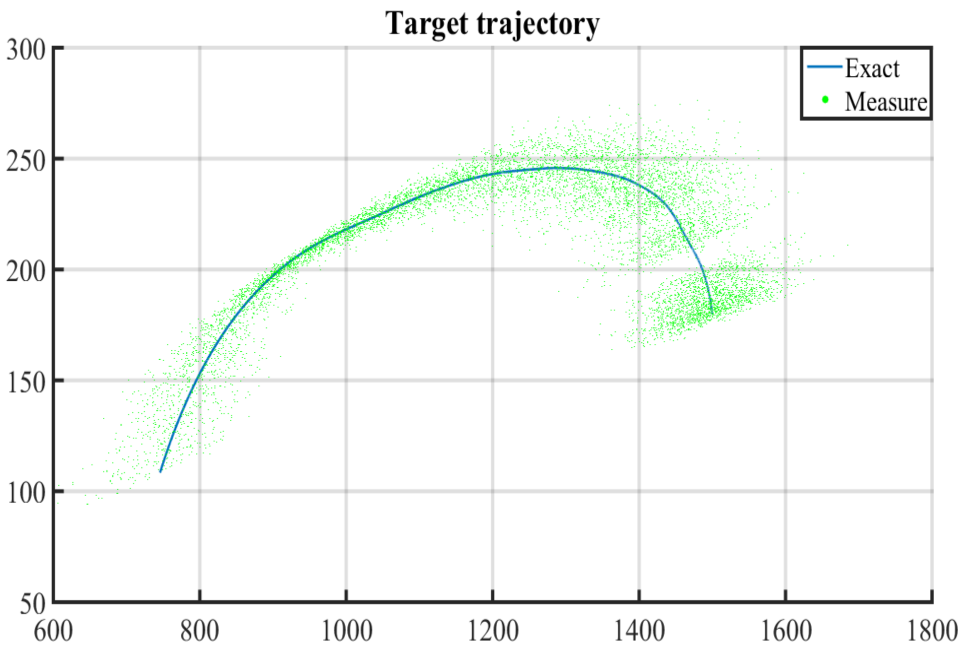

Figure 4.7: Maneuvering target trajectory.

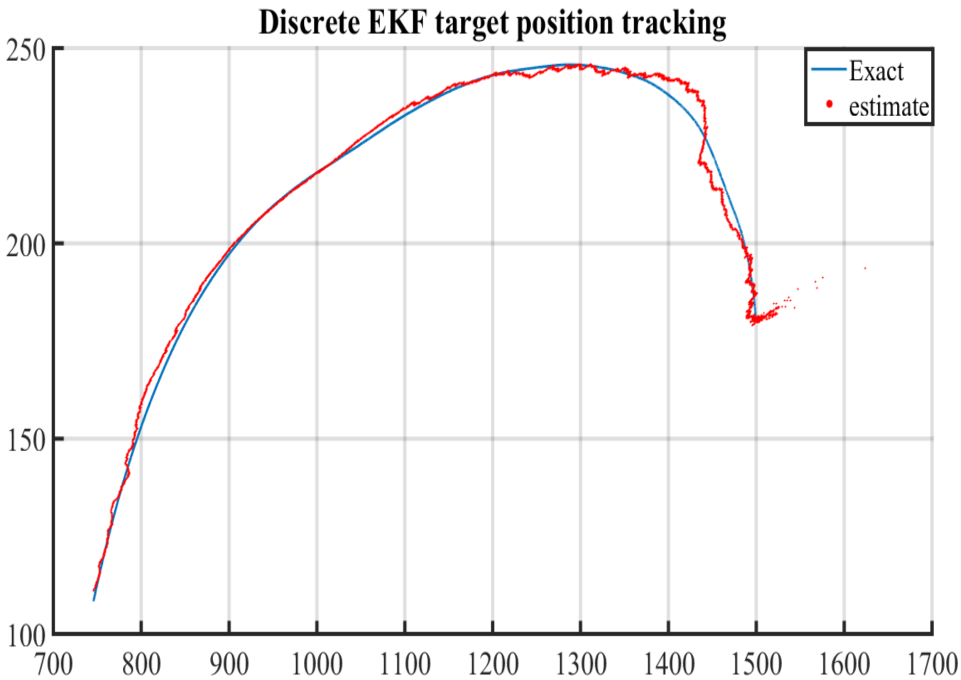

Figure 4.8: Maneuvering target tracking using discrete extended Kalman filter.

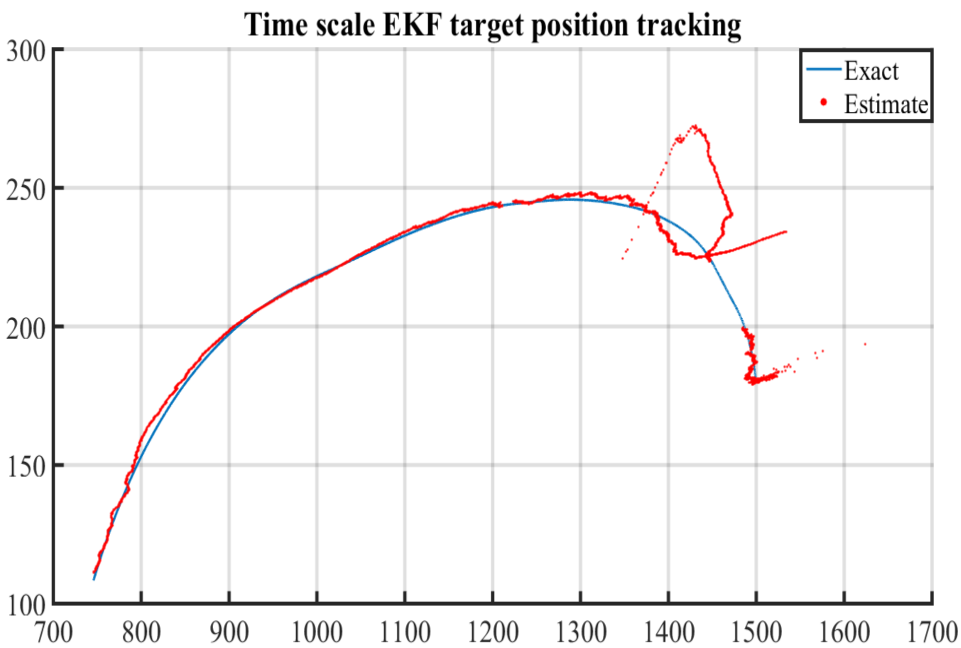

Figure 4.9: Maneuvering target tracking using time scale extended Kalman filter.

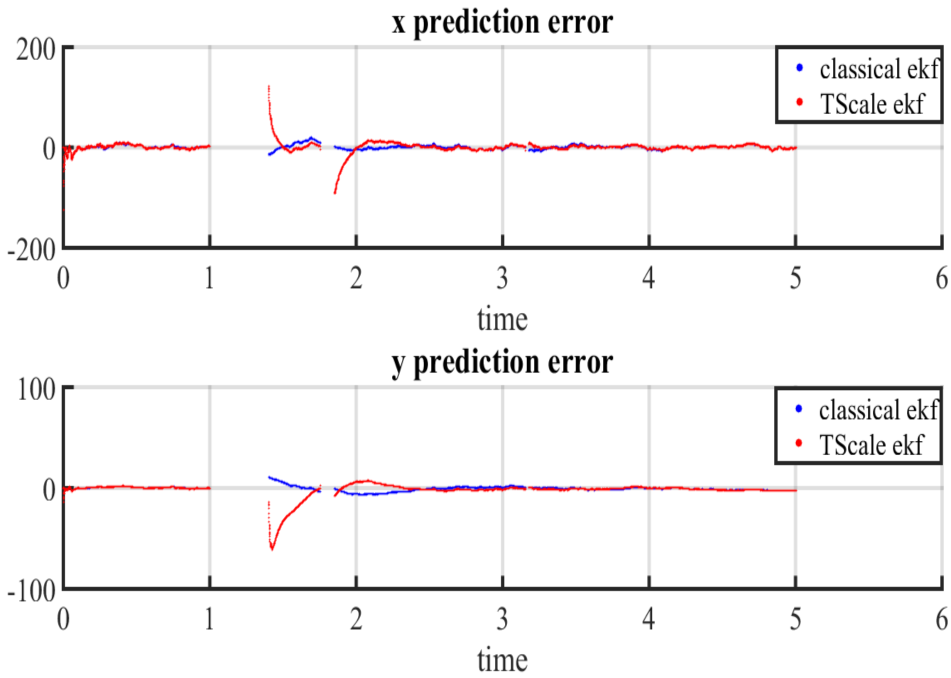

Figure 4.10: Maneuvering target position estimation error.

Comments on results

The time scale Kalman filter performs the radar target position tracking with a very satisfying accuracy in presence of extremely corrupted measurements.
We still observe the usual deviation of the estimate from the signal when the data are missing (which is implied by an increase of the graininess), the estimation accuracy is quickly recovered when the measurements get back (which is due to the graininess value decrease). It's important to notice that the error peak of the discrete filter is less important than the one observed for the time scale EKF in the maneuvering case.
In the non maneuvering case, the time scale filter appears to perform with lesser accuracy, unfortunately the absence of measurements drives the estimation error to highly increase and it takes more time to recover its initial accuracy than the maneuvering case. Moreover, the discrete EKF has a better accuracy than the time scale EKF even when the measures are accessible to the observer. Nevertheless, whatever the case this error is still bounded.
The difference of the graininess increase impact on the error pick between the discrete and time scale Kalman filter suggests that the time scale Kalman filter introduced in [6] should be improved to overcome this issue.

4.4 Conclusion

In this chapter, we evaluated the time scale extended Kalman filter performance in a concrete scenario where non uniform measurements are involved.
The particularity of this simulated scenario is the fact that the non-uniformities that usually characterize the time scale systems are just virtual.
Indeed, they only appear in the measurements or the feedback loop while the state of the system is characterized by a classical discrete dynamic.
The results of these simulations are interesting regarding to the relevance of the information obtained about this time scale filter estimation capacity.
We have seen that the time scale extended Kalman filter is able to perform the radar target tracking with an accuracy globally equivalent to its discrete version.
The implementation of this new filter omens a promising potential for practical applications in any engineering area which could be subjected to non-uniformities in the dynamics of their processes.

General Conclusion

State observers represent a major asset in control engineering and control theory to solve the issue of systems inaccessible inner state signals measure. the introduction of this type of tools for time scale systems is of important interest, since this new theory is still poorly supplied with advanced observation techniques and strategies.

In this context, the main purpose of this thesis was the development of observers with the objective to perform state estimation for systems that are characterized with non uniform or hybrid dynamics.

At first, we reminded the fundamentals of time scale calculus and introduced the main notions and definitions around time scale systems and their dynamical properties. We presented then the generalities relative to model based fault diagnosis and gave an overview of some observer based diagnosis strategies and techniques.

In the main chapter that gathers all our contributions to the topic, we introduced first the time scale Kalman filter and added to it a fault diagnosis feature. We developed its extended version to nonlinear systems and established its time scale stochastic stability. We ended this part by studying the observer based control case and discussing the LQG/LTR issue for the non zero graininess time scale case.

After that, we proposed a study where we generalized to the random time scale general case the adaptive observers (fast fault estimation and PI observers) by generalizing their error stability conditions for any graininess value. We also extended to time scales the H_∞ filtering approach to design the PI observer introduced in [20].

The method followed to provide the proofs of this thesis important results mainly relied on establishing the time scale equivalent of the already established proofs that ensured the stability properties of the introduced filters and observers in continuous or discrete time sets using the theoretical tools of time scale calculus.

This approach has proven to be successful, since it allows the establishment of powerful

results by combining the conventional continuous and discrete control theory results and time scale calculus.
During the simulations, all the newly introduced observers have shown interesting performances regarding to their global accuracy and convergence rates. However, we have seen that the estimation error tends to increase due to the error stability configuration which is highly influenced by the graininess operator that shrinks the stability domain when this operator increases. The Loop transfer recovery controller proposed seems to work with good performance on unions of nonzero graininess time scales, unfortunately it fails to reject the noise impact when the graininess takes random values.
In the last chapter, we proposed a radar target tracking scenario where the radar sometimes looses its target to assess the time scale Kalman filter performances. The filter performance were similar to what has been observed in chapter 3. These results signify that this new filter can be used in real applications where systems with non uniform measurements are involved. Moreover, the time scale Kalman filter is of major interest for any application with non-uniform dynamics or hybrid systems.

Future outlook

There are several directions to consider for future developments in view of the work done in this thesis. Next years students should inquire for a solution to the error pick issue observed in Kalman filter estimation for high values graininess. They could find a new and better formulation for this filter that could fix this issue.
A frequency description of time scale systems should be developed in future works. Indeed, the frequency description of continuous and discrete systems is very useful to quantify systems dynamical properties and ease the performance analysis of a controller or observer capacity to reject noises or respond with a given rate and accuracy. Such a description would allow a truly rigorous development of the LQG/LTR controller and overcome the issues that we met. Beyond that, it will allow a better understanding of time scale systems robustness properties and subsequently find a way to strengthen these properties under high graininess.
The last important thing to improve concerns the adaptive non linear fault estimation observers. We gave in theorems 3.7.1, 3.7.2 and 3.7.3 the gains conditions that ensure the estimation error stability of each observer. It would be suitable to translate these LMI conditions into LMI optimization problems to allow a more easier evaluation of the observer gains.

Bibliography

[1] ATKINSON.K.E and HAN.W. *Theoretical numerical analysis: a functional analysis framework.* World publishing corporation, 2013.

[2] Bartosiewicz.Z and Piotrowska.E. "On stabilisability of nonlinear systems on time scales". In: *International Journal of Control* 86.1 (2013), pp. 139–145. DOI: 10.1080/00207179.2012.72563.

[3] Bartosiewicz.Z, Piotrowska.E, and Wyrvas.M. "Stability, Stabilization and Observers of Linear Control Systems on Time Scales". In: *46th IEEE Conference on Decision and Control New Orleans, LA, USA* (2007), pp. 2803–2808.

[4] BESANCON.G. "Remarks on nonlinear adaptive observer design". In: *Systems & control letters* 41.4 (2000), pp. 271–280.

[5] BOHNER.M and PETERSON.A. *Dynamic Equations on Time Scales: An Introduction With Applications.* 2001 ed. BIRKHAÜSER Boston Inc., 2001.

[6] Bohner.M and Wintz.N. "The Kalman filter for linear systems on time scales." In: *Journal of Mathematical Analysis and Applications.* 406 (2013), pp. 419–436.

[7] Chen.B.M, Saberi.A, and Sannuti.P. "A new stable compensator design for exact and approximate Loop Transfer Recovery". In: *Automatica* 27 (1991), pp. 257–280.

[8] Clempner.Jo.B and W.yu. *New Perspectives and Applications of Modern Control Theory.* 1st ed.2018. Springer International Publishing, 2018.

[9] DJOUATI.M.S. "Poursuite de Cibles Manoeuvrantes par Vision Active". Thése de Doctorat. Ecole Nationale Polytechnique, d'Alger, 2006.

[10] Doan.T.S, Kalauch.A, and Siegmund.S. "Exponential Stability of Linear Time-invariant Systems on Time Scales". In: *Nonlinear Dynamics and Systems Theory* 9.1 (2009), pp. 37–50.

[11] DRIS.L. "Les Algorithmes Adaptatifs de Poursuite de Cible". thése de Magistère. Ecole Nationale Polytechnique, Departement d'électronique, 2008.

[12] DRISS.Y. "Poursuite de cible par le filtrage de Kalman non linéaire (EKF)". Ingénieur. Université Saad Dahleb Blida, 2010.

[13] FLOQUET.T, EDWARDS.C, and SPURGEON.S.K. "On sliding mode observers for systems with unknown inputs". In: *International journal of Adaptive Control and Signal Processing* 21 (2007), pp. 638–656.

[14] HILGER.S. "Ein Maßkettenkalkül mit Anwendung auf Zentrumsmannigfaltigkeiten". PhD Thesis. Universität Würzburg, 1989.

[15] ISERMANN.R and BALLE.P. "Trends in the application of model-based fault detection and diagnosis of technical processes". In: *Control Engineering Practice* 5 (1997), pp. 709–719.

[16] JACKSON.B.J. "A general linear systems theory on time scales: Transforms, stability and control". PhD thesis. Baylor Univesity, 2007.

[17] Jan Lunze and Françoise Lamnabhi-Lagarrique. *Handbook of Hybrid Systems Control:Theory, Tools, Applications*. Cambridge University Press, 2009.

[18] Mudry.F. *Modélisation et régulation d'un pendule inversé*. URL: `http://freddy.mudry.org/public/NotesApplications/na_pendinvc.pdf`. accessed: 09.03.2020.

[19] NOLL.D. *A generalization of the Linear Quadratic Gaussian Loop Transfer Recovery procedure (LQG/LTR)*. URL: `https://www.math.univ-toulouse.fr/~noll/lqg_ltr.html`. accessed:23.04.2020.

[20] OUCIEF.N. "Contribution à la synthèse d'observateurs adaptatifs pour l'estimation des défauts dans une classe de systèmes non lineaires". Thése de Doctorat en Sciences. Ecole Nationale Polytechnique, Département d'Automatique, Laboratoire de Commande des Processus, 2017.

[21] OUCIEF.N, TADJINE.M, and LABIOD.S. "A new methodology for an adaptive state observer design for a class of nonlinear systems with unknown parameters in unmeasured state dynamics". In: *Transactions of the institute of Measurement and Control* 40.4 (2016), pp. 1297–1308. DOI: `10.1177/0142331216680288`.

[22] Poulsen.D and Wintz.N. "The Kalman filter on stochastic time scales". In: *Nonlinear Analysis: Hybrid Systems* 33 (2019), pp. 151–161.

[23] RAGHAVAN.S and HEDRICK.J.K. "Observer design for a class of nonlinear systems". In: *International Journal of Control* (1994), pp. 515–528.

[24] RAOUFI Reza, MARQUEZ HJ, and ZINOBER Alan. “H_∞ sliding mode observers for uncertain nonlinear Lipschitz systems with fault estimation synthesis.” In: *International Journal of Robust and Nonlinear Control* 20.16 (2010), pp. 1785–1801.

[25] TADJINE.M, M’SAAD.M, and DUGARD.L. “An overview on the LQG/LTR method using the delta operator”. In: *Proc. 31st Conf.Decision Contr .* 4 (1992), pp. 3728–3733. DOI: 10.1109/CDC.1992.371190.

[26] TADJINE.M, M’SAAD.M, and DUGARD.L. “On loop transfert recovery at the plant output”. In: *Proc. IFAC 1993 World congress. Sydney, Australia* (1993), pp. 185–188.

[27] *The Hilger Complexe Plane.* URL: https://www.timescales.org/Time_Scales_Tutorial/index_files/5.html.

[28] *Using the Kalman filter for price direction prediction.* URL: https://www.mql5.com/en/articles/3886.

[29] WINTZ.N.J. “THE KALMAN FILTER ON TIME SCALES.” DOCTOR OF PHYLOSOPHY. MISSOURI UNIVERSITY OF SCIENCE and TECHNOLOGY., 2009.

[30] YAZ.E.E. “Stochastic stability of the discrete-time extended Kalman filter”. In: *IEEE Transactions on Automatic Control* 44.4 (1999), pp. 714–728. DOI: 10.1109/9.754809.